with low <mu> data

W-Ai measurements

Daniil Ponomarenko

3-February-2023

Plan of the talk

- Motivation
- Brief analysis overview
- Updates on MJ estimation

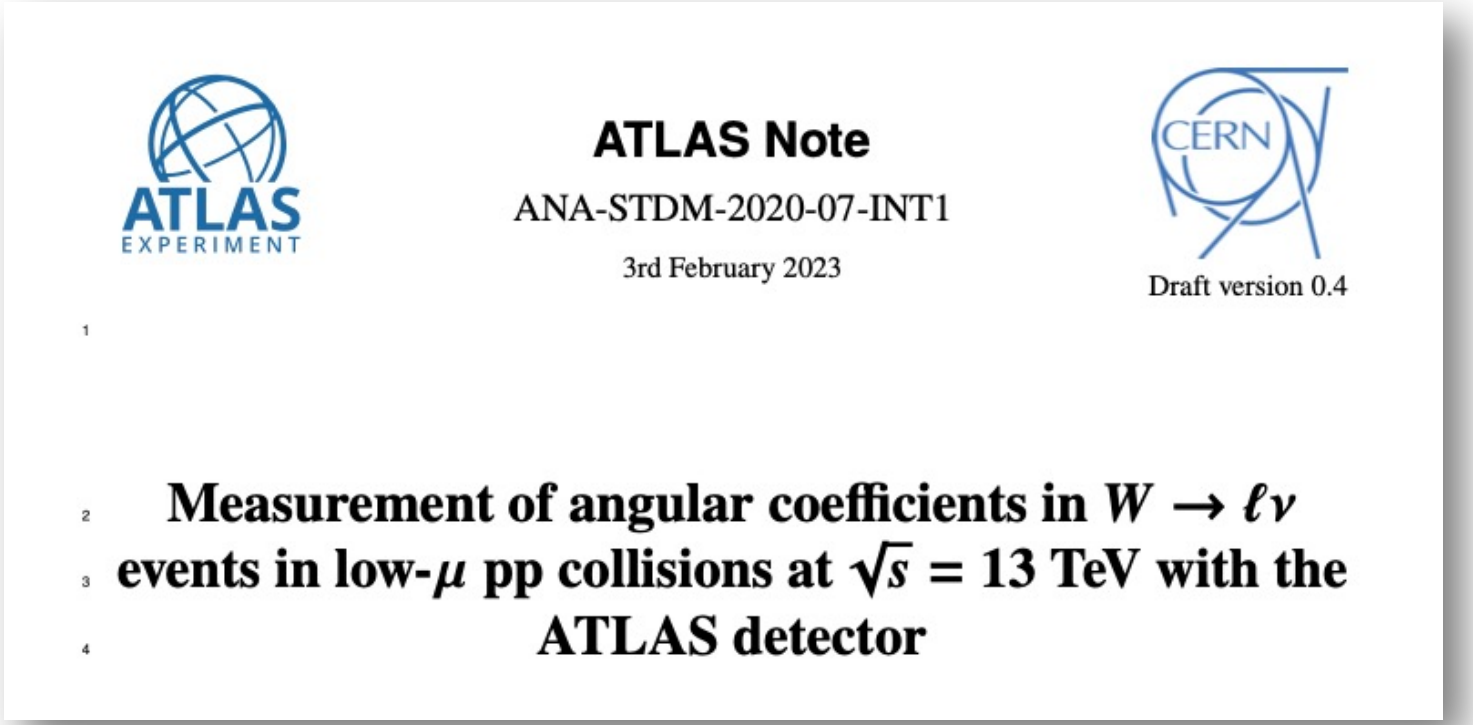

ATLAS EXPERIMENT

ATLAS Note

ANA-STDM-2020-07-INT1

3rd February 2023

CERN

Draft version 0.4

Measurement of angular coefficients in $W \to \ell\nu$ events in low-μ pp collisions at $\sqrt{s} = 13$ TeV with the ATLAS detector

Link to CDS: https://cds.cern.ch/record/2824052 (last modified 2022-09-30).
Latest version of supporting note is in attachments to the agenda.

Motivation

W mass measurement

$M_W = 80369.5 \pm 6.8\ (\text{stat}) \pm 10.6\ (\text{exp.syst.}) \pm 13.6\ (\text{model.syst.})\ \text{MeV}$

Limited by data

Experimental: modelling of lepton momentum measurement and hadronic recoil

Theoretical: understanding of vector boson production and decay

Combined categories	Value [MeV]	Stat. Unc.	Muon Unc.	Elec. Unc.	Recoil Unc.	Bckg. Unc.	QCD Unc.	EW Unc.	PDF Unc.	Total Unc.	χ^2/dof of Comb.
m_T-p_T^ℓ, $W^\pm$, e-μ	80369.5	6.8	6.6	6.4	2.9	4.5	8.3	5.5	9.2	18.5	29/27

- Larger source of modelling uncertainty from PDFs
- Total uncertainty on ATLAS W mass measurement ~19MeV still larger than 8MeV from electroweak fit

Why measure Ai in W events?

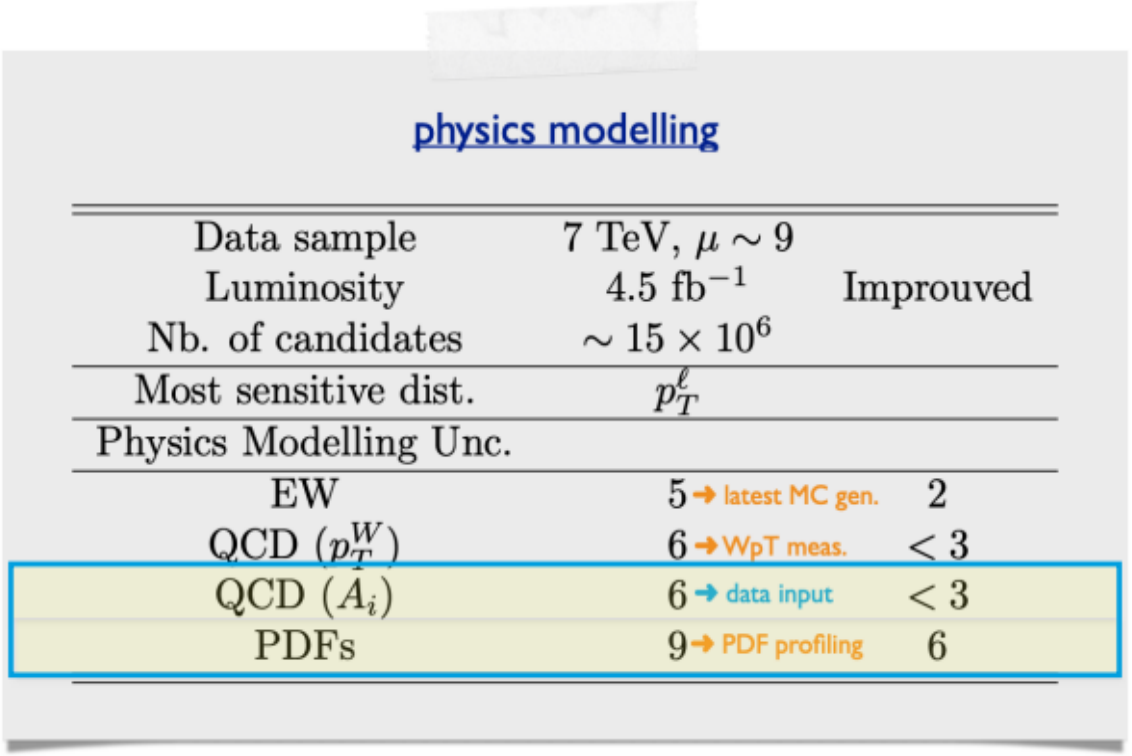

physics modelling

Data sample	7 TeV, $\mu \sim 9$	
Luminosity	4.5 fb^{-1}	Improuved
Nb. of candidates	$\sim 15 \times 10^6$	
Most sensitive dist.	p_T^ℓ	
Physics Modelling Unc.		
EW	5 → latest MC gen.	2
QCD (p_T^W)	6 → WpT meas.	< 3
QCD (A_i)	6 → data input	< 3
PDFs	9 → PDF profiling	6

- W-Ai analysis (+ x-section):
  - A_i: Stringent test of QCD & physics modelling!
  - X-section measurement as function of the Y.
    - All previous measurements at the LHC are done with lepton η.
  - Charge asymmetry measurement: Input for PDF fits
- Full set of A_i have never been measured before for the W boson!
  - Only A_2 and A_3 were measured by CDF (Phys. Rev. D 73, 052002)

Vector boson production and decay

- Drell Yan $pp \rightarrow V \rightarrow l\bar{l}$ cross section can be factorised into an **unpolarised** cross-section and **8 angular coefficients** (A_i).

$$\frac{d\sigma}{dp_1 dp_2} = \left[\frac{d\sigma(m)}{dm}\right]\left[\frac{d\sigma(y)}{dy}\right]\left[\frac{d\sigma(p_T,y)}{dp_T dy}\left(\frac{d\sigma(y)}{dy}\right)^{-1}\right]\left[(1+\cos^2\theta)+\sum_{i=0}^{7} A_i(p_T,y)P_i(\cos\theta,\phi)\right]$$

Breit Wigner | Parton shower | Fixed order pQCD

- The angular coefficients:
  - A_0, A_1, A_2 sensitive to vector boson **polarisation**
    - $A_0 - A_2 = 0$ but violated due to higher order QCD effects (e.g. multi-gluon emission..)
  - A_3, A_4 sensitive to **vector and axial couplings** of the boson
    - A_4 directly related to A_{FB}, probes electroweak mixing
  - A_5, A_6, A_7 non-zero only at $\mathcal{O}(\alpha_s^2)$
- QCD production dynamics fully contained in A_i coefficients, while decay kinematics fully contained in coupled angular polynomials

In Collins-Soper frame:

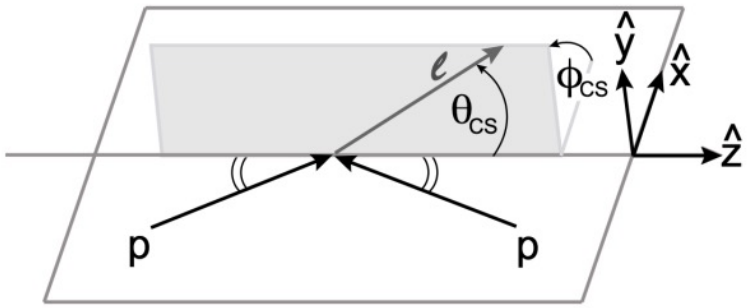

JHEP08(2016)159

Analysis overview

W Ai analysis overview

- Supporting note: ANA-STDM-2020-07-INT1
- Dataset:
  - ATLAS 13 TeV low pileup datasets 335.18 pb^{-1}
  - Statistically limited by small datasets but provides hadronic recoil resolution needed
- Able to measure 1D in p_T^W and separately in y^W
- We focus on the larger coefficients A_0, A_2, A_3, A_4
  - Other coefficients are also get measured, but the analysis is far from having sensitivity to A_5, A_6, A_7
- Channels:
  - $W^- \to e^-\nu, W^+ \to e^+\nu, W^- \to \mu^-\nu, W^+ \to \mu^+\nu$
- Looking forward for EB request

Event selection

Electron	Muon
Tight ID	Medium ID
p_T > 25 GeV	
|η| < 2.4	
1.37 < |η| < 1.52	
ptvarcone20/p_T < 0.1	
topoetcone20/p_T < 0.05	
|d_0 sig| < 5	|d_0 sig| < 3
$\Delta z_0 \sin\theta$ < 0.5	

- We use signal region selection based on pTW analysis with optimizations for better A_i sensitivity
  - Use same physics objects calibrations
  - + estimate and apply corrections specific for Wai analysis
- Relaxed kinematic cuts:
  - No $E_T^{miss} > 25\ GeV$ cut
  - No $m_T^W > 50\ GeV$ cut
- Use *TightLH* working point for electrons
- Tighter isolation selection:
  - $ptvarcone20/pt$<0.1 && $topoetcone20/pt$<0.05

Analysis

Angular definitions require fully constructed neutrino (will cover in next slides):

- Using Hadronic recoil solve for Neutrino p_z with mass constrain.
- Once the mass constraint is chosen φ_{CS} is solved while the 2 solutions corresponds to a sign ambiguity in $\cos\theta_{CS}$.
- Discovered that adding sign ambiguity only in y^W, not in $\cos\theta_{CS}$ drives our A_4 sensitivity.

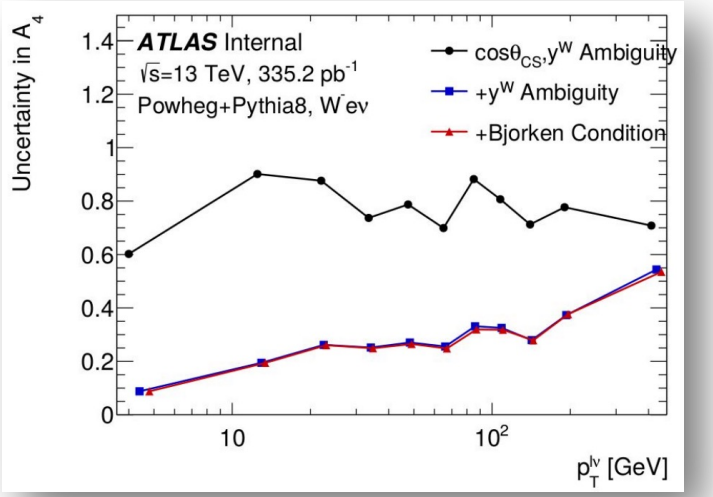

MJ shape estimation follows procedure used by pTW analysis (slides in backup):

- Calculate MJ normalization by linear extrapolation fit for different anti-isolation slices
- Calculate MJ template shape by applying bin-by-bin linear shape extrapolation
- To get MJ shape as a function of |Y| and $p_T^{l,\nu}$ MC samples used: $b\bar{b} + c\bar{c}$ for W→μν channels, JF17 for W→eν channels
- Calorimetric isolation used for e± and track isolation used for μ± channels:
  - Slicing ptvarcone20/pt for W→μν: 8 slicing bins from 0.1 to 0.5
  - Slicing in topoetcone20/pt for W→eν: 8 slicing bins from 0.05 to 0.45

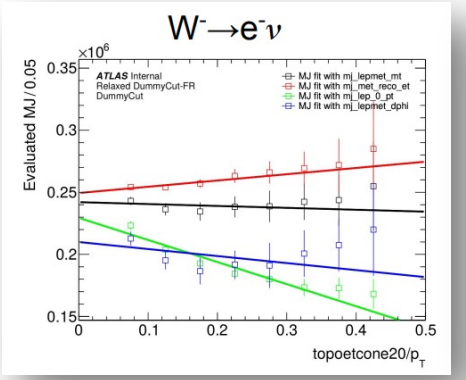

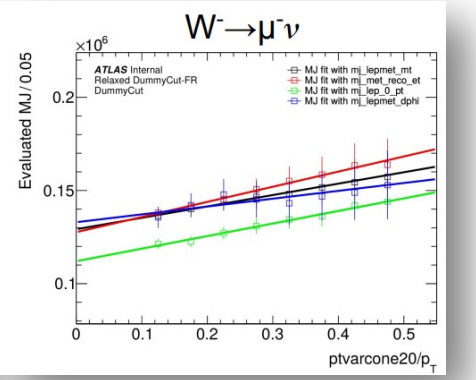

Control plots in the Signal Region for $W^- \to e^- \nu$

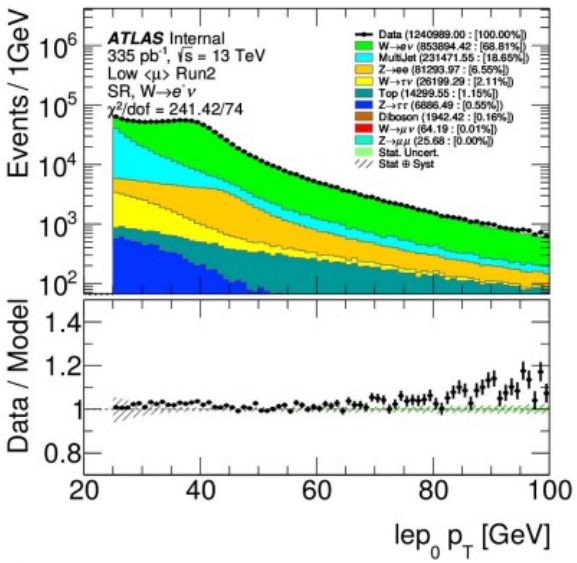

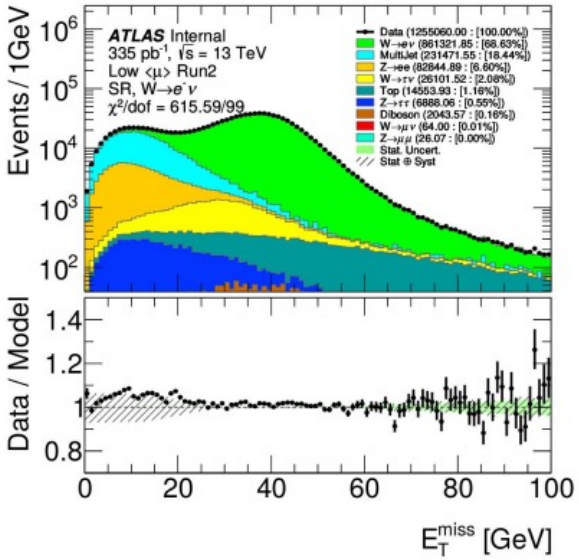

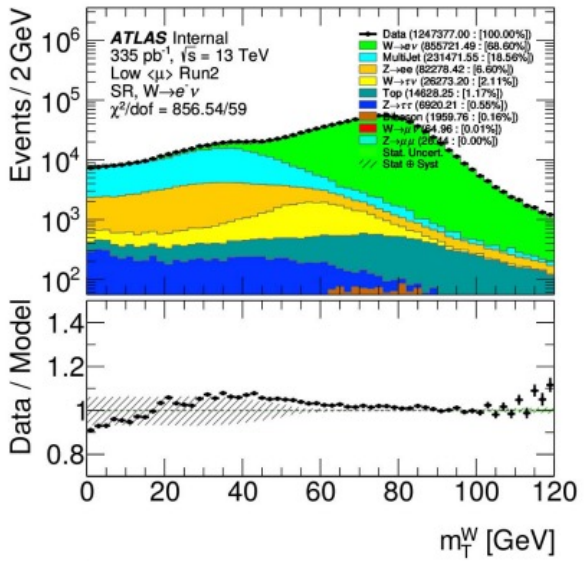

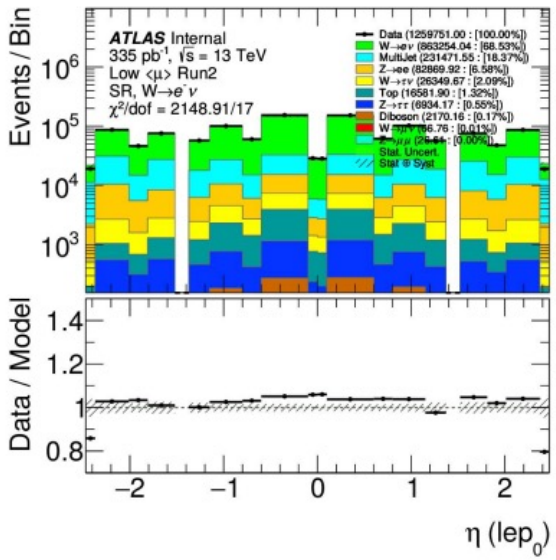

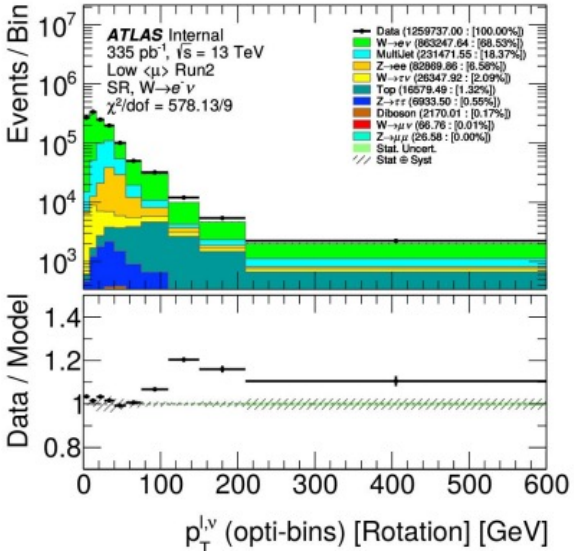

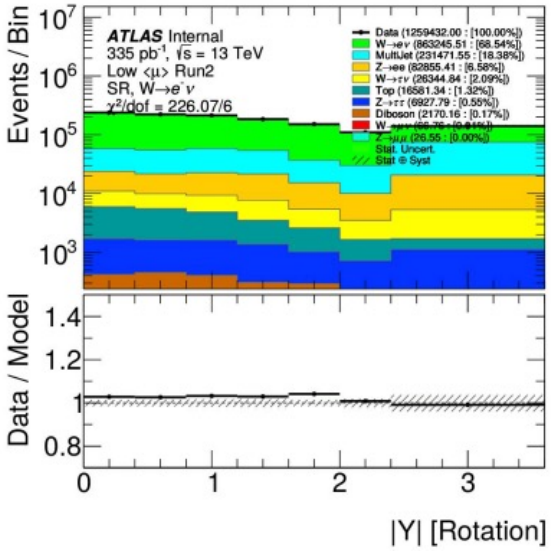

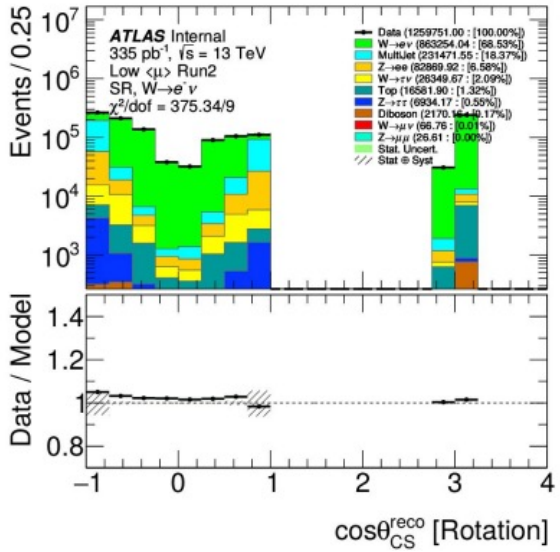

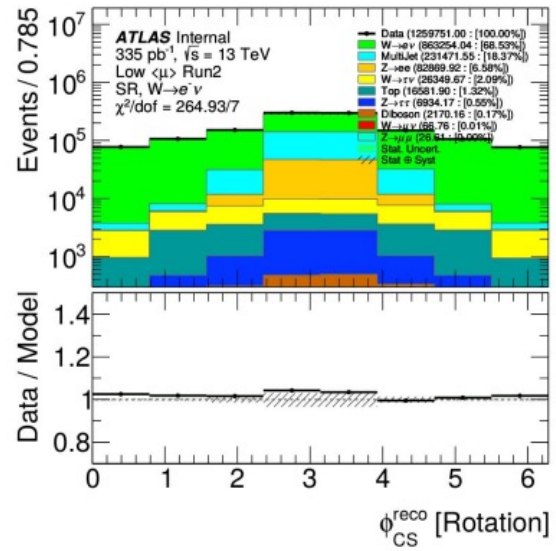

Control plots in the Signal Region for $W^- \to \mu^- \nu$

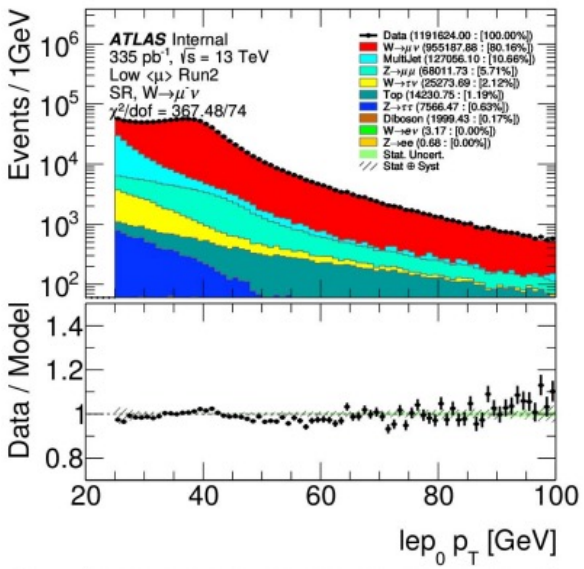

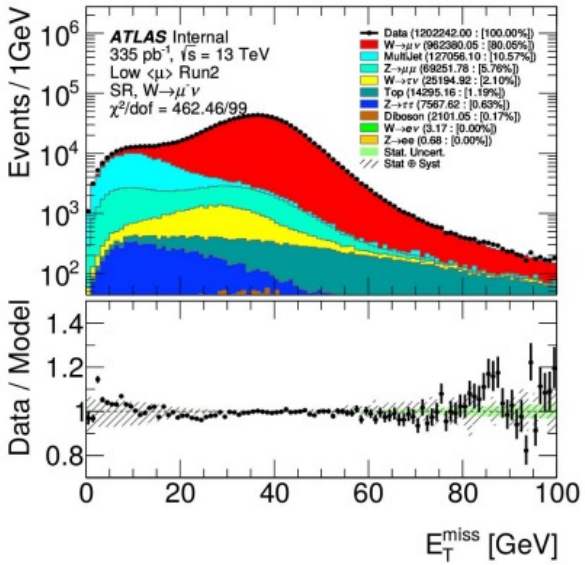

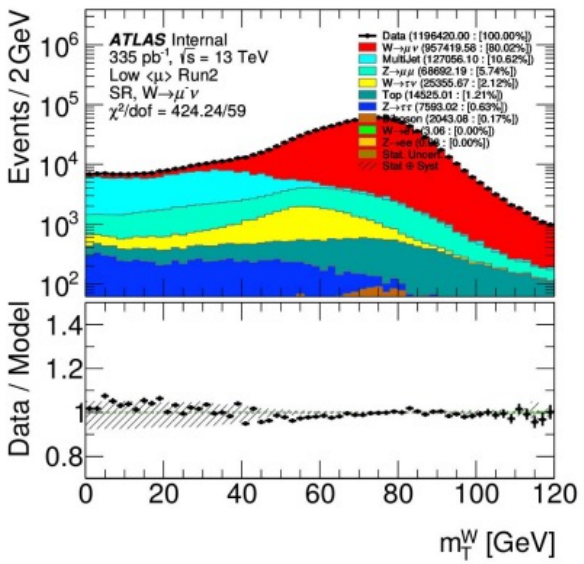

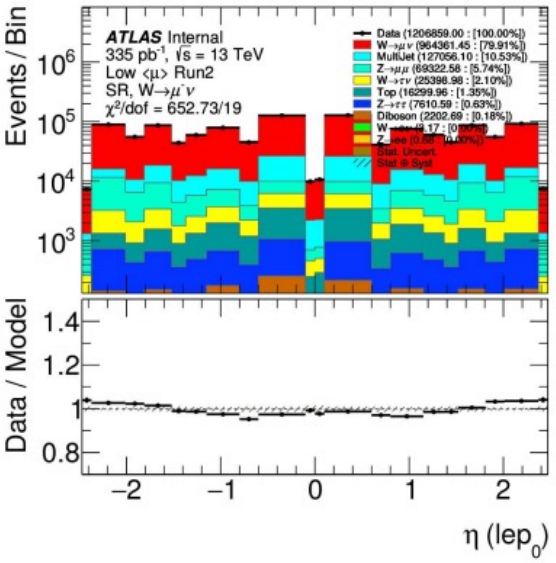

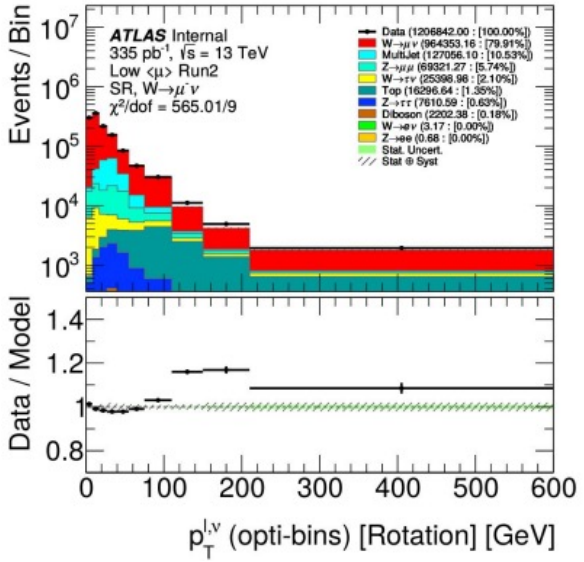

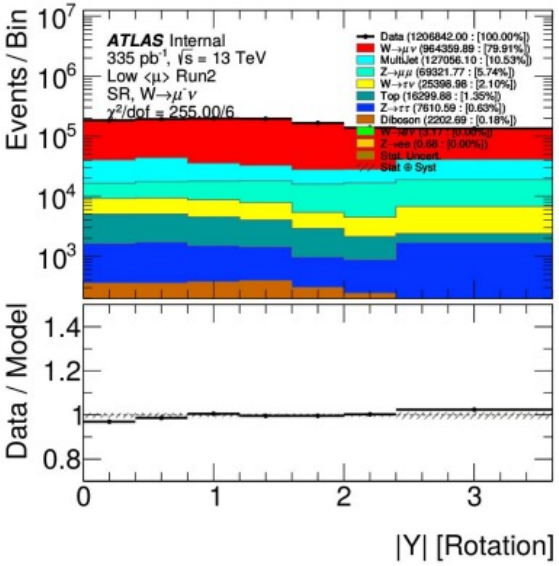

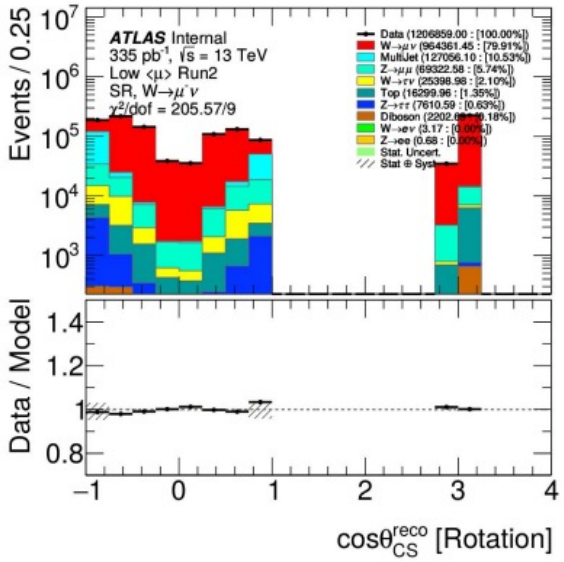

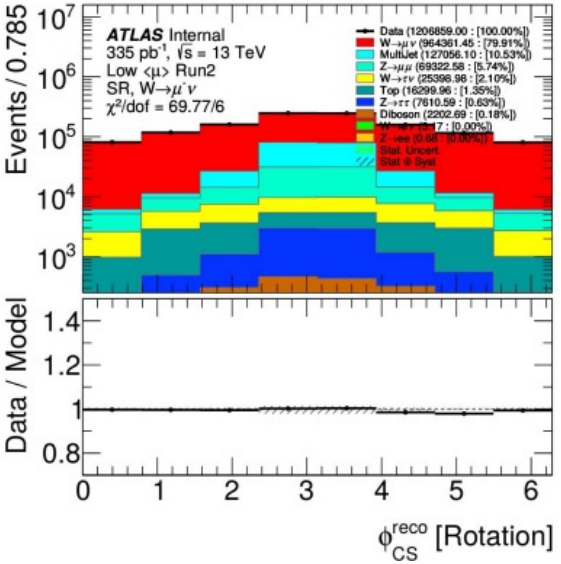

Fitting method

Reference coefficients created by taking moments of the polynomials using truth MC

$$\langle P_i(\theta,\varphi)\rangle = \frac{\int d\sigma(p_T,m,y,\theta,\varphi)\,P_i(\theta,\varphi)\,d\cos\theta d\varphi}{\int d\sigma(p_T,m,y,\theta,\varphi)\,d\cos\theta d\varphi} \rightarrow \langle\cos\theta\rangle = \frac{1}{4}A_4$$

Truth phase space is folded into the reco phase space through polynomial templates.

$$T_{ij} = \sum_{event\in\Delta_j} \frac{P_i\left(\cos\theta_{CS}^{Reco},\varphi_{CS}^{Reco}\right) w_{event}(r,t)}{\sigma_j\left\{P_8\left(\cos\theta_{CS}^{Truth},\varphi_{CS}^{Truth}\right) + \sum_{i=0}^{7} A_{ij}^{ref} P_i\left(\cos\theta_{CS}^{Truth},\varphi_{CS}^{Truth}\right)\right\}}$$

Extraction of coefficients through likelihood fit of MC templates in $p_T^{l,\nu}$ and $y^{l,\nu}$ bins.

$$\mathcal{L}(A_{ij},\mu_j|N) = \prod_{events}^{N}\left\{\sum_{j=1}^{N_{pT}^{bins}}\mu_j\left[T_{8,j}+\sum_{i=0}^{7}A_{ij}\times T_{ij}\right] + \sum_{B}^{bkgds} T_B + T_{Fakes}\right\}$$

Polynomial templates differ to ZAi analysis by extending $\cos\theta_{CS}$ range to save information for events with no real solution.

Systematics

- Have largest expected systematics included (MJ, cross-section variation, hadronic recoil, and MC stat) and understood.
- Adding remaining systematics (PDF[1] and lepton)
- Large constraint on MJ systematics from very conservative estimation[2].

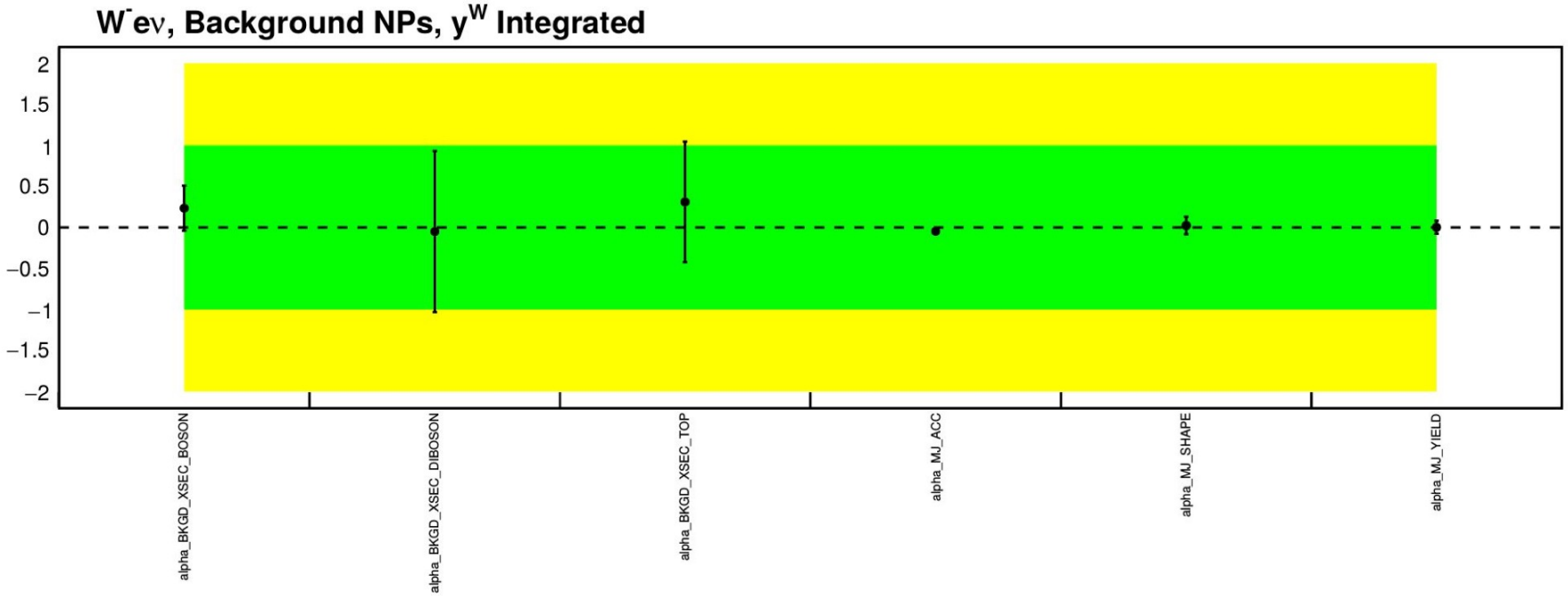

Systematics

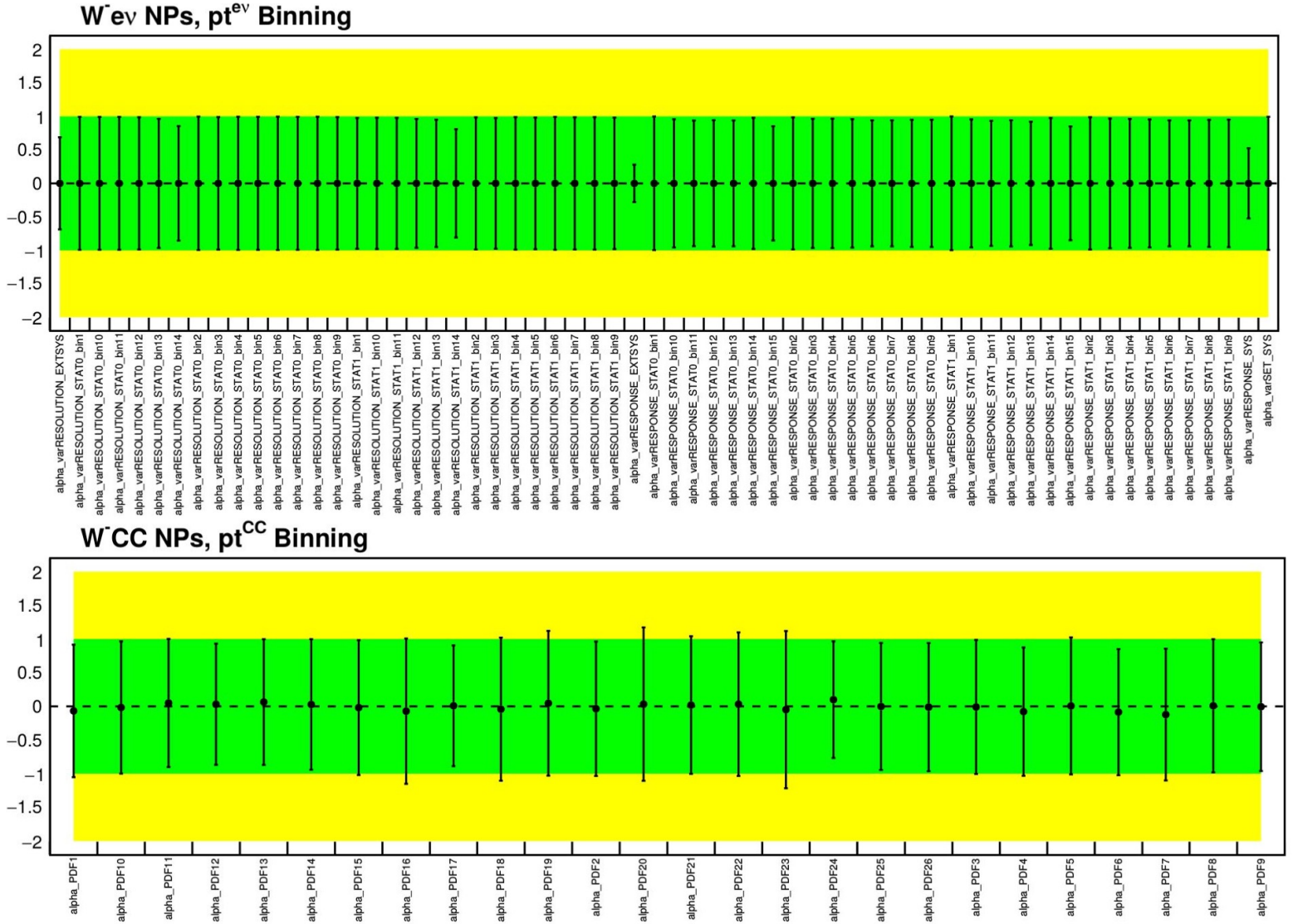

Pseudo data ($p_T^{l,\nu}$)

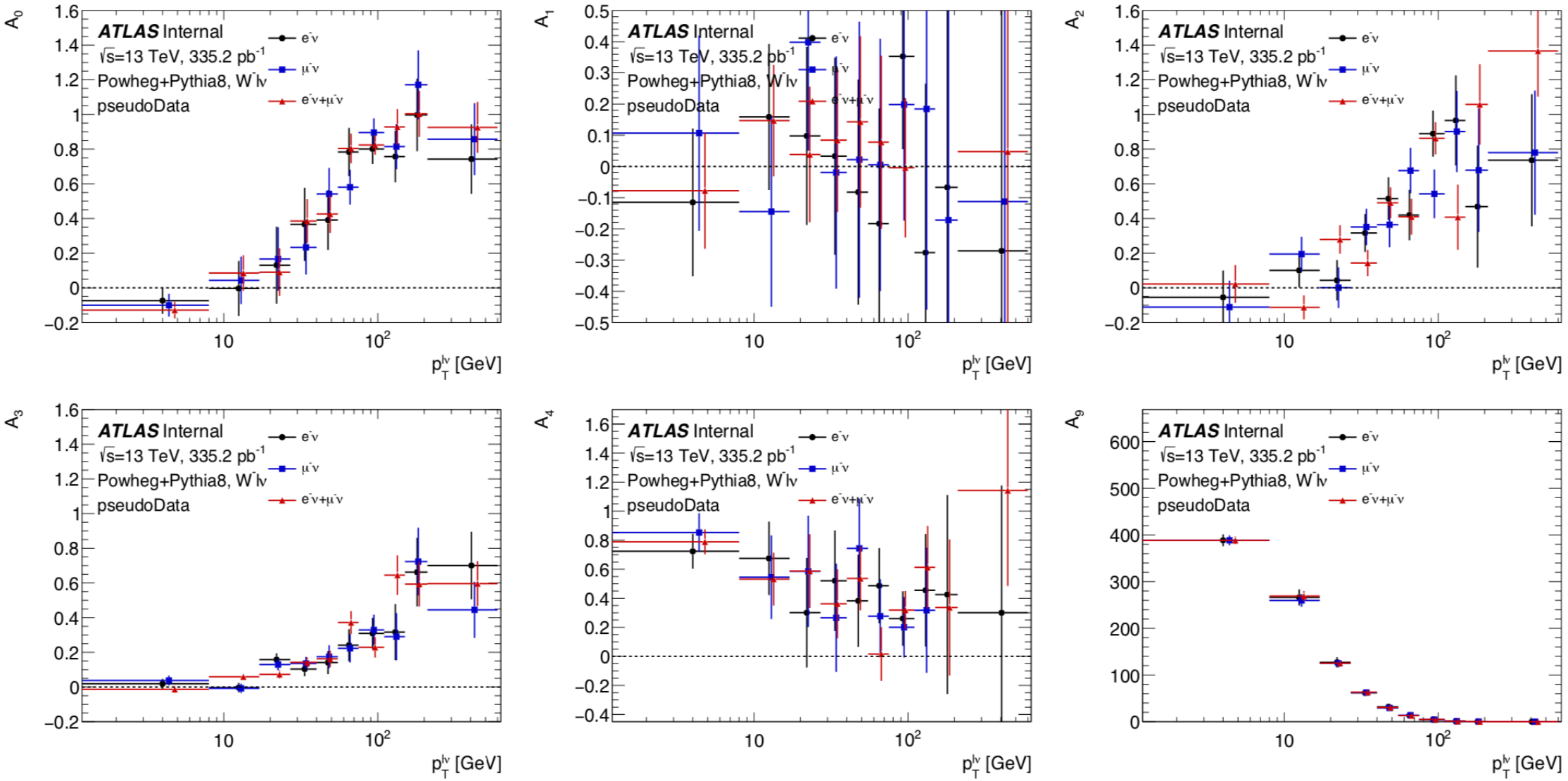

Systematic uncertainties ($p_T^{l,\nu}$)

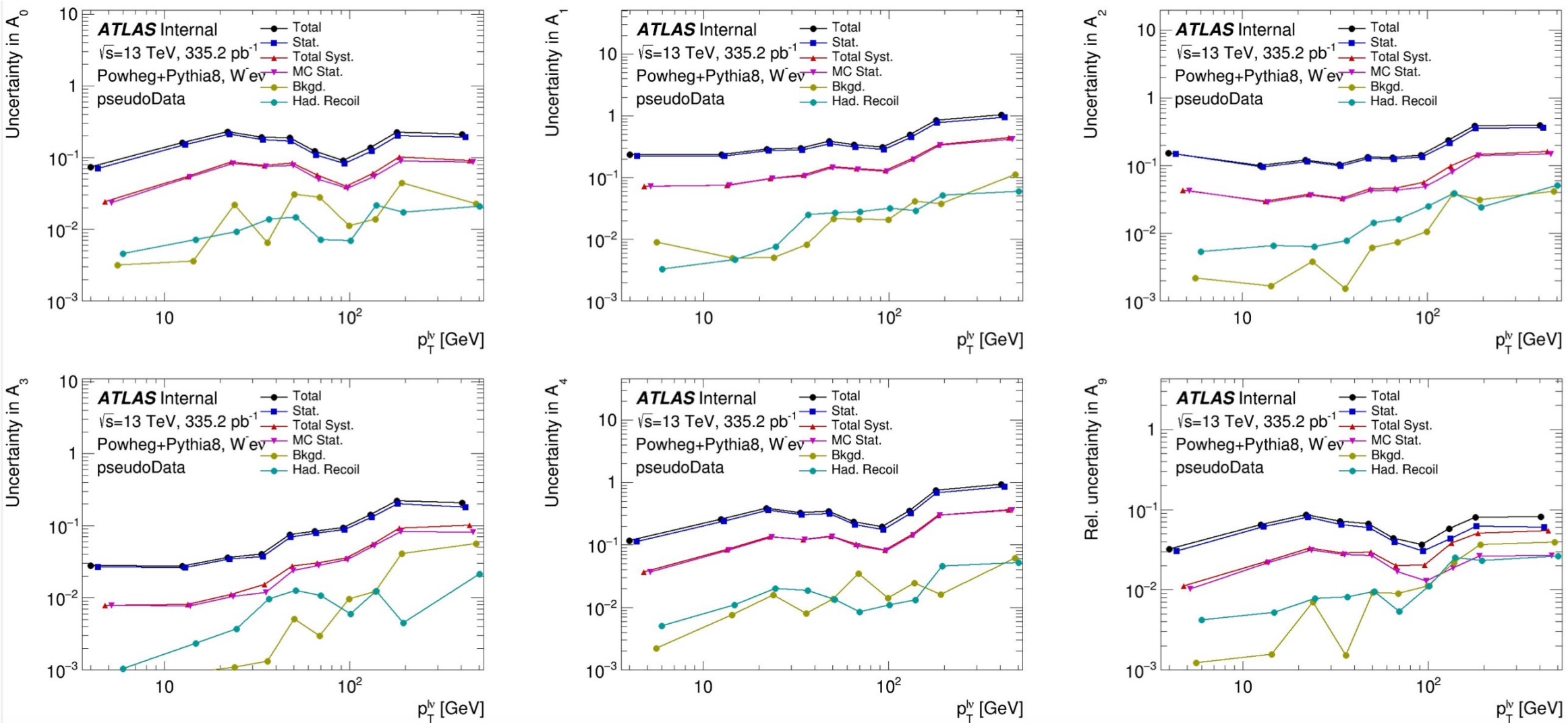

- Expect uncertainty to be stat dominated for all bins for both p^W and y^W differential measurements

Pseudo data ($y^{l,\nu}$)

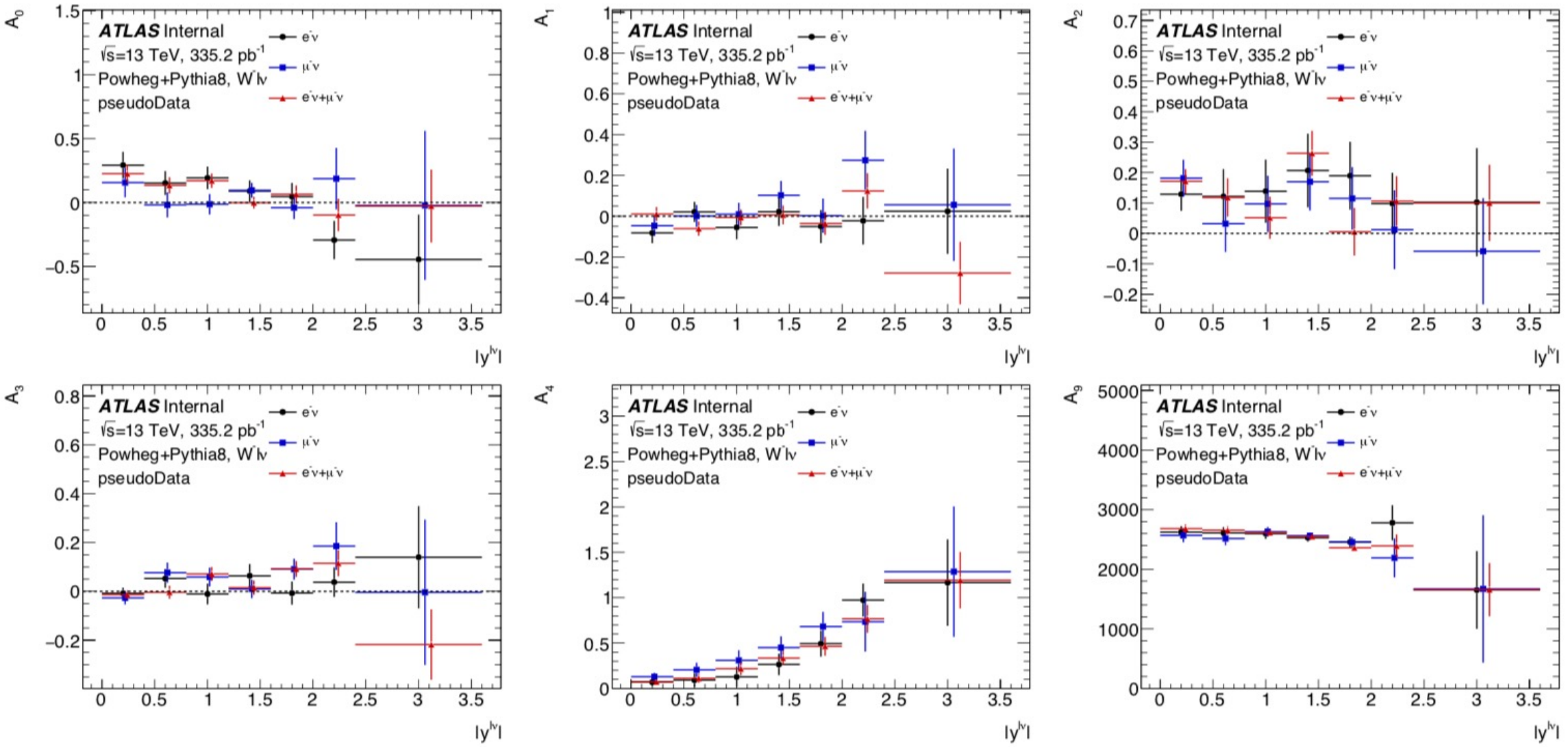

Systematic uncertainties ($y^{l,\nu}$)

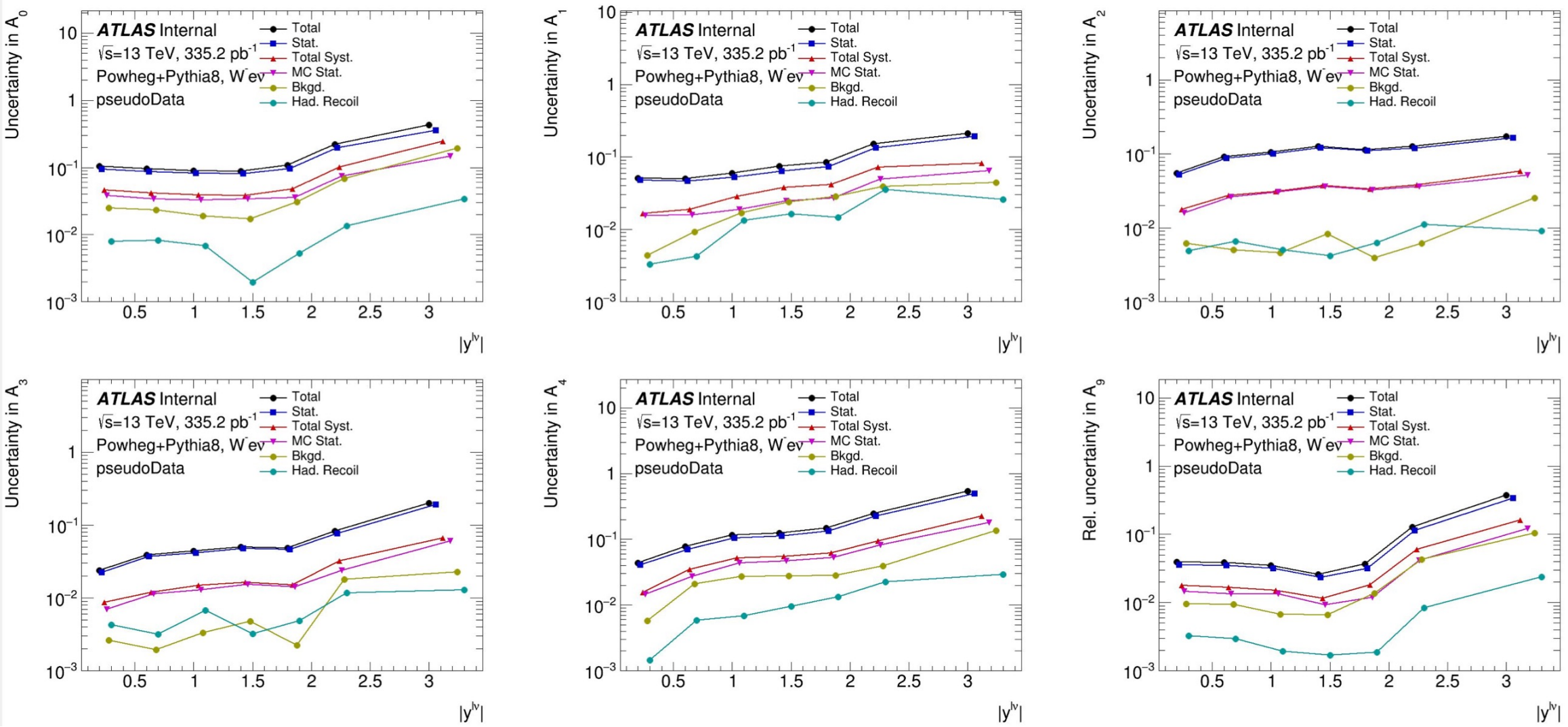

- Expect uncertainty to be stat dominated for all bins for both p^W and y^W differential measurements

Current status

- Goal of the measurement
  - measure A_i in W events
  - important input to W mass measurement and PDF fits
  - main targets: A_4 (forward-backward asymm.), $A_0 - A_2$ (Lam-Tung), charge asymmetry
- Measurement status:
  - Use W events in low-μ data (less statistics, but better hadronic recoil resolution)
  - Solve for neutrino p_z via W mass constraint
  - Study of sensitivity of this analysis to A_4
  - MJ background estimate is in place. Other backgrounds added and understood.
  - Inclusion of hadronic recoil systematics and background systematics.
  - Electron and muon channel combined fit also working.
- ToDo:
  - Refine MJ systematics correlation uncertainty model (MJ NPs heavily constrained, still being understood)
  - Fit doesn’t work with real data
  - Add remaining systematics
  - Prepare for EB request

MJ estimation updates

MJ background in WAi analysis (1): inclusive SR

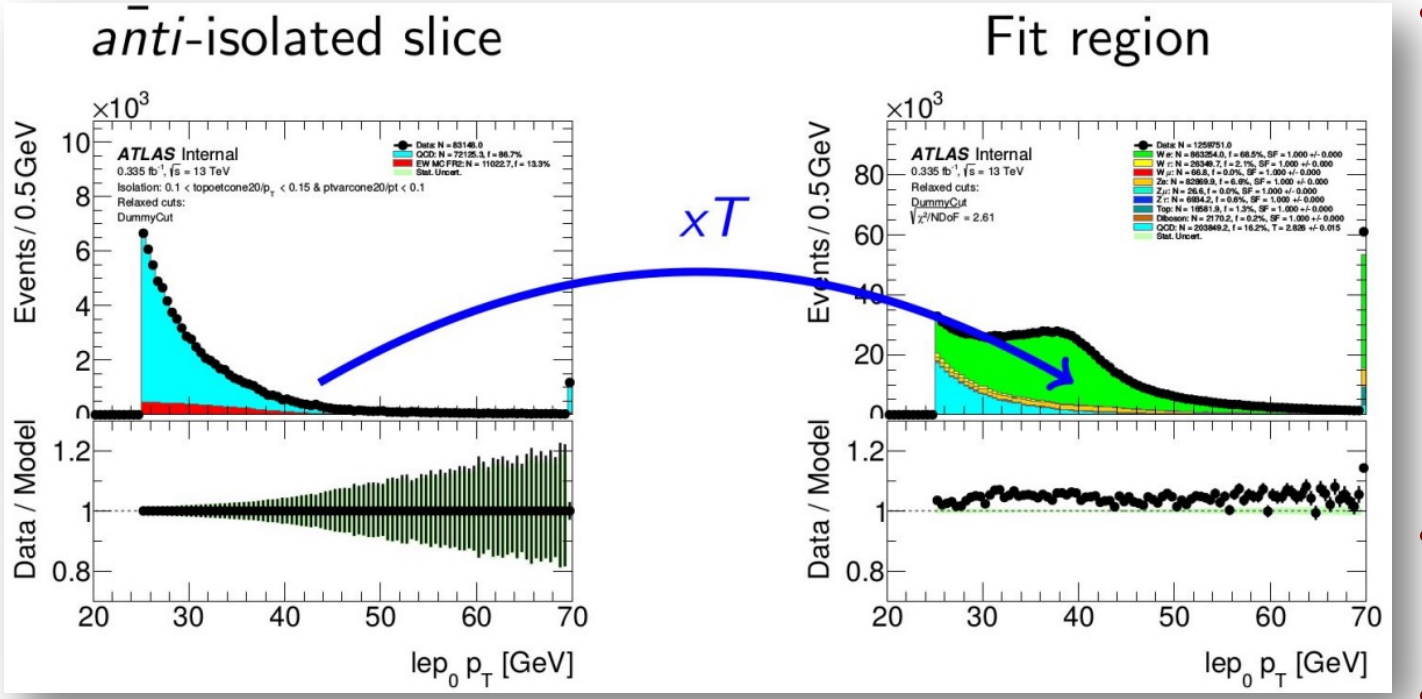

- Calorimetric isolation used for e± and track isolation used for μ± channels:
  - Slicing ptvarcone20/pt for W→μν: 8 slicing bins from 0.1 to 0.5
  - Slicing in topoetcone20/pt for W→eν: 8 slicing bins from 0.05 to 0.45

- MJ bkgd estimate has 2 “steps”:
  - Calculate MJ normalization
    - Repeat MJ estimation for different anti-isolation slices
    - Fit linear function
    - Extrapolate back to SR
  - Calculate MJ template shape:
    - MJ distributions in anti-iso slices don’t match SR shape
    - Apply bin-by-bin linear shape extrapolation
    - Assign 100% uncertainty
- Use 4 discriminative variables:
  - p_T^l, m_T, E_T^{miss}, $|\Delta\varphi(l, E_T^{miss})|$
- In the fit use fixed EWT background normalization.
- To get MJ shape as a function of |Y| and $p_T^{l,\nu}$ following samples used:
  - $b\bar{b} + c\bar{c}$ for W→μν channels
  - JF17 for W→eν channels

MJ background in WAi analysis (2): inclusive SR

MJ normalization

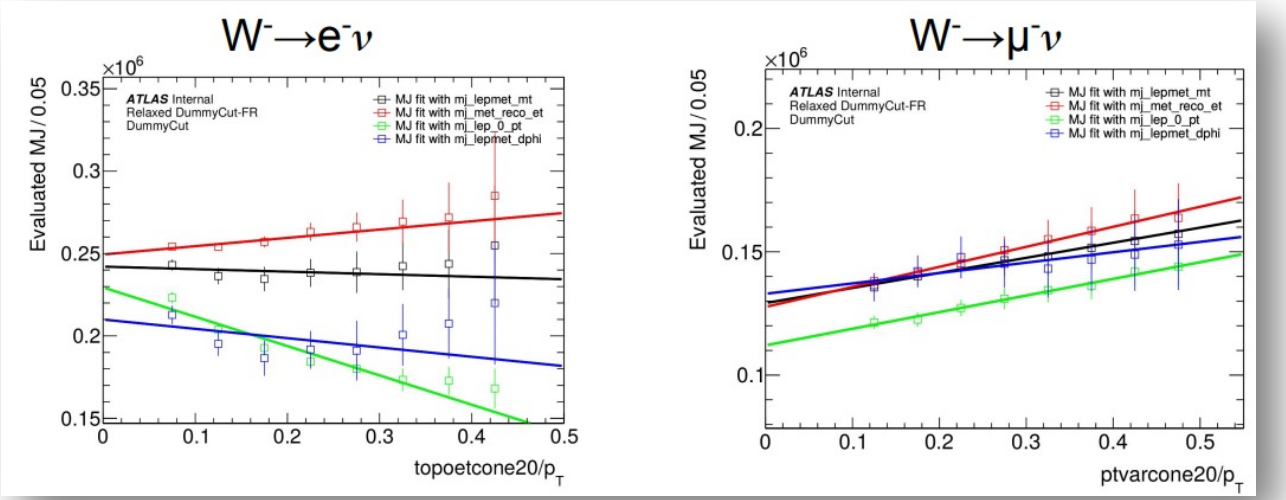

- The error bars are multiplied by $\sqrt{\chi^2/NDoF}$
- Take final MJ yield as mean at $ptvarcone20/pt$=0.025
- Less MJ background contribution for muon channel (as expected).
- Dominant MJ yield uncertainty comes from intersection point.

MJ template shape

In assumption, extrapolation is linear:

$$H_{MJ}^{[0.A,0.B]}[X] = H_{Data}^{[0.A,0.B]}[X] - H_{MC}^{[0.A,0.B]}[X]$$

$$\Delta H[X] = \frac{1}{4}\{\frac{H_{MJ}^{0.1,0.15} - H_{MJ}^{0.3,0.35}}{4} + \frac{H_{MJ}^{0.15,0.2} - H_{MJ}^{0.35,0.4}}{4} + \frac{H_{MJ}^{0.2,0.25} - H_{MJ}^{0.4,0.45}}{4} + \frac{H_{MJ}^{0.25,0.3} - H_{MJ}^{0.45,0.5}}{4}\}$$

$$H_{MJ}^{sig}[X] = H_{MJ}^{0.1,0.15}[X] + 2 \cdot \Delta H[X]$$

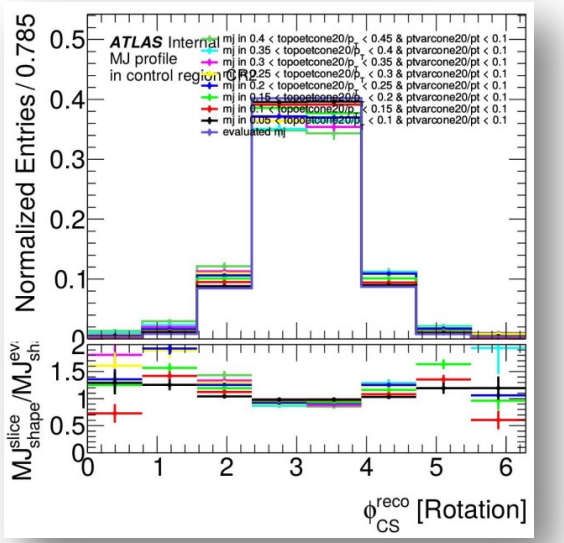

- Calculate shape correction using isolation slices for final MJ templates.
- Given the large statistical uncertainty and the linear approximation used, the shift ΔH[X] applied is assigned a 100% relative uncertainty.
  - Small wrt intersection point.

MJ Systematics Summary (inclusive signal region)

Channel	Using $topoetcone20/p_T$ $W \to e^-\nu$	Using $topoetcone20/p_T$ $W \to e^+\nu$	Using $ptvarcone20/p_T$ $W \to \mu^-\nu$	Using $ptvarcone20/p_T$ $W \to \mu^+\nu$
Total Number of MJ bkg	**231472**	**232268**	**127056**	**132995**
Luminosity and cross section	±7199 (3.11%)	±9098 (3.92%)	±547 (0.43%)	±698 (0.52%)
Intersection point	±22928 (9.91%)	±24910 (10.72%)	±13313 (10.48%)	±12276 (9.23%)
Extrapolation target	±1246 (0.54%)	±1172 (0.50%)	±1575 (1.24%)	±1433 (1.08%)
Choice of hists	±7643 (3.30%)	±8303 (3.57%)	±4438 (3.49%)	±4092 (3.08%)
Isolation correction	N/A	N/A	N/A	N/A
Correlated Uncertainty	±24032 (10.38%)	±26519 (11.42%)	±13324 (10.49%)	±12296 (9.25%)
Data Stat.	±490 (0.21%)	±463 (0.20%)	±795 (0.63%)	±809 (0.61%)
MC Stat.	±262 (0.11%)	±229 (0.10%)	±990 (0.78%)	±880 (0.66%)
Shape Correction	±2961 (1.28%)	±2769 (1.19%)	±927 (0.73%)	±915 (0.69%)
Uncorrelated Uncertainty	±3012 (1.30%)	±2816 (1.21%)	±1572 (1.24%)	±1505 (1.13%)

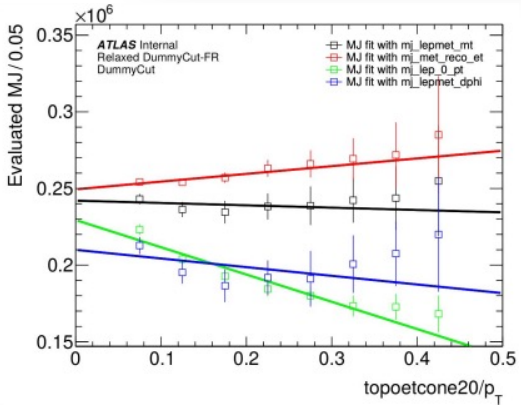

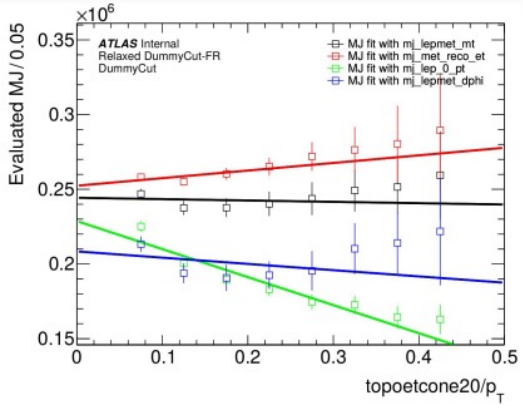

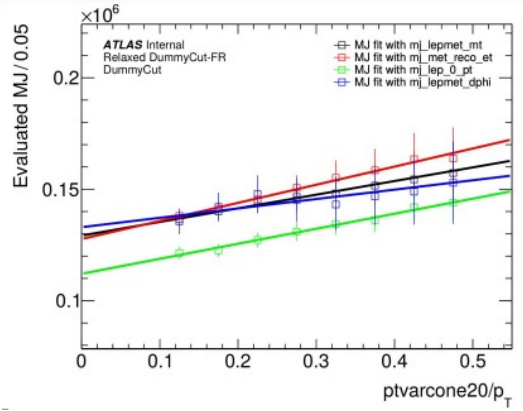

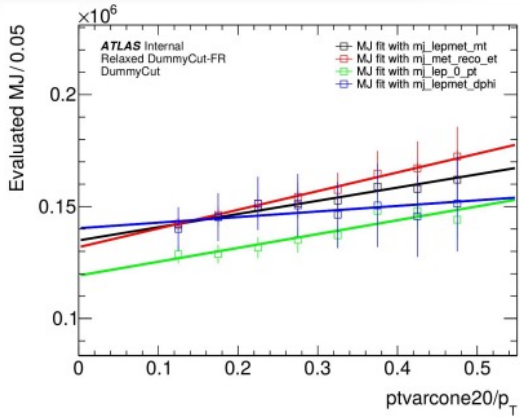

MJ templates for $\cos\theta_{CS}$ vs. φ_{CS} : inclusive SR

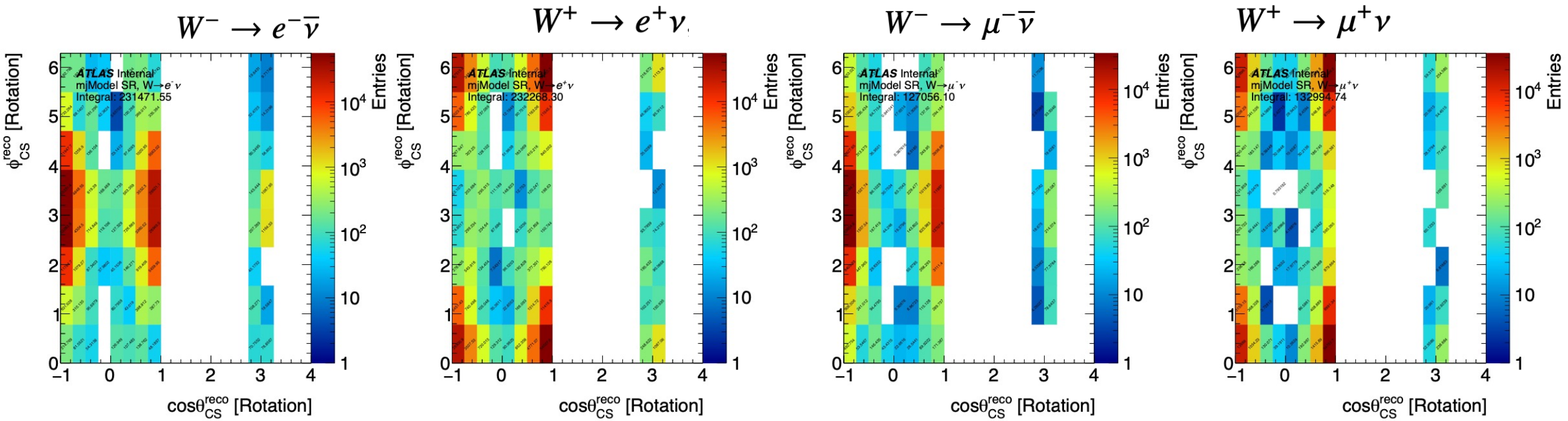

- The 2D templates are derived in the same way as described for 1D histograms

MJ shape as function of |Y| and $p_T^{l,\nu}$: task definition

1D control plots in SR (only stat unc. + MJ systematics are shown.):

$W^- \to e^- \nu$

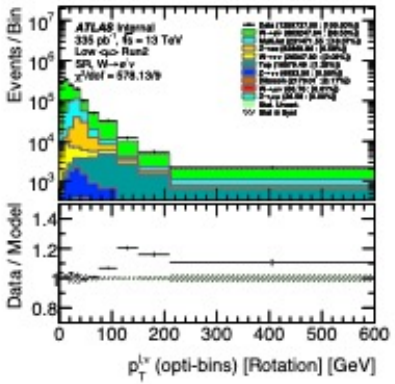
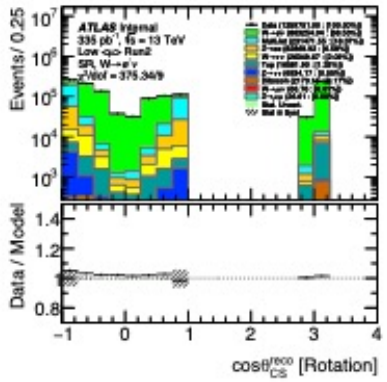
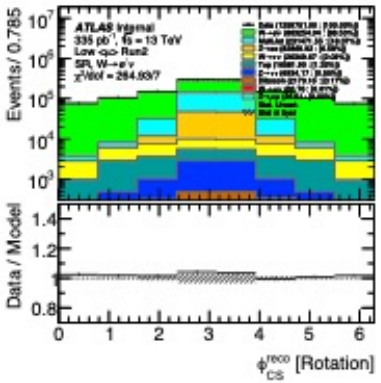

$W^- \to \mu^- \nu$

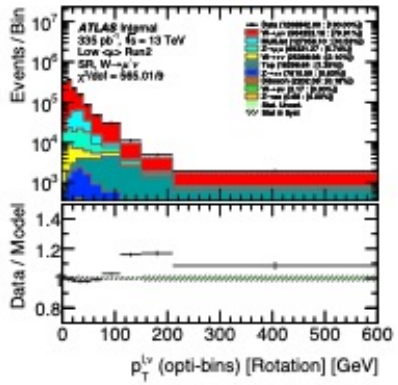
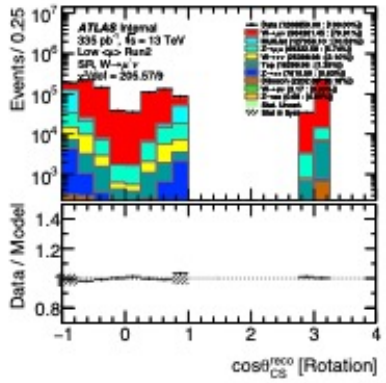
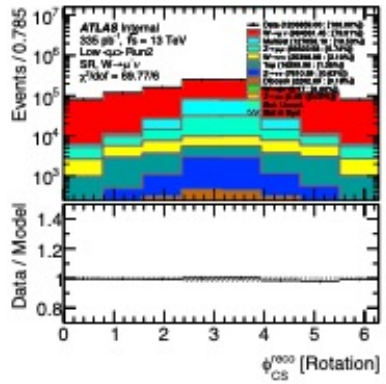

W-Ai analysis uses more complicated approach:

- Building 2D histograms $\cos\theta_{CS}$ vs. ϕ_{CS} as function of η or $p_T^{\ell,\nu}$

$$p_T^{\ell,\nu} : [0, 8, 17, 27, 40, 55, 75, 110, 150, 210, 600];$$
$$|Y| : [0, 0.4, 0.8, 1.2, 1.6, 2.0, 2.4, 3.6]$$

- Above 100 GeV the data/MC agreement in the $p_T^{\ell,\nu}$ degradate due to missing truth p_T^W reweighting correction above this range.

Closure test by DD method: coarse bins

$p_T^{\ell,\nu}$: [0, 17, 55, 600];
$|Y|$: [0, 0.8, 2.0, 3.6]

$W^- \to e^- \bar{\nu}$

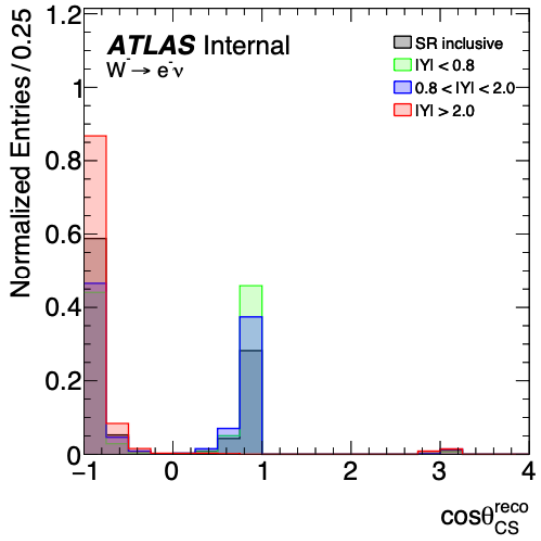

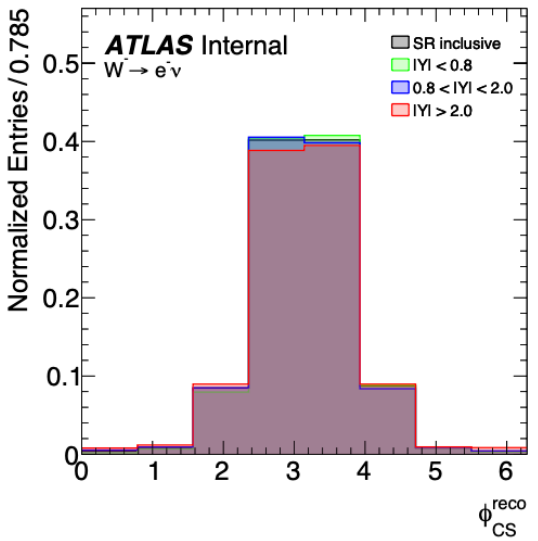

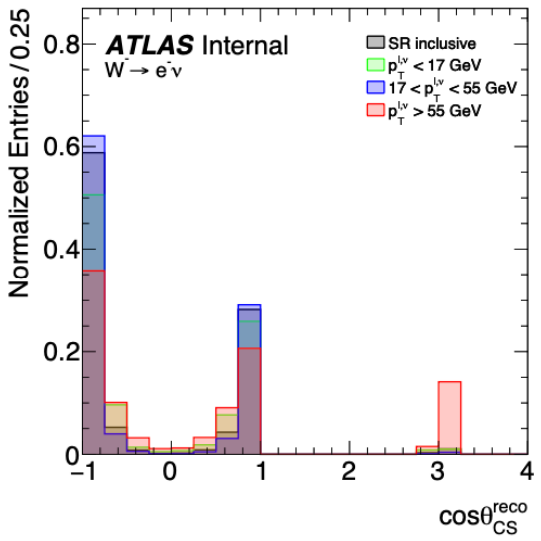

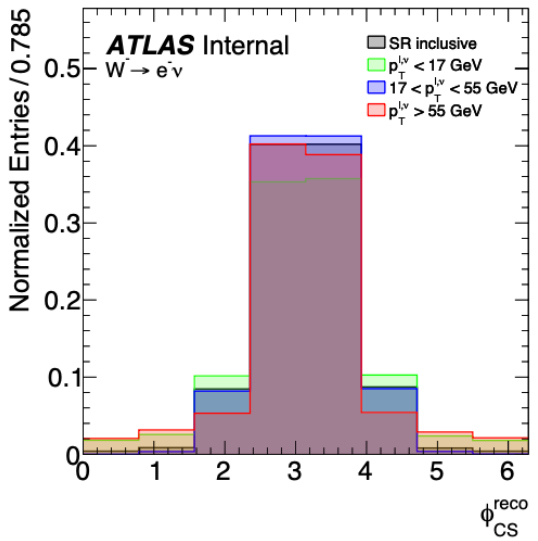

$W^- \to \mu^- \bar{\nu}$

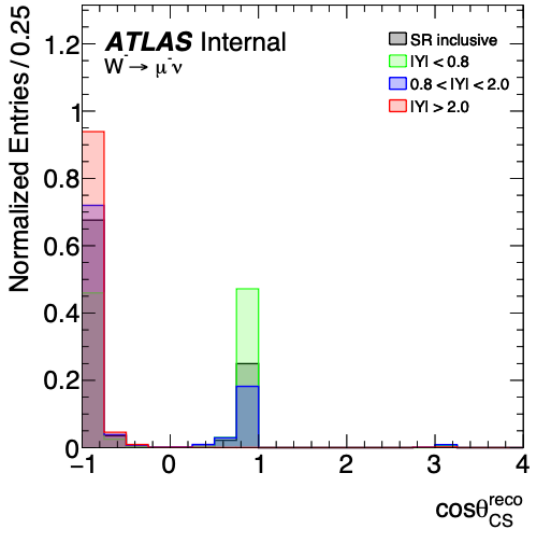

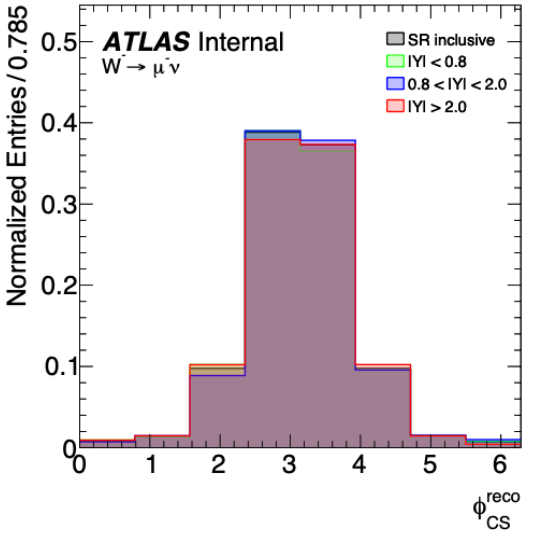

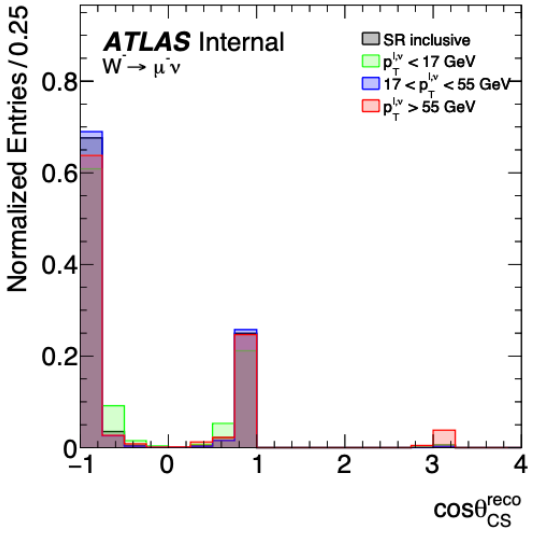

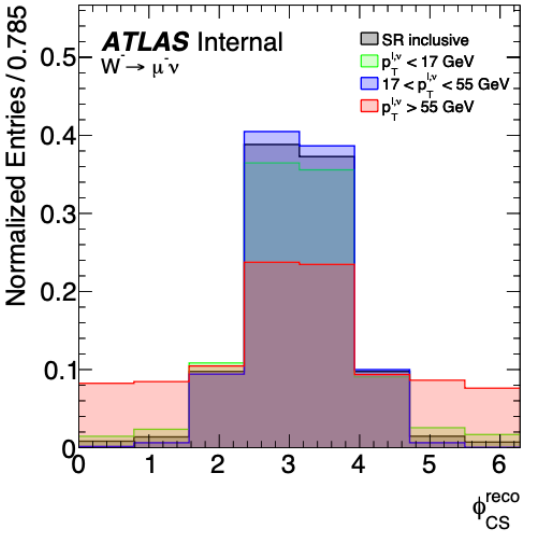

MJ shape as function of |Y| and $p_T^{l,\nu}$: studies

$p_T^{\ell,\nu}$: $[0, 17, 55, 600]$;
$|Y|$: $[0, 0.8, 2.0, 3.6]$

- There are strong dependence of the $\cos\theta_{CS}$ MJ template shape as function of $|Y^{l,\nu}|$ and φ_{CS} as a function of $p_T^{l,\nu}$
- Acceptance correction functions were built to correct MJ data-driven template derived in the SR to the given $|Y^{l,\nu}|$ or $p_T^{l,\nu}$ slice using the samples:
  - $b\bar{b} + c\bar{c}$ for W→μν channels
  - JF17 for W→eν channels

$$A_j = h_{MC}^{bin_j} / h_{MC}^{SR} \qquad h_{MJ}^{bin_j} = h_{MJ,data}^{SR} \times A_j$$

- Acceptance correction functions for number of $|Y^{l,\nu}|$ bins, fully uncorrelated uncertainty on these acceptance correction functions is applied on the MJ estimate:

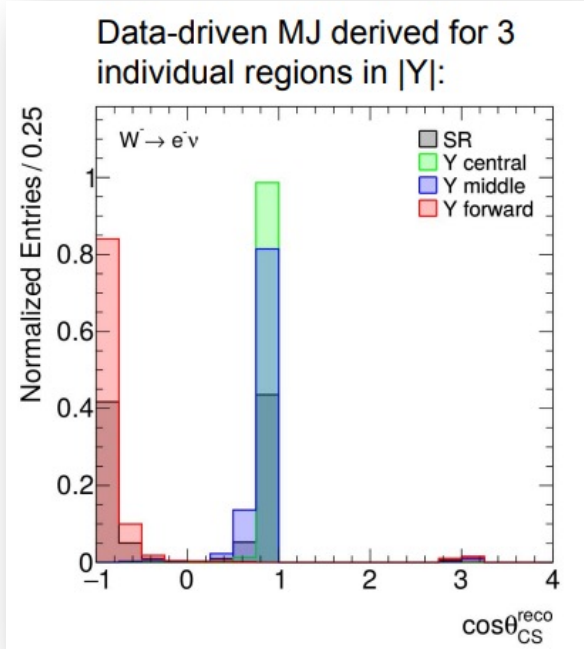

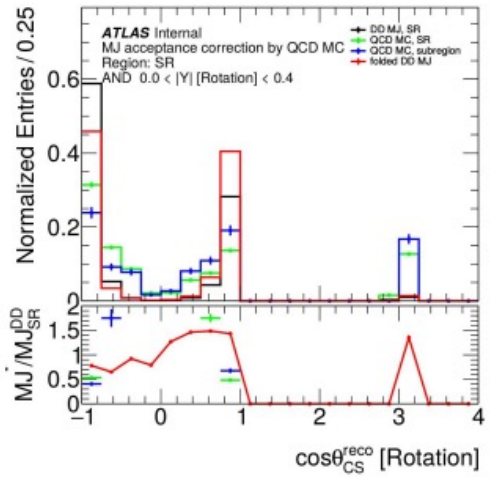

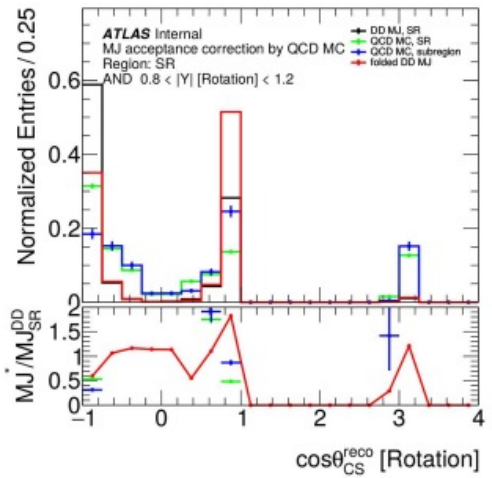

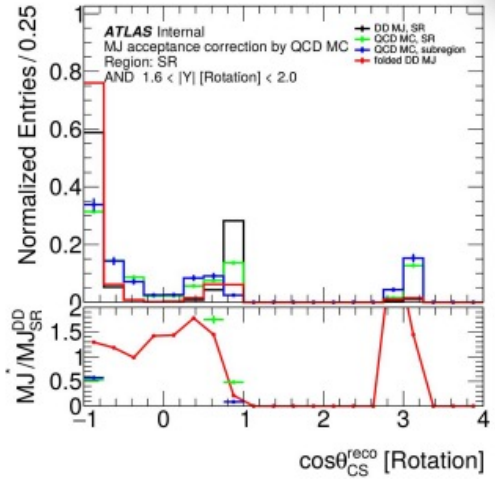

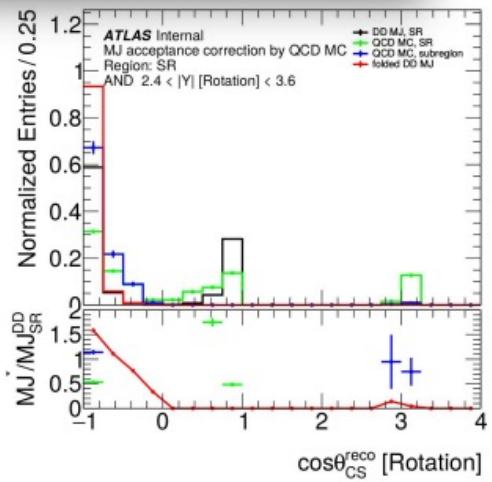

Acc. corr. function: closure test

$p_T^{\ell,\nu}: [0, 17, 55, 600];$
$|Y|: [0, 0.8, 2.0, 3.6]$

$W^- \to e^-\bar{\nu}$

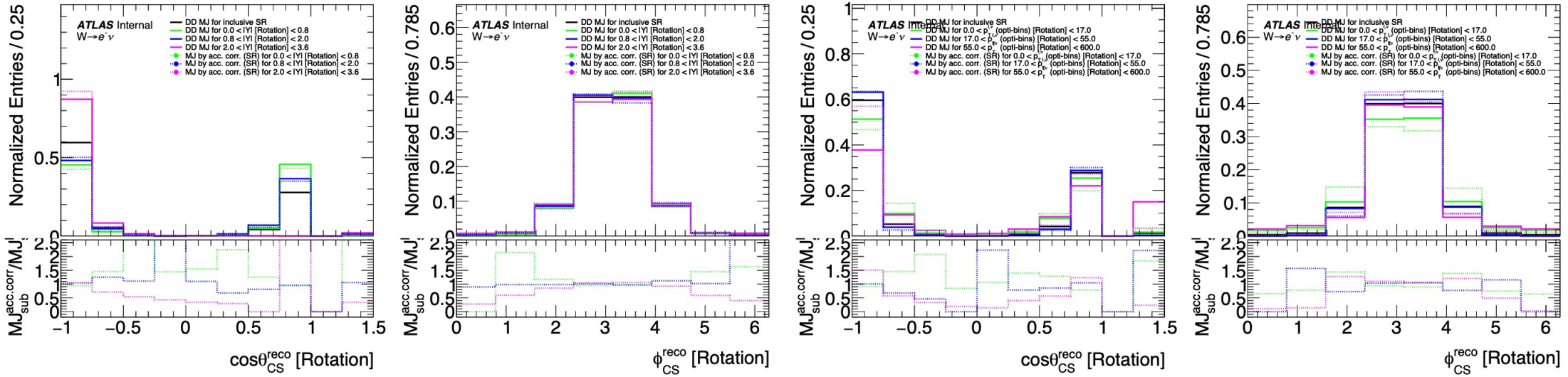

$W^- \to \mu^-\bar{\nu}$

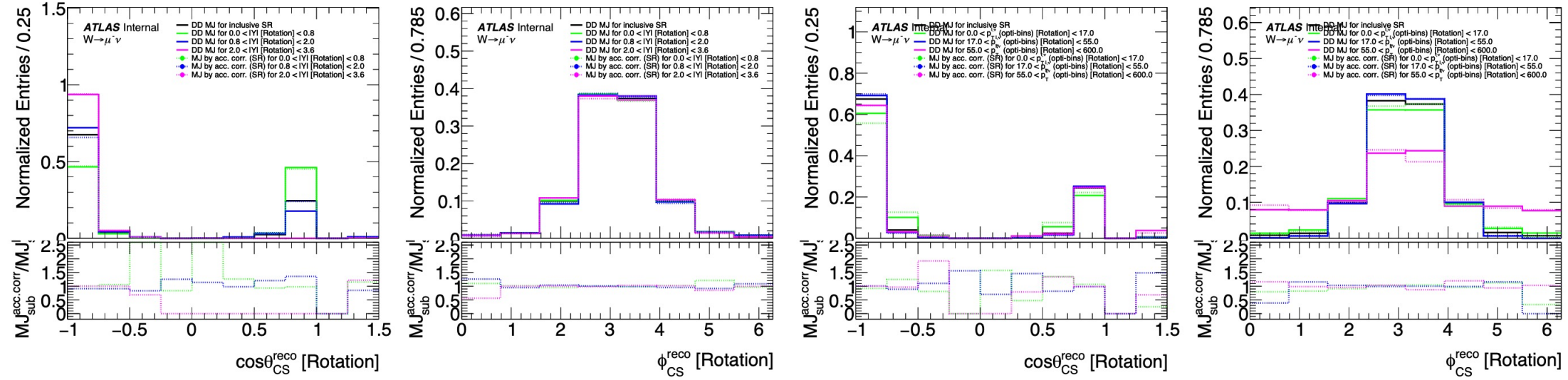

MJ shape as function of $|Y|$ and $p_T^{\ell,\nu}$

- There are strong dependence of the $\cos\theta_{CS}$ MJ template shape as function $|Y|$ and ϕ_{CS} as function of $p_T^{\ell,\nu}$
- Acceptance correction functions were build using QCD MC samples to correct MJ data-driven template derived in the SR to the given $|Y|$ or $p_T^{\ell,\nu}$ slice:

$$h_{MJ}^{bin_i} = h_{MJ}^{SR} \cdot h_{QCDMC}^{bin_i} / h_{QCDMC}^{SR}$$

Closure test for Data-driven MJ and Acc.Corr MJ derived for 3 individual regions in $p_T^{\ell,\nu}$:

$W^- \to e^- \nu$ $\quad$ $W^- \to \mu^- \nu$

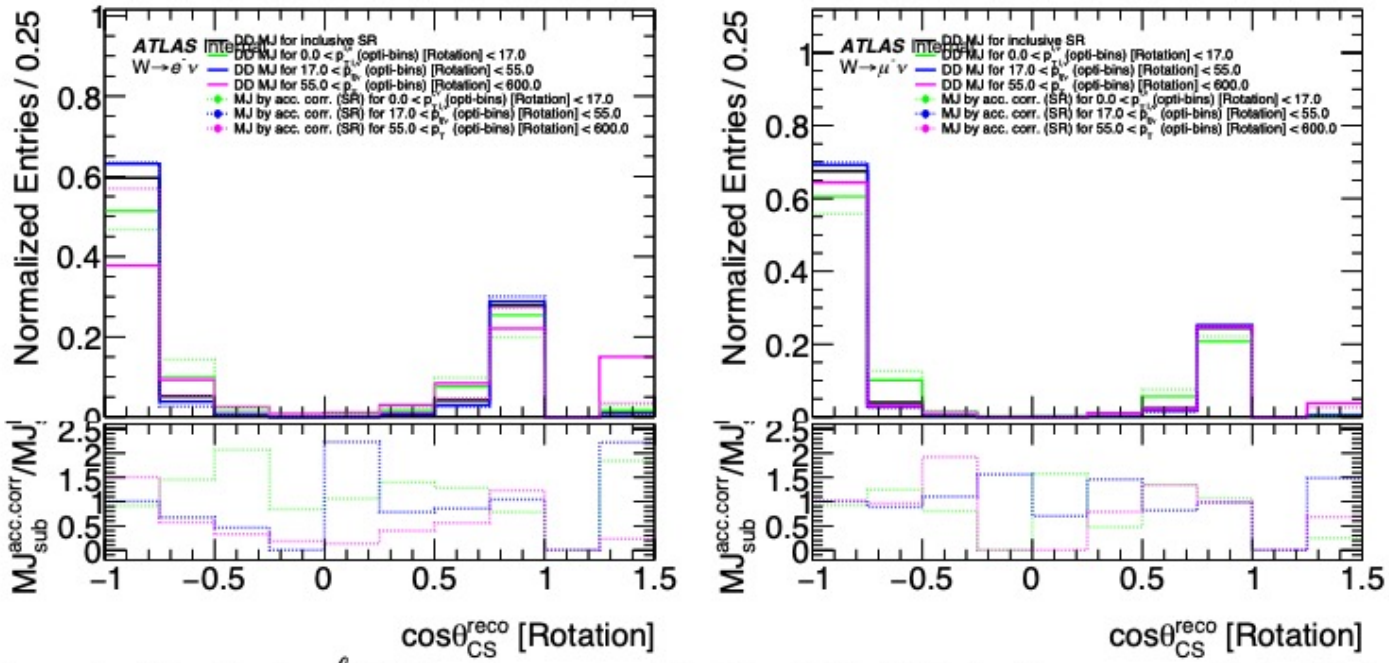

Problem:

- Comparing to MJ template given by AccCocc in the last $p_T^{\ell,\nu}$ bin for e^- with the DD MJ, last one predicts higher MJ contribution to the no solution bin + overall shape differs a lot.
- **DD MJ template derived from SR might be "too far" from DD MJ template derived for $p_T^{\ell,\nu} > 55$ GeV bin.**
- We might not see this effect in muons due to the fact this channel is "cleaner".
- Integrated distributions for Y coarse bins looks good due to small MJ fraction for the last coarse $p_T^{\ell,\nu}$ bin.

Solution:

- Instead of using SR use the coarse bins: $h_{QCDMC}^{CoarseBin_k}$ and $h_{MJ}^{CoarseBin_k}$.

$$p_T^{\ell,\nu} : [0, 17, 55, 600];$$
$$|Y| : [0, 0.8, 2.0, 3.6]$$

Some W-Ai control plots and e/μ compatibility

Compare 2 $p_T^{\ell,\nu}$ bins: $17 < p_T^{\ell,\nu} < 27$ GeV and $150 < p_T^{\ell,\nu} < 210$ GeV

Before

$17 < p_T^{\ell,\nu} < 27$ GeV

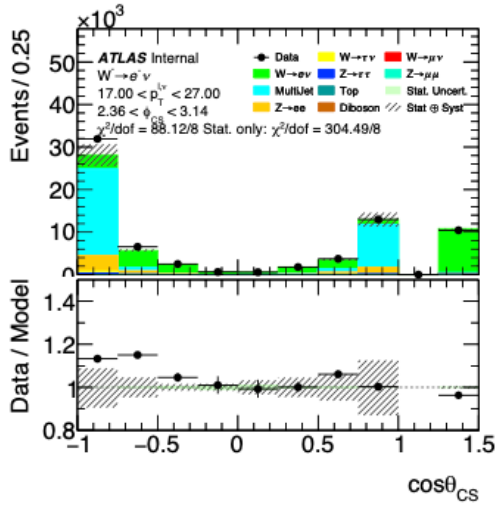

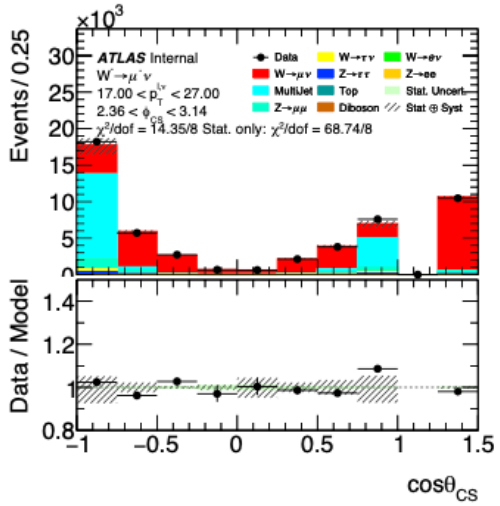

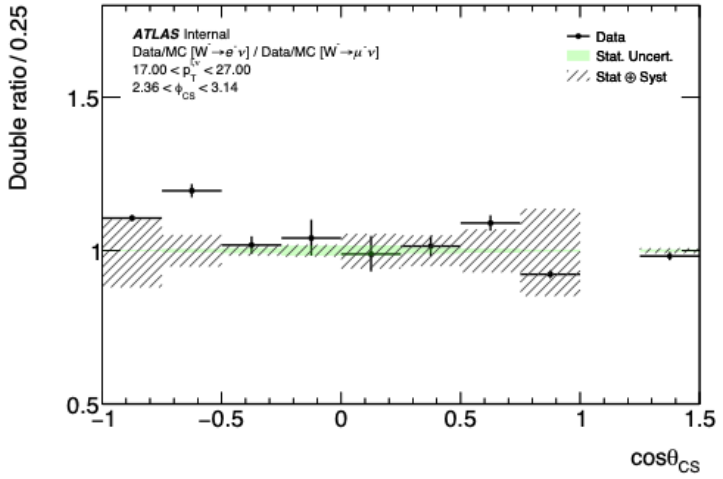

$150 < p_T^{\ell,\nu} < 210$ GeV

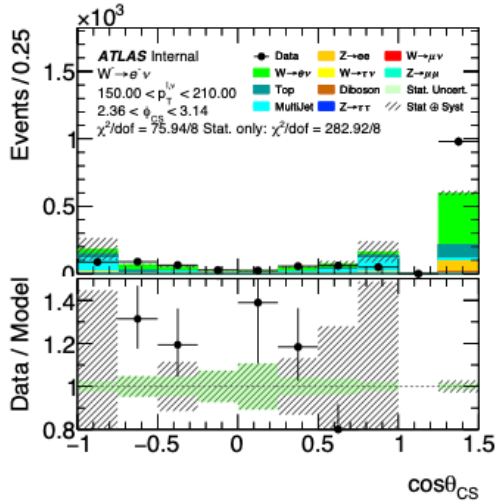

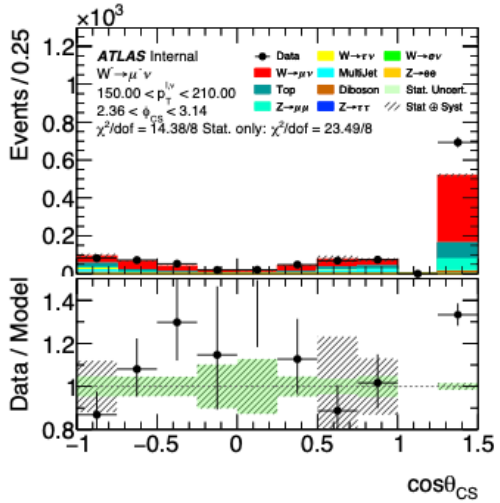

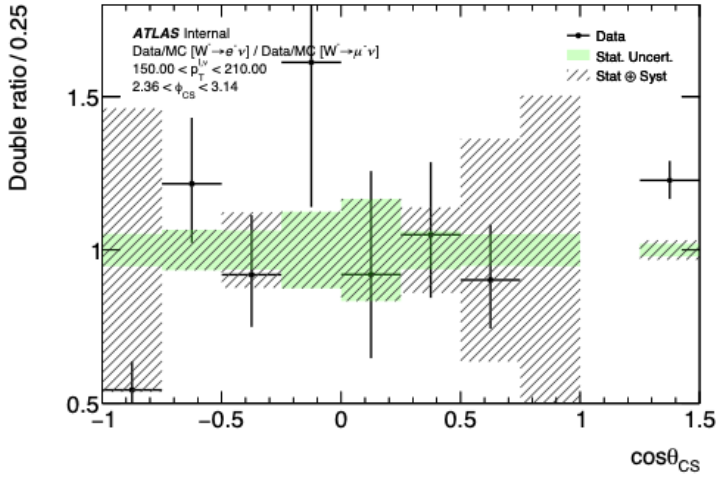

Note: discrepancy in the no solution bins in pTW>100 GeV is from absence of the PTRW

Test with 1D $\cos\theta_{CS}$ integrated over ϕ_{CS} in some $p_T^{\ell,\nu}$ bins

Instead of using SR, use the coarse bins: $h_{QCDMC}^{CoarseBin_k}$ and $h_{MJ}^{CoarseBin_k}$.

Before

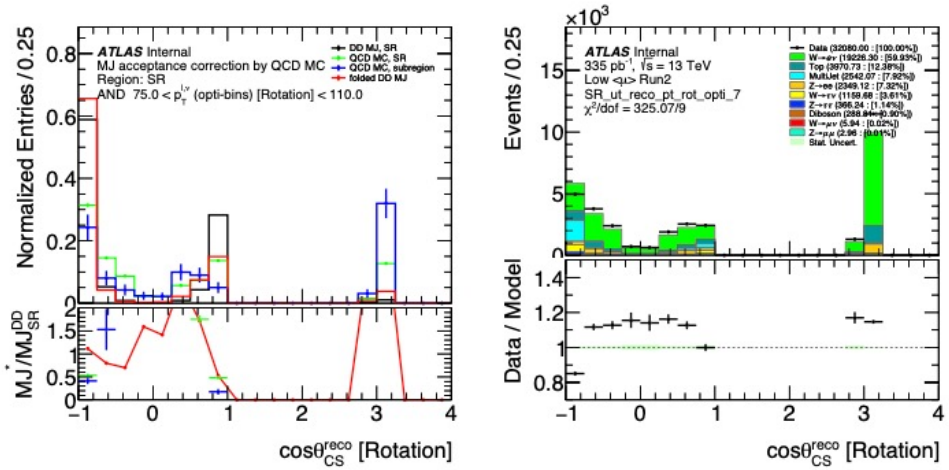

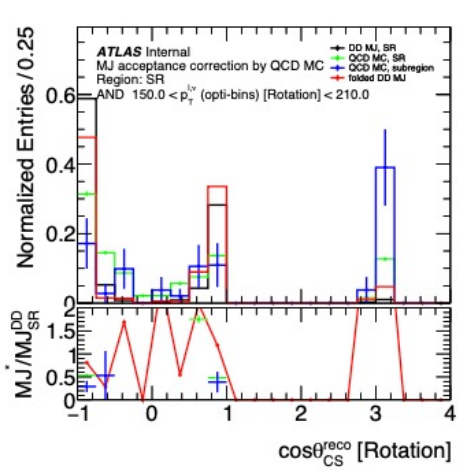

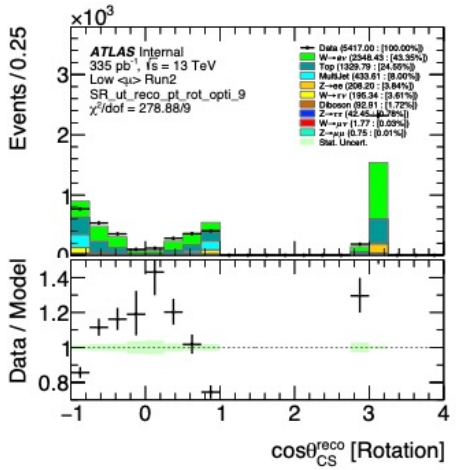

After

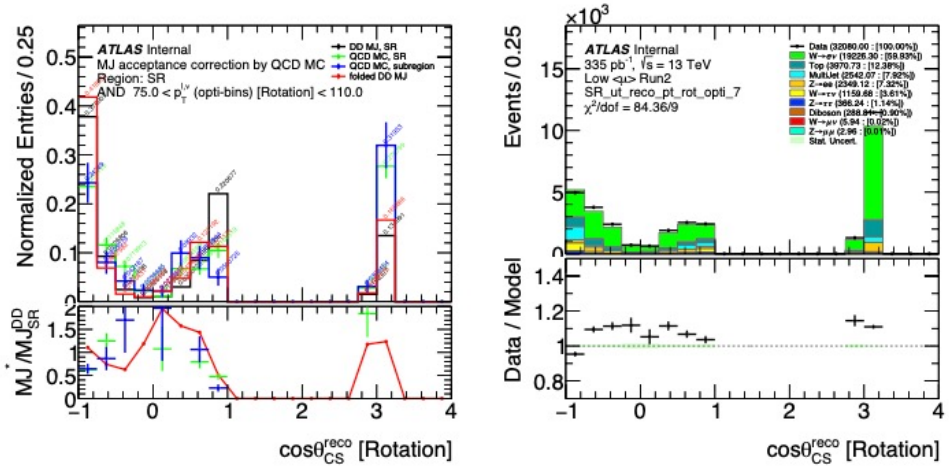

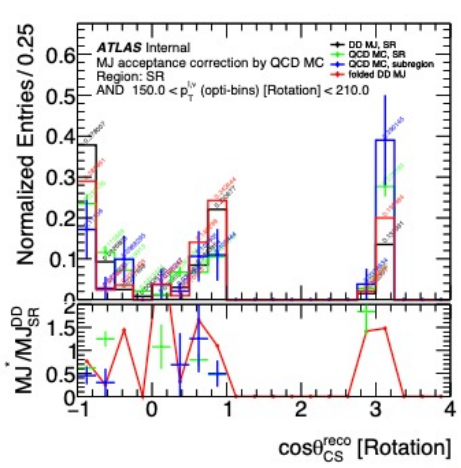

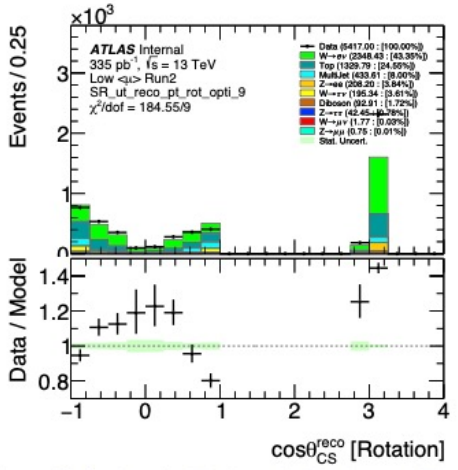

Note: discrepancy in the no solution bins in pTW>100 GeV is from absence of the PTRW

Test with 3D W-Ai control plots

Before

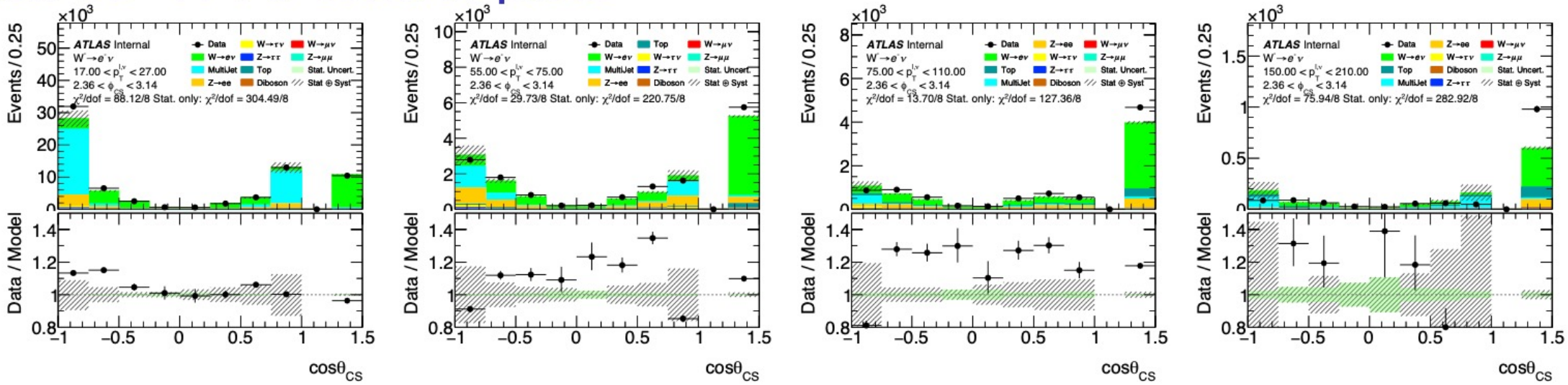

After

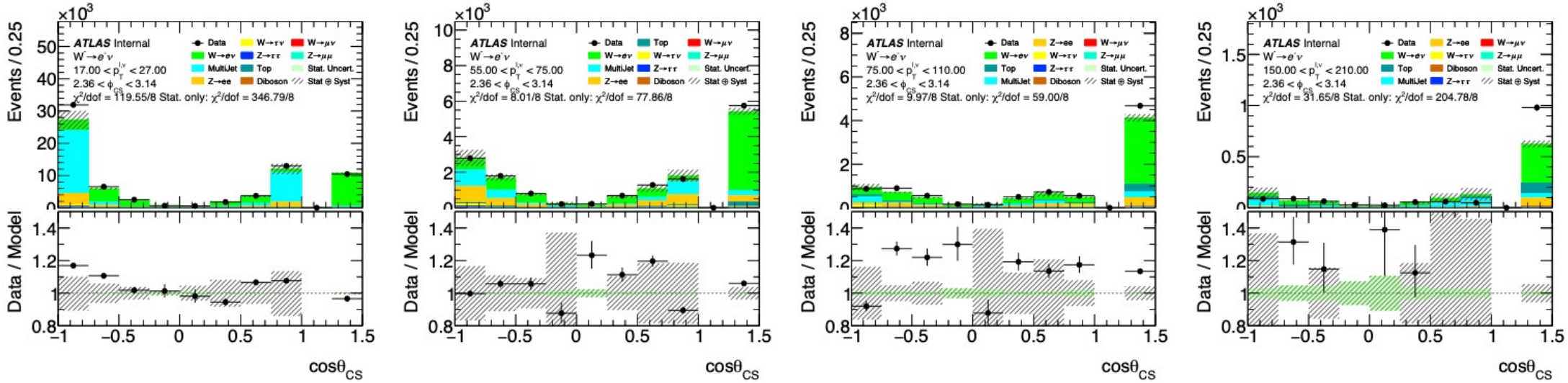

Only some $p_T^{\ell,\nu}$ coarse bins and ϕ_{CS} slices are shown.

Note: discrepancy in the no solution bins in pTW>100 GeV is from absence of the PTRW

MJ templates for W-Ai analysis in $p_T^{l,\nu}$ binnning

$W^- \rightarrow e^- \overline{\nu}$

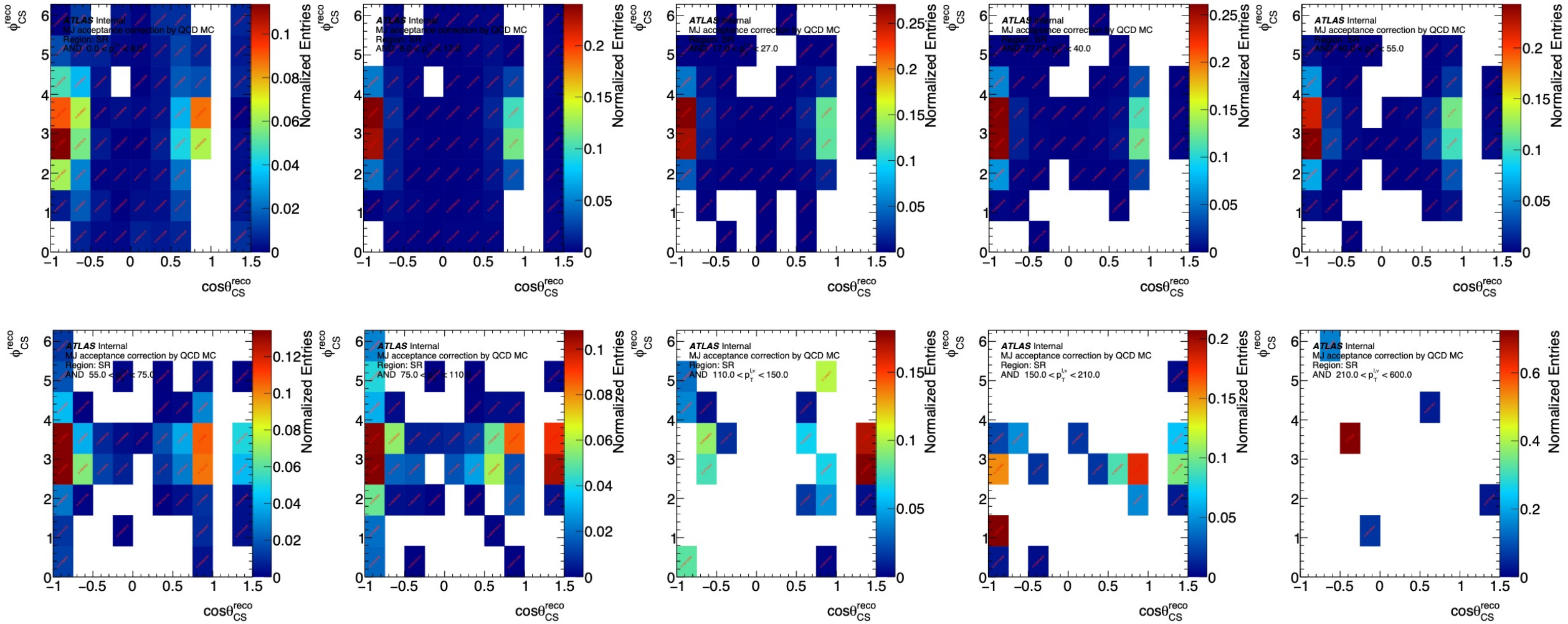

$$p_T^{\ell,\nu} : [0, 8, 17, 27, 40, 55, 75, 110, 150, 210, 600];$$

MJ templates for W-Ai analysis in $|Y|$ binnning $W^- \rightarrow e^- \bar{\nu}$

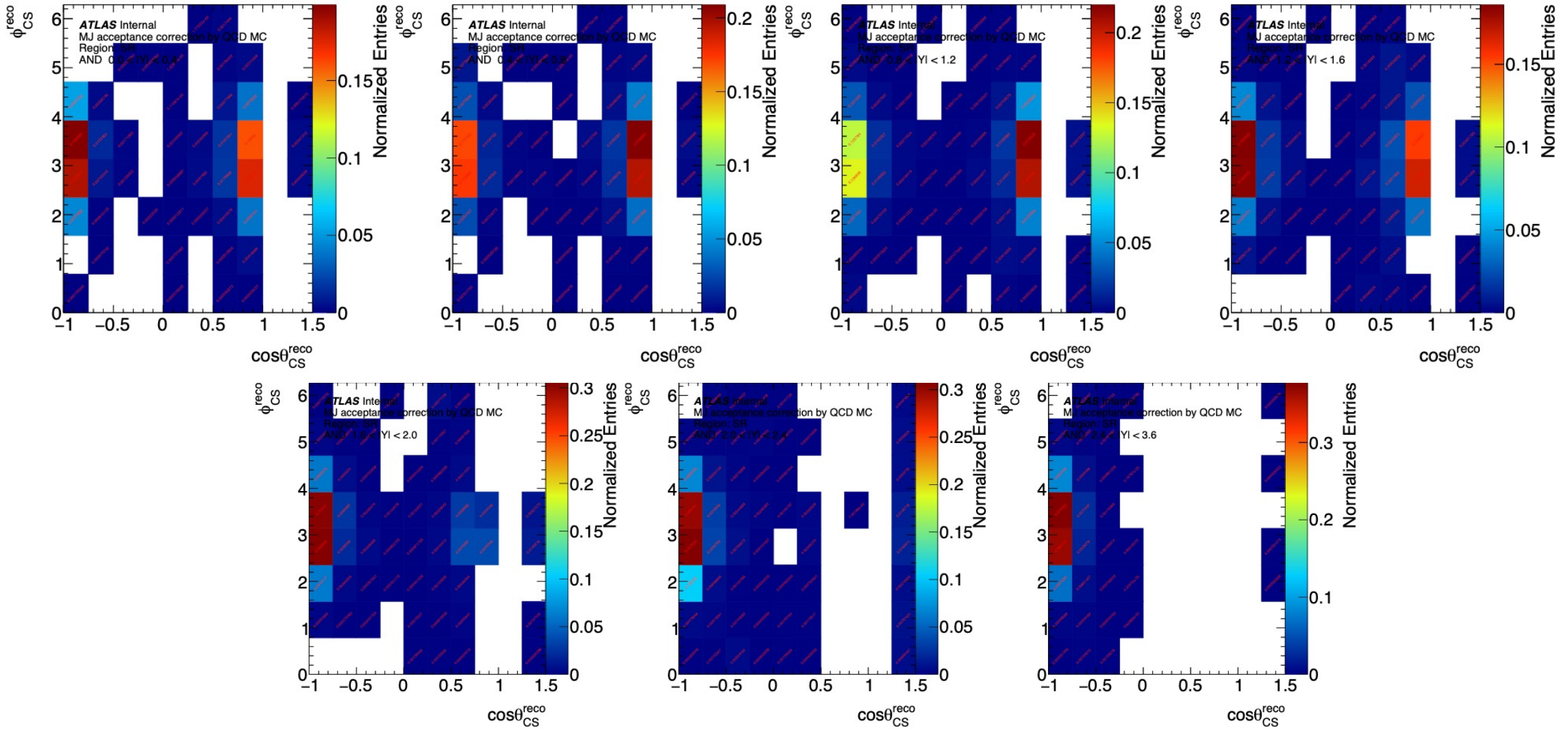

$$|Y| : [0, 0.4, 0.8, 1.2, 1.6, 2.0, 2.4, 3.6]$$

MJ templates for W-Ai analysis in $p_T^{l,\nu}$ binnning $W^- \to \mu^- \bar{\nu}$

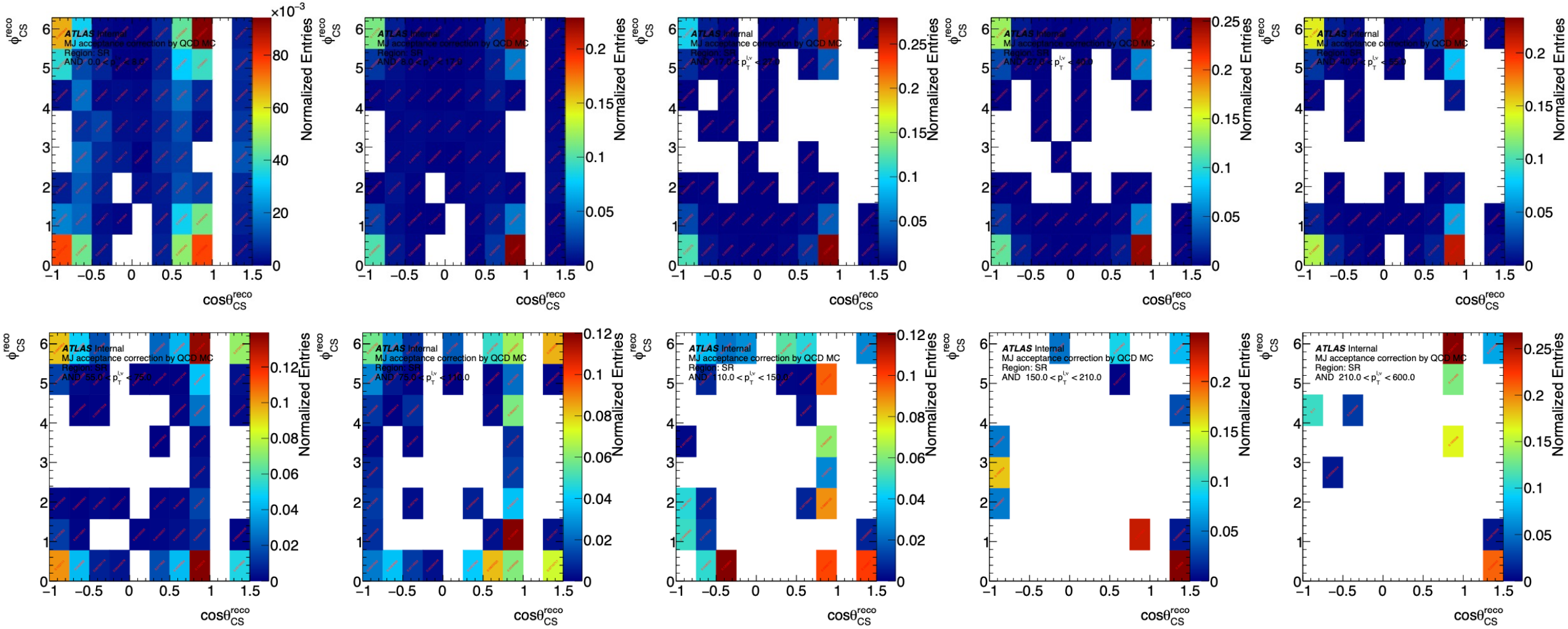

$$p_T^{\ell,\nu} : [0, 8, 17, 27, 40, 55, 75, 110, 150, 210, 600];$$

MJ templates for W-Ai analysis in $|Y|$ binnning $W^- \to \mu^- \bar{\nu}$

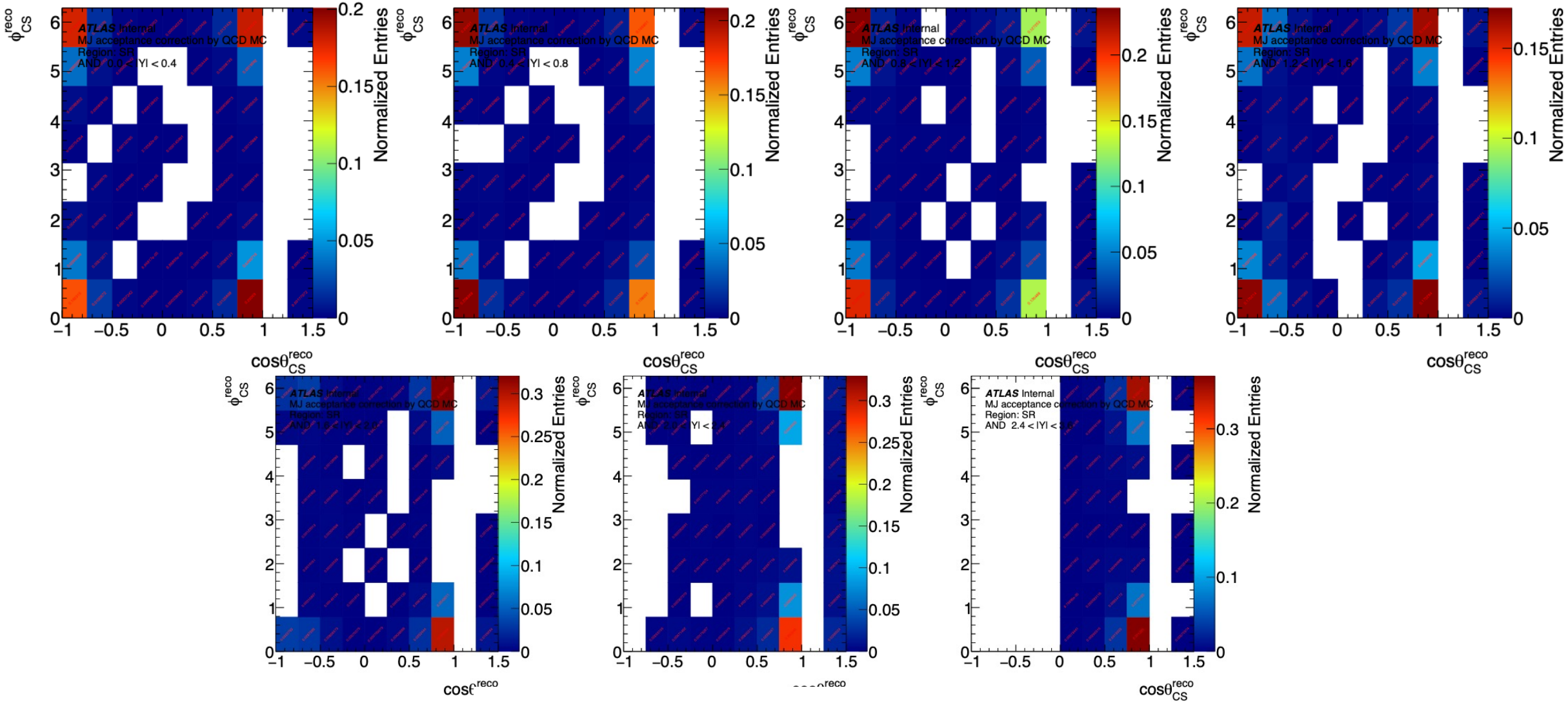

$$|Y| : [0, 0.4, 0.8, 1.2, 1.6, 2.0, 2.4, 3.6]$$

Systematic uncertainties

systematic uncertainty on new acc correction [h_bin_i_QCD_MC / h_CORSE_BIN_k_QCD_MC] should be

1. correlated sources within the bin_k the relative difference between h_CORSE_BIN_k_MJ and h_CORSE_BIN_k_QCD_MC
2. uncorrelated sources 2 possible approach:
    1. a) 100% on the acceptance correction it-slef
    2. b) stat error on the MC the acceptance correction it-slef

where

- bin i correspond to pTW and Y_W measurement bins
- bin k correspond to corse pTW and and Y_W bins so that bin_k >> bin_i

- For Electron channel :
    - mj_Yieldcorr_E
    - mj_Yielduncor_E
    - mj_acc_cor_closureE0 , mj_acc_cor_closureE1 , mj_acc_cor_closureE2 (for the 3 corse binning in pT_V and Y_V)
    - mj_acc_cor_statE0, mj_acc_cor_statE1, mj_acc_cor_statE2, mj_acc_cor_statE3, mj_acc_cor_statE4, mj_acc_cor_statE5 (as many as pT_V and Y_V bins)
- For Muon channel :
    - mj_Yieldcorr_M
    - mj_Yielduncor_M
    - mj_acc_cor_closureM0 , mj_acc_cor_closureM1 , mj_acc_cor_closureM2 (for the 3 corse binning in pT_V and Y_V)
    - mj_acc_cor_statM0, mj_acc_cor_statM1, mj_acc_cor_statM2, mj_acc_cor_statM3, mj_acc_cor_statM4, mj_acc_cor_statM5 (as many as pT_V and Y_V bins)

From inclusive SR (MJ yield and shape of the pTW and Y)

From inclusive SR (MJ yield and shape of the pTW and Y)

From coarse bin to fine bin accCorr functions

From limited QCD MC statistics

Systematic uncertainties breakdown

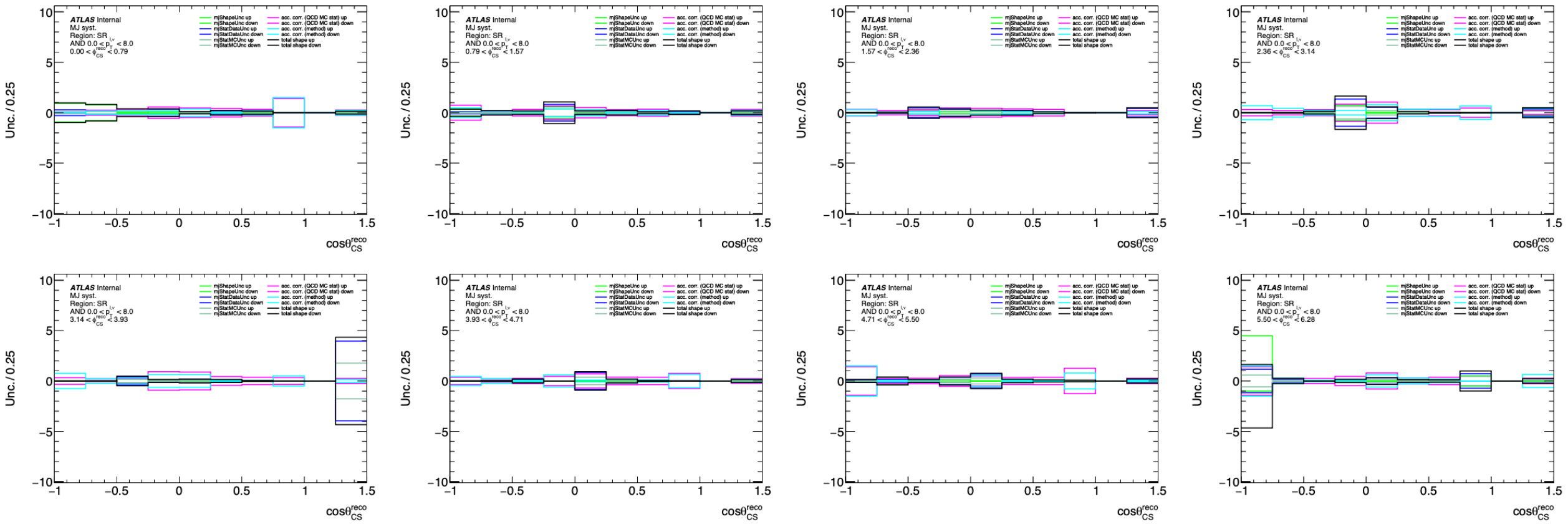

Figure 237: Multi-jet background shape systematics breakdown for $\cos\theta_{CS}$ as slices of ϕ_{CS} for $0 < p_T^{\ell,\nu} < 8$ GeV bin for $W^- \to e^-\overline{\nu}$ channel.

Systematic uncertainties breakdown

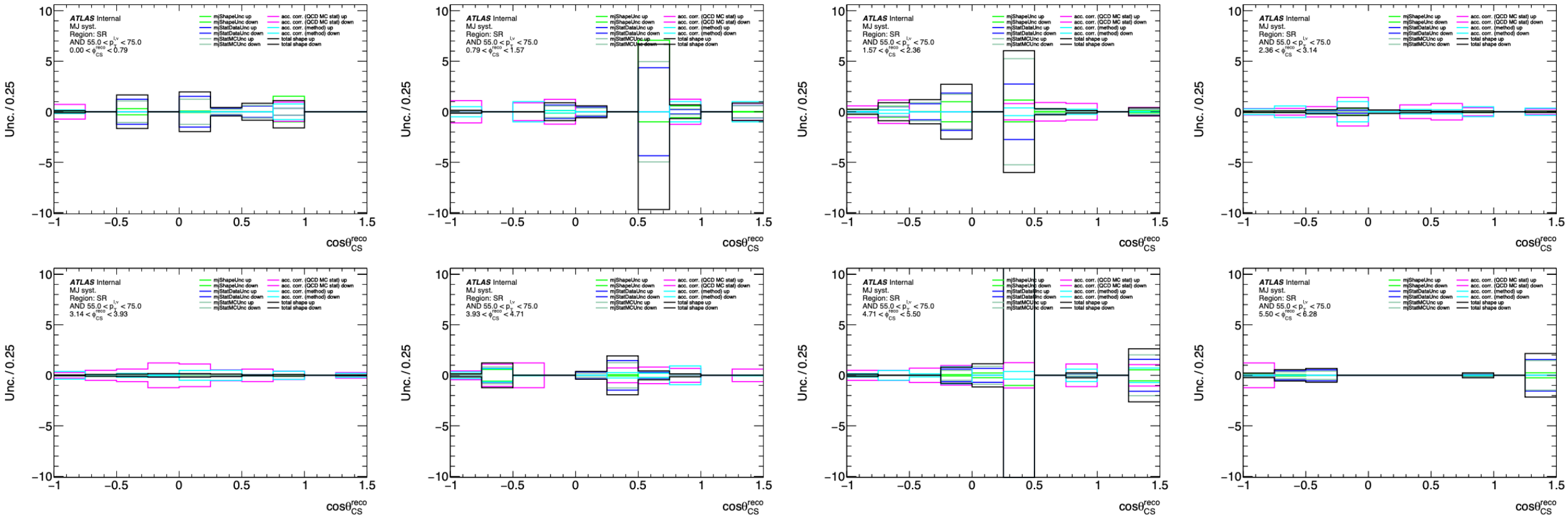

Figure 242: Multi-jet background shape systematics breakdown for $\cos\theta_{CS}$ as slices of ϕ_{CS} for $55 < p_T^{\ell,\nu} < 75$ GeV bin for $W^- \to e^-\overline{\nu}$ channel.

Systematic uncertainties breakdown

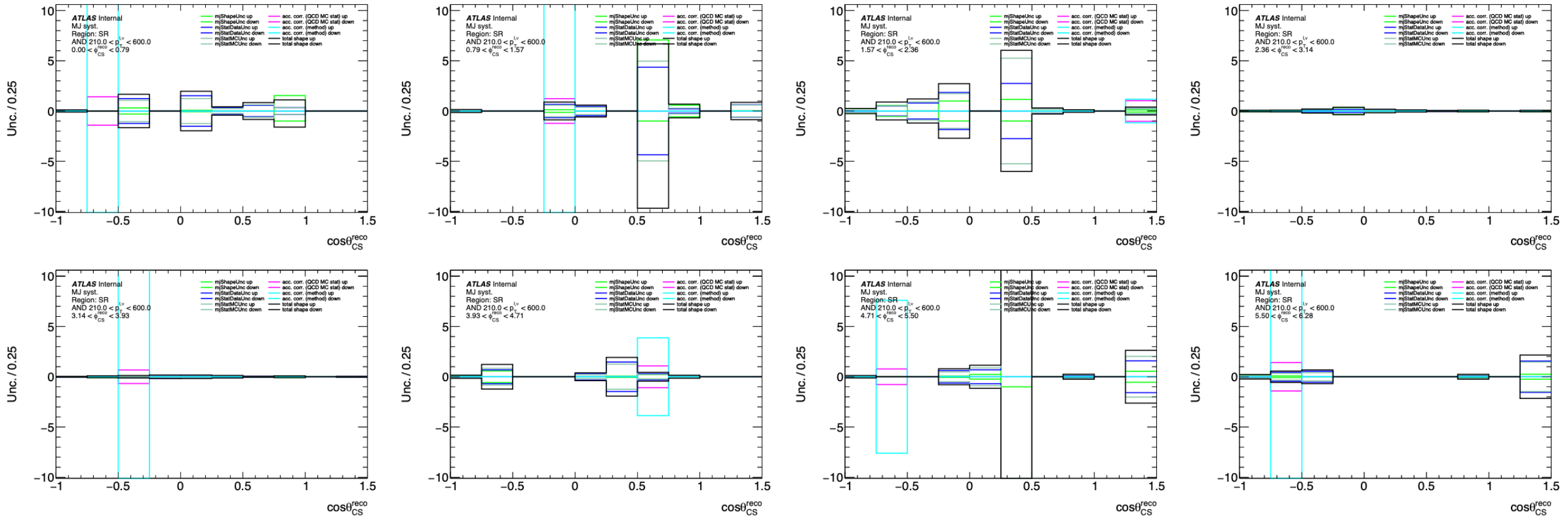

Figure 246: Multi-jet background shape systematics breakdown for $\cos\theta_{CS}$ as slices of ϕ_{CS} for $210 < p_T^{\ell,\nu} < 600$ GeV bin for $W^- \to e^-\overline{\nu}$ channel.

Thanks for attention!

Control Plots in the Signal Region for $W^+ \rightarrow e^+\nu$

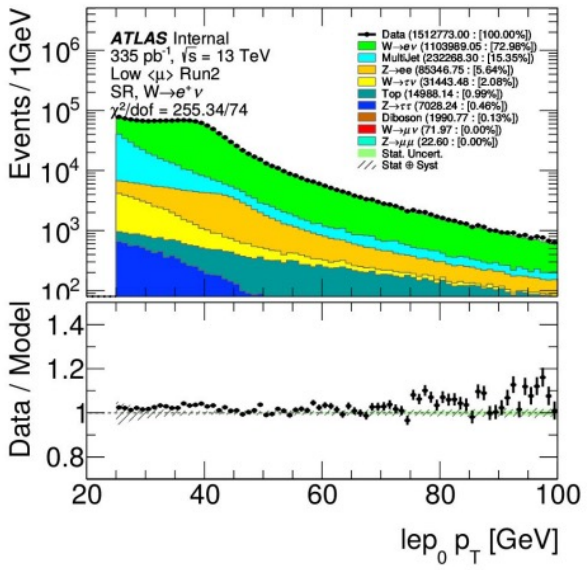

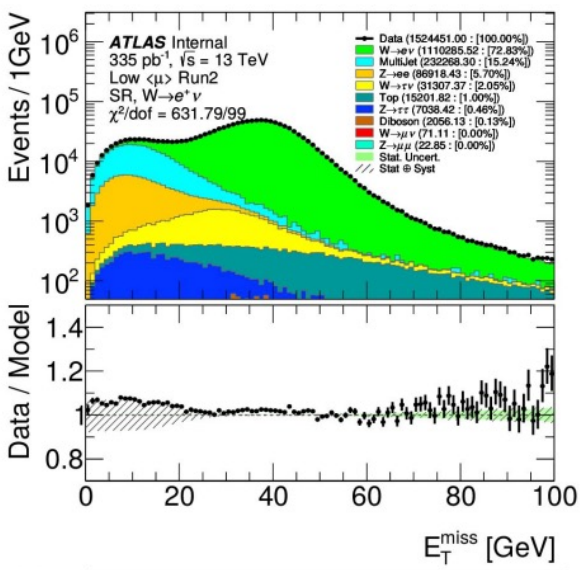

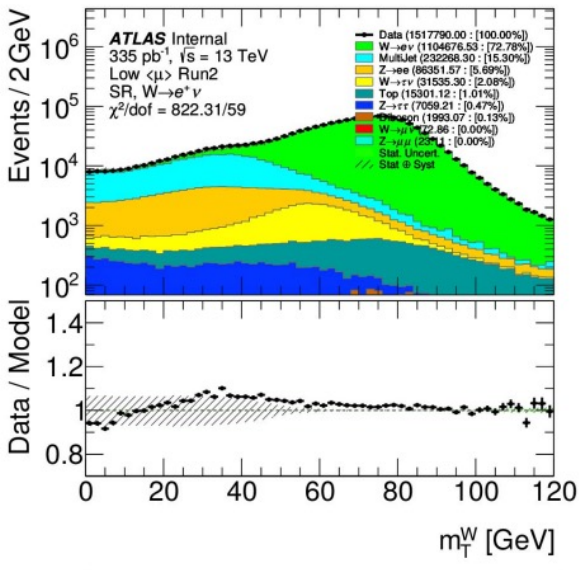

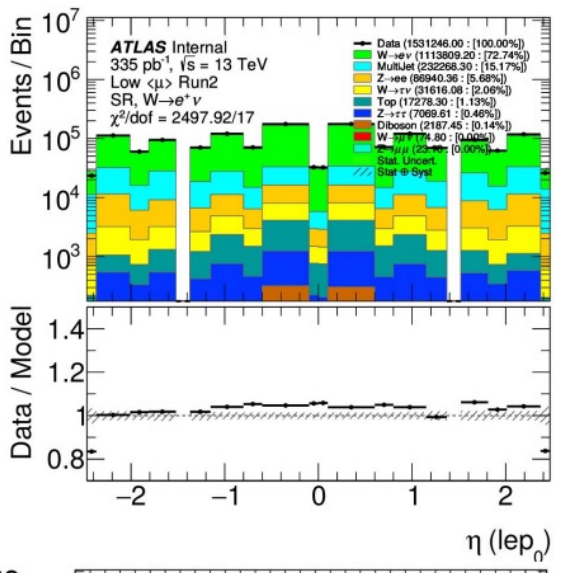

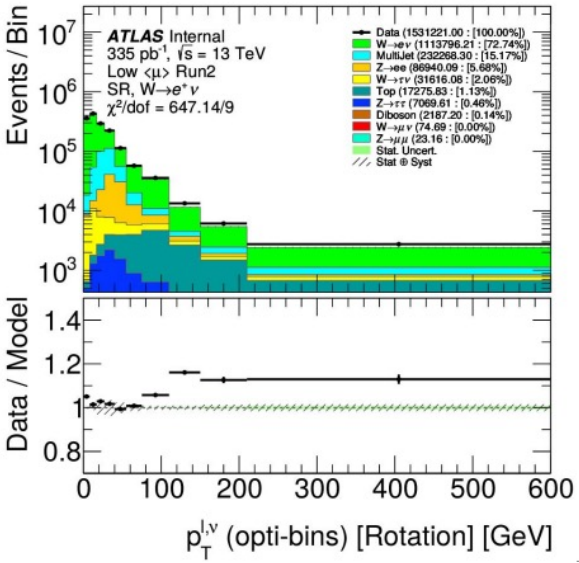

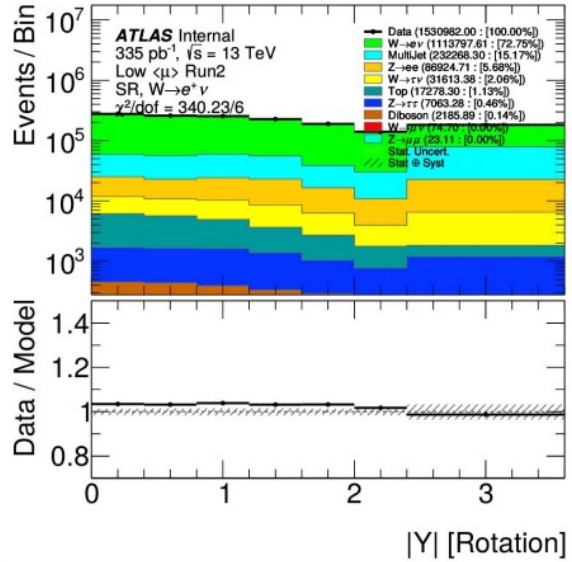

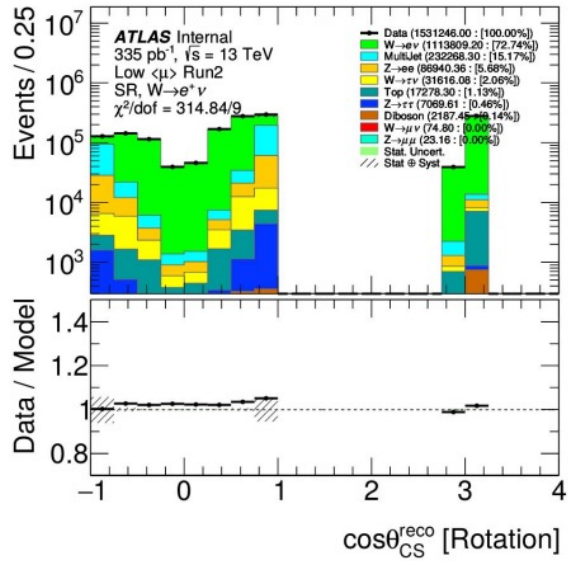

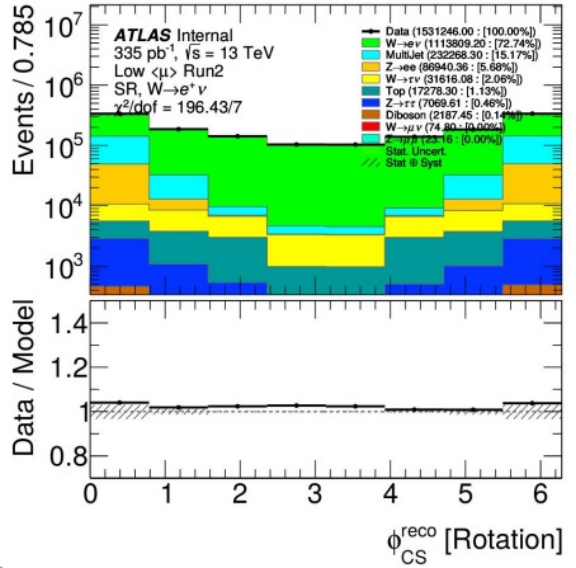

Control Plots in the Signal Region for $W^+ \to \mu^+\nu$

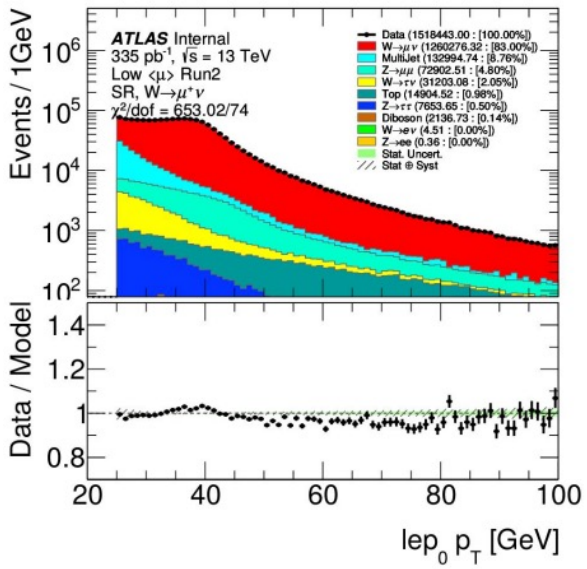

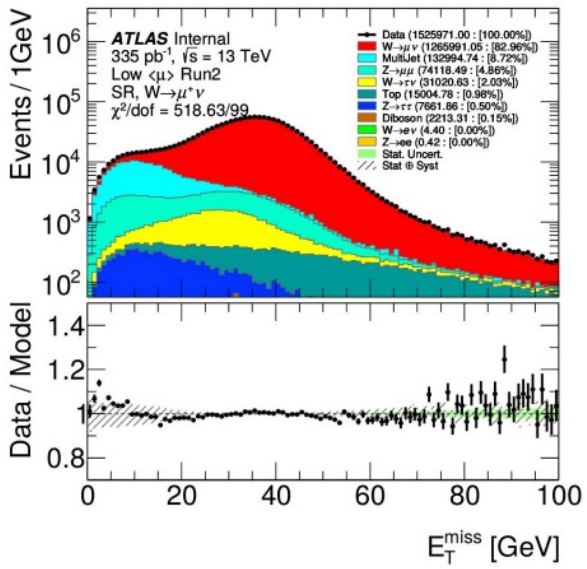

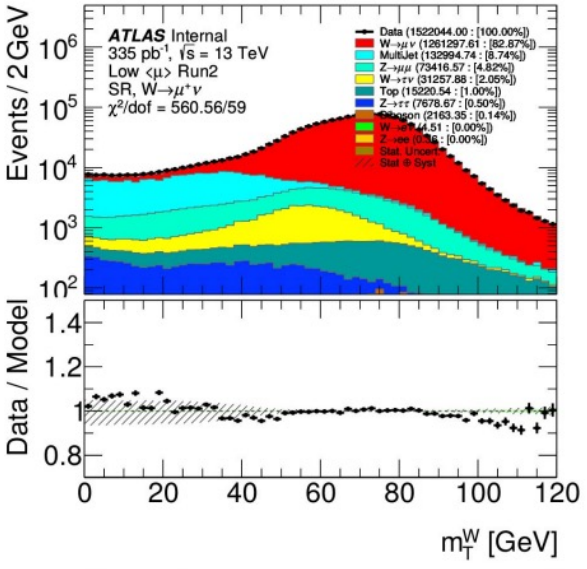

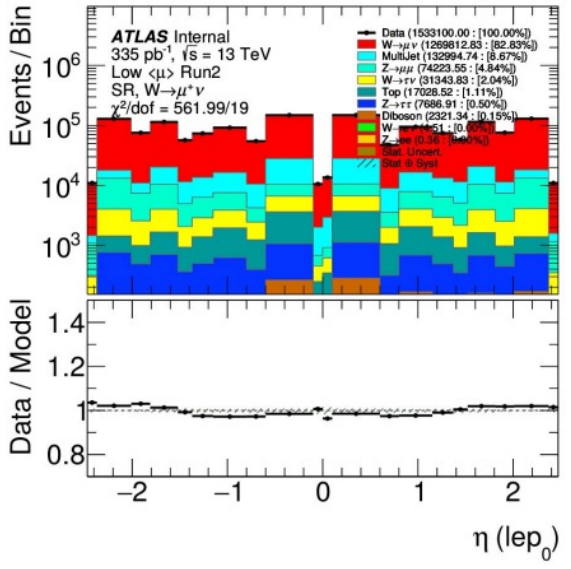

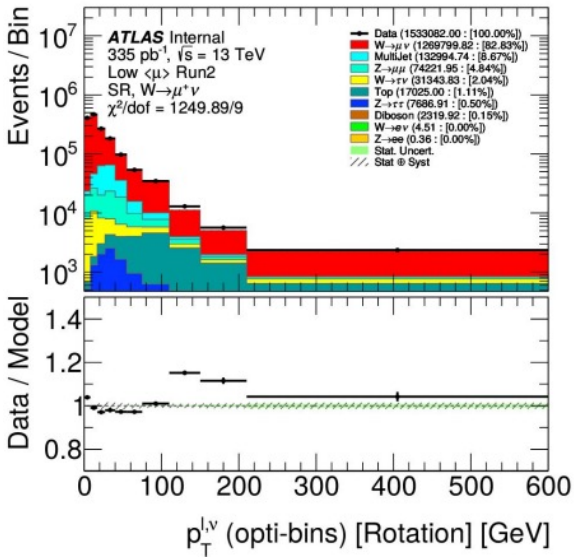

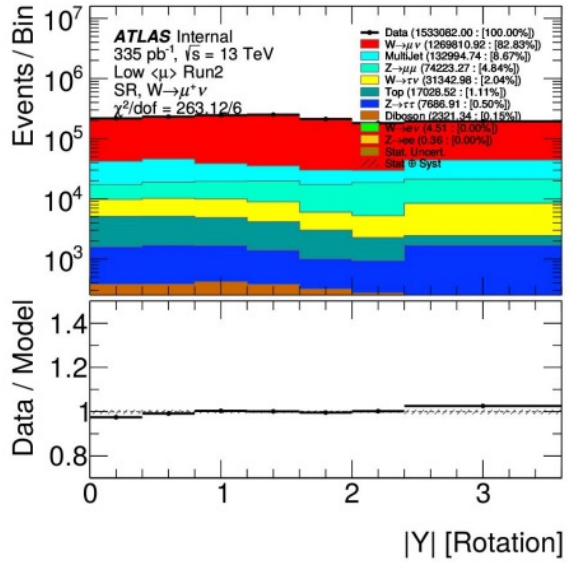

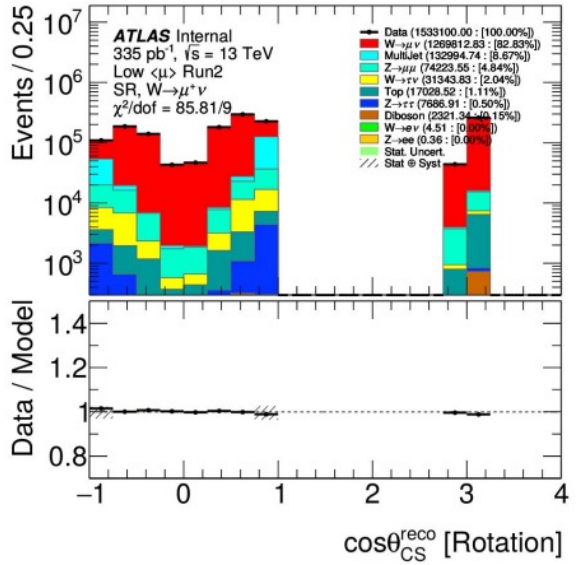

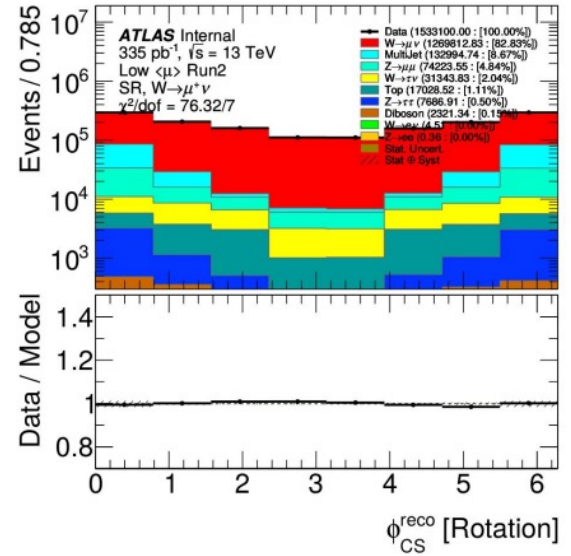

Collins Soper Frame

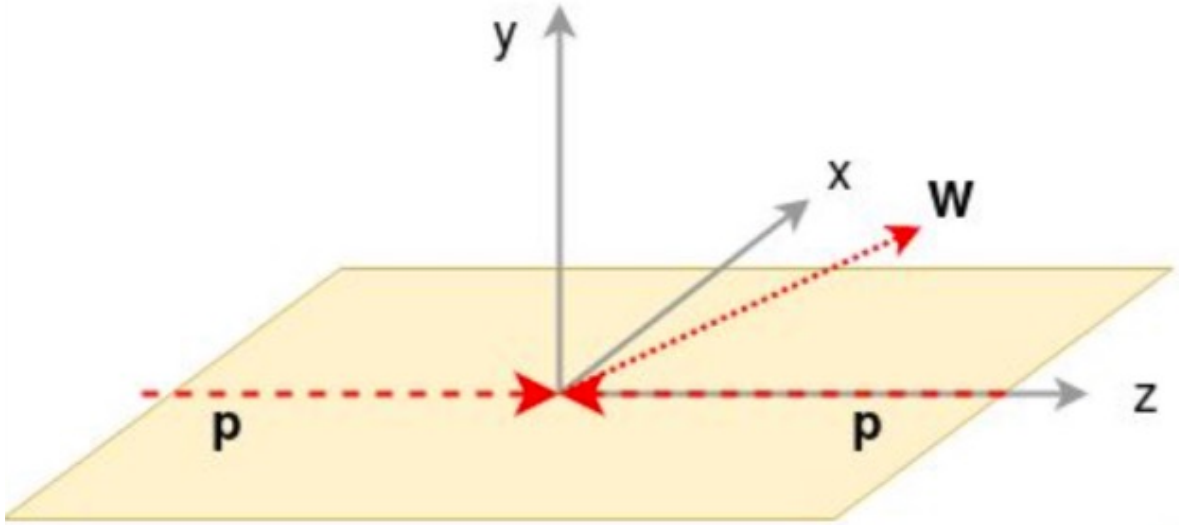

Lab Frame

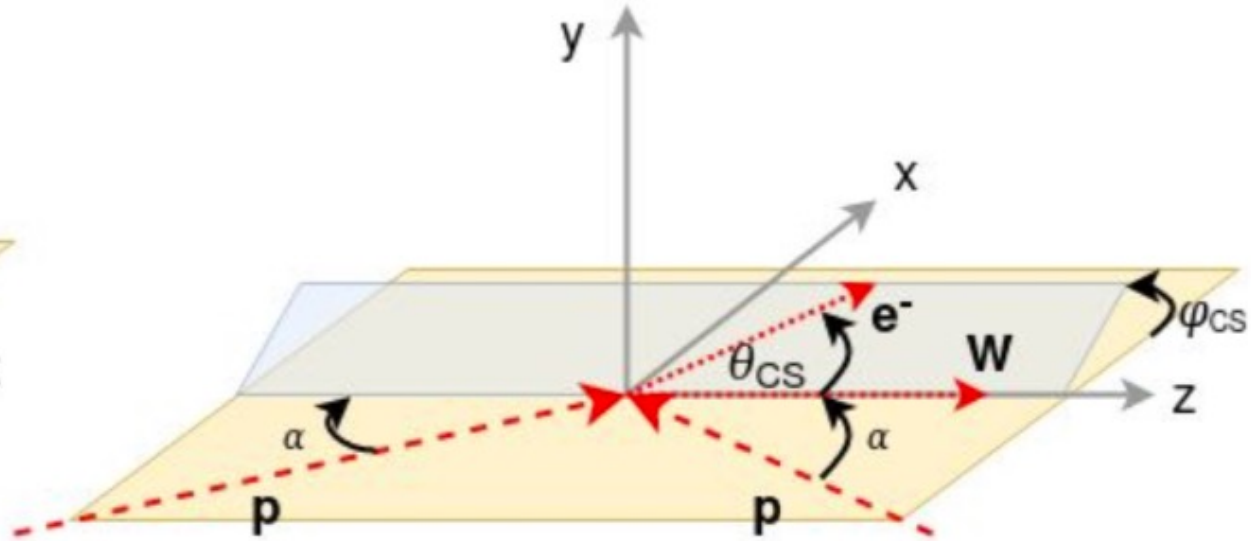

CS Frame

- Special W boson rest frame where angles are defined by lepton and proton kinematics.
- Define using “negative” lepton, so for W+ case this is the neutrino

Polynomial Information

A_i	P_i	$Y_l^m(\theta,\phi)$	Coupling	Non-Zero
A_0	$1/2\left(1-3\cos^2\theta\right)$	Y_2^0		$O\left(\alpha_S^1\right)$
A_1	$\sin 2\theta\cos\phi$	$\left(Y_2^{-1}-Y_2^1\right)$	$\left(v_\ell^2+a_\ell^2\right)\left(v_q^2+a_q^2\right)$	$O\left(\alpha_S^1\right)$
A_2	$1/2\sin^2\theta\cos 2\phi$	$\left(Y_2^{-2}+Y_2^2\right)$		$O\left(\alpha_S^1\right)$
A_3	$\sin\theta\cos\phi$	$\left(Y_1^{-1}-Y_1^1\right)$	$v_\ell a_\ell v_q a_q$	$O\left(\alpha_S^1\right)$
A_4	$\cos\theta$	Y_1^0		$O\left(\alpha_S^0\right)$
A_5	$\sin^2\theta\sin 2\phi$	$\left(Y_2^{-2}-Y_2^2\right)$	$\left(v_\ell^2+a_\ell^2\right)\left(v_q a_q\right)$	$O\left(\alpha_S^2\right)$
A_6	$\sin 2\theta\sin\phi$	$\left(Y_2^{-1}+Y_2^1\right)$		$O\left(\alpha_S^2\right)$
A_7	$\sin\theta\sin\phi$	$\left(Y_1^{-1}+Y_1^1\right)$	$\left(v_\ell a_\ell\right)\left(v_q^2+a_q^2\right)$	$O\left(\alpha_S^2\right)$

Physics Modelling

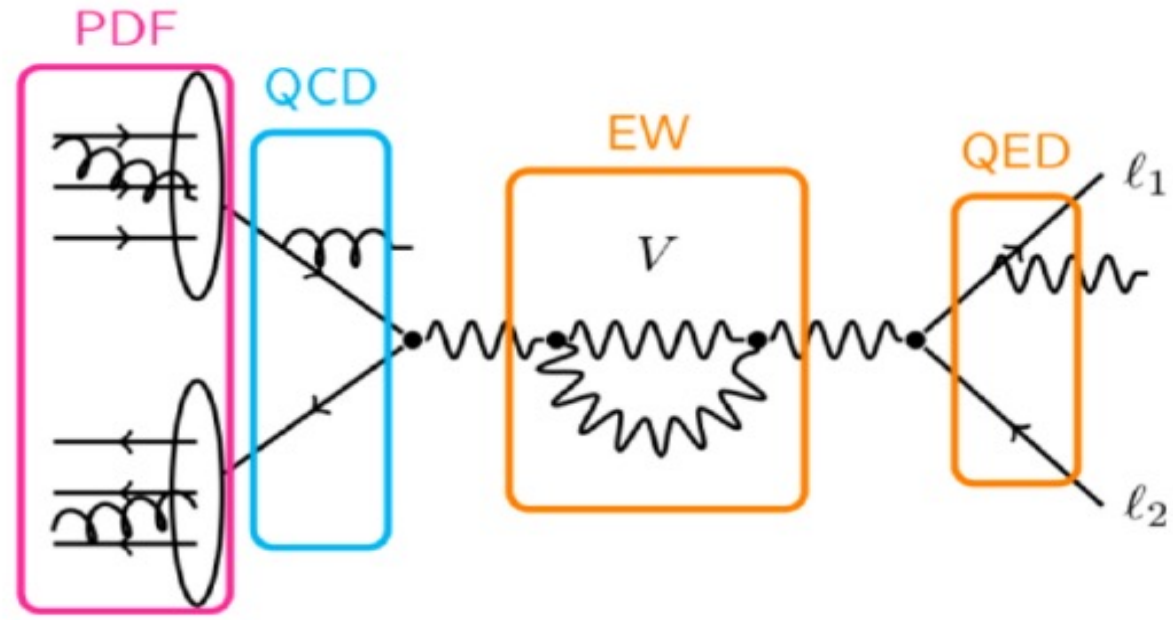

Angular Coefficients

$$\frac{d\sigma}{dp_{\mathrm{T}}^{W}\,dm^{W}\,dy^{W}\,d\cos\theta d\phi} = \frac{3}{16\pi}\frac{d\sigma^{U+L}}{dp_{\mathrm{T}}^{W}\,dm^{W}\,dy^{W}}\Big\{\big(1+\cos^2\theta\big) + \frac{1}{2}A_0\big(1-3\cos^2\theta\big) + A_1\sin 2\theta\cos\phi + \frac{1}{2}A_2\sin^2\theta\cos 2\phi + A_3\sin\theta\cos\phi + A_4\cos\theta + A_5\sin^2\theta\sin 2\phi + A_6\sin 2\theta\sin\phi + A_7\sin\theta\sin\phi\Big\}.$$

Non-zero at LO
Non-zero at NLO
Non-zero at NNLO

- Full angular cross-section parameterization
- QCD production dynamics fully contained in Ai coefficients, while decay kinematics fully contained in coupled angular polynomials

Neutrino reconstruction

- Angular definitions require fully constructed neutrino
- Hadronic recoil:
  - Vectorial sum of all transverse momenta of ISR objects
  - ATLAS: uses PFlow objects (neutral+charged)
- Solving for Neutrino p_z:
  - Take mass constraint resulting in quadratic equation
    - $(q_l + q_\nu)^\mu \, (q_l + q_\nu)_\mu = m_W^2$
  - $m_T < m_W$ gives 2 solutions
    - one chosen at random but can statistically resolve correct distributions
  - No real solution when $m_T > m_W$, still can use events for φ_{CS} information
- Once the mass constraint is chosen φ_{CS} is solved while the 2 solutions corresponds to a sign ambiguity in $\cos\theta_{CS}$

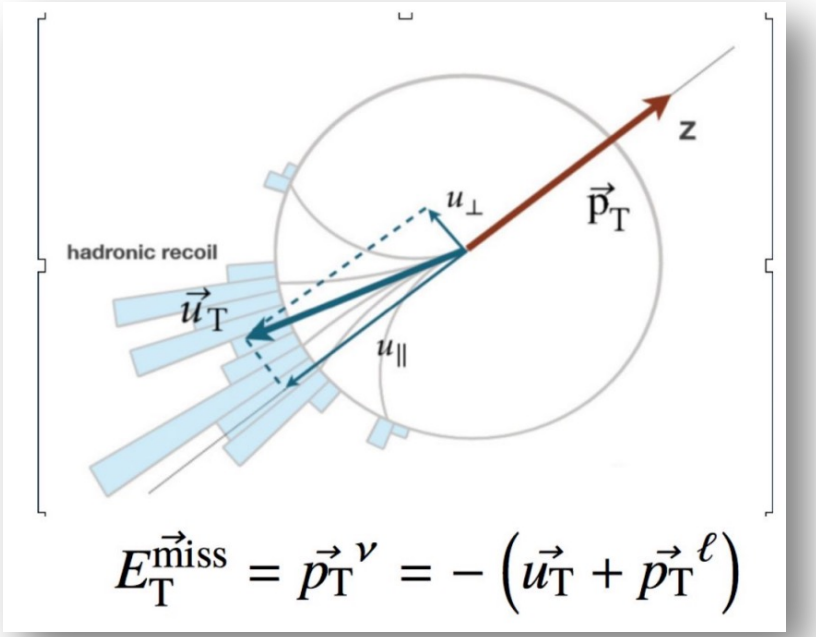

$cos\theta_{CS}$ ambiguity (1)

More info

- How can we statistically resolve $cos\theta_{CS}$?

$$\cos\theta = 2\frac{(l^+\bar{l}^- - l^-\bar{l}^+)\cdot \mathrm{sign}(y_{\ell\ell})}{m_{\ell\ell}\sqrt{m_{\ell\ell}^2 + \vec{p}_T^{\,2}}},$$

$$l^{\pm} = E \pm p_z \text{ for the lepton/neutrino}$$
$$\bar{l}^{\pm} = E \pm p_z \text{ for the antilepton/antineutrino}$$

- Only choose correct p_z 50% of the time, incorrect p_z can still be used

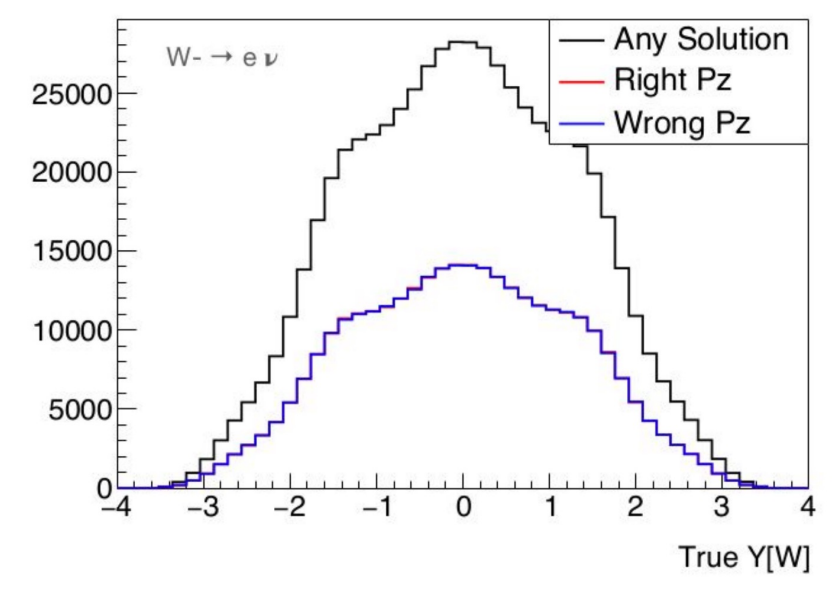

- Can solve it in 2 cases:
  - 1) Solutions where y_{ll}^1 and y_{ll}^2 have opposite signs
    - sign flips in orange and blue cancel
  - 2) One of the solutions violates Bjorken condition x < 1
    - neutrino has more p_z than beam energy → unphysical

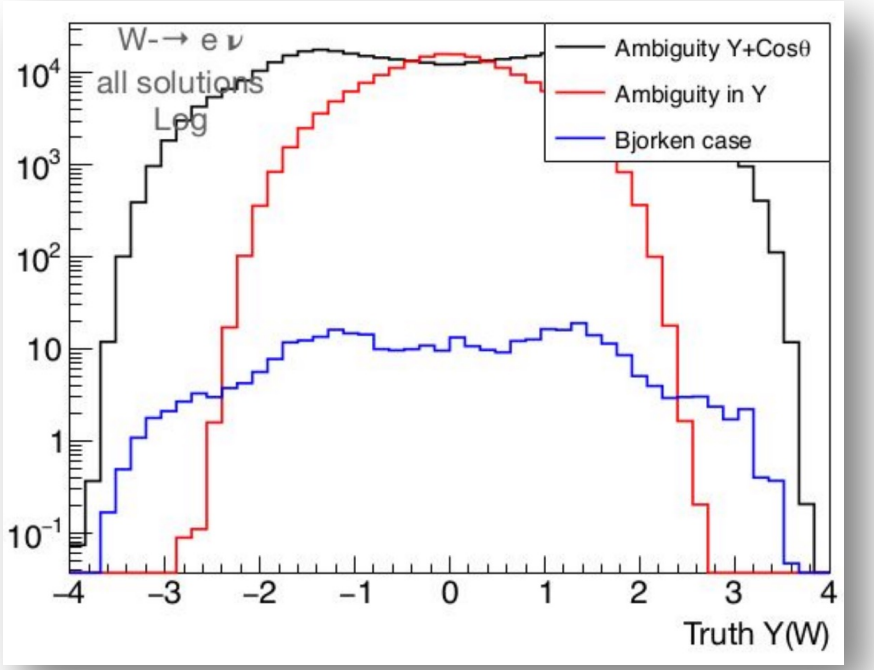

$\cos\theta_{CS}$ ambiguity (2)

- Red are events where we picked right p_z to get right sign of $\cos\theta_{CS}$
- Green are events where we picked wrong p_z but y_{ll} flipped so we get correct $\cos\theta_{CS}$, these are the events where we get our sensitivity.

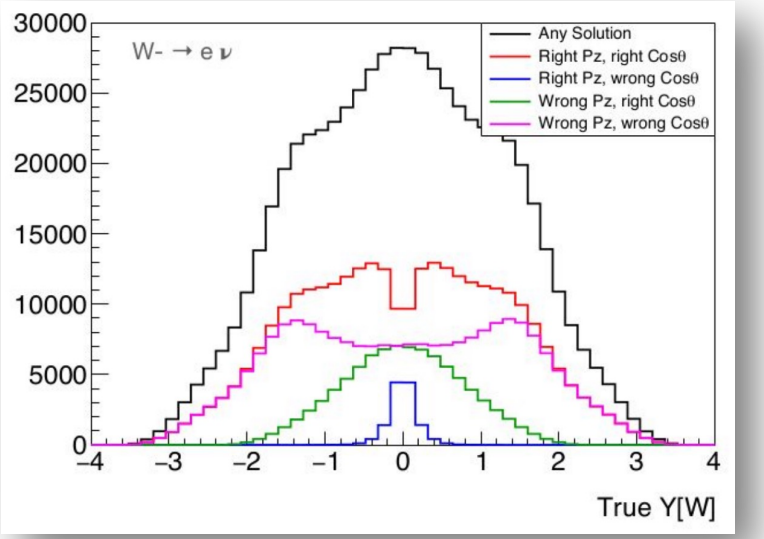

1) Both $\cos\theta_{CS}$ and y_{ll} have sign ambiguity so right 50%, no A_4 sensitivity

2) Adding to 1): only y^W has ambiguity which cancels with $\cos\theta_{CS}$ → right 100% (where we gain our sensitivity)

3] Adding to 2): One solution doesn't satisfy Bjorken condition (x < 1) → right 100% but pretty rare

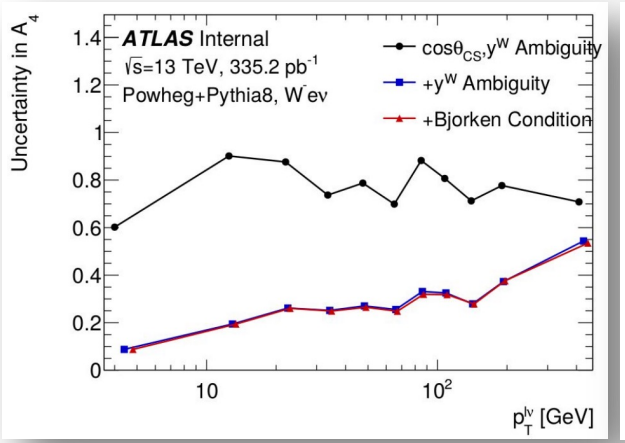

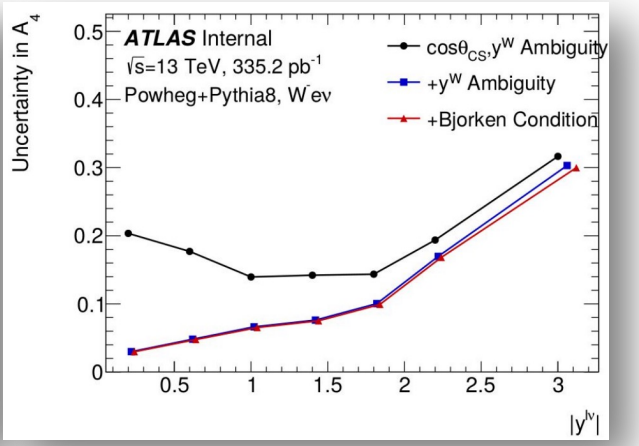

Top Background (1)

When first adding background, the increase in uncertainty was larger than expected especially at high $p_T^{l,\nu}$.

Due to larger top background contributions.

Preliminarily we thought a $|\Delta\phi| > \pi/4$ cut should help reduce the top background but doesn't as shown on the next slide.

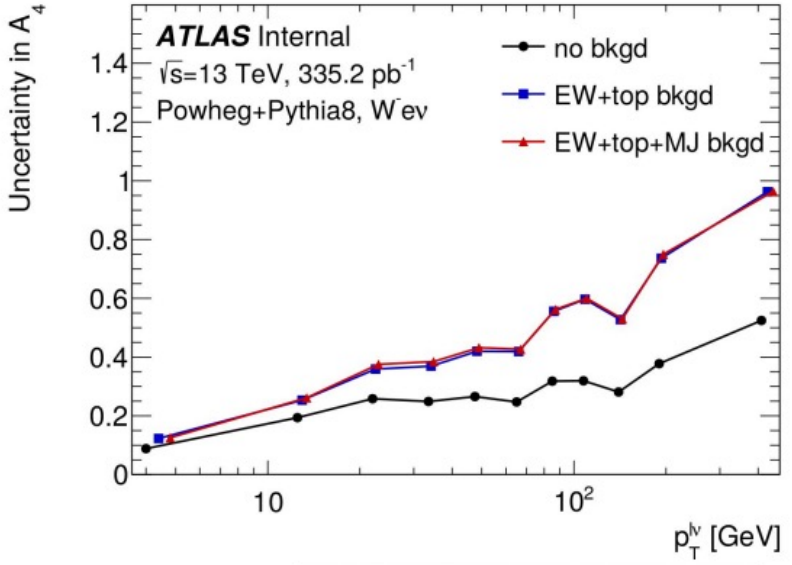

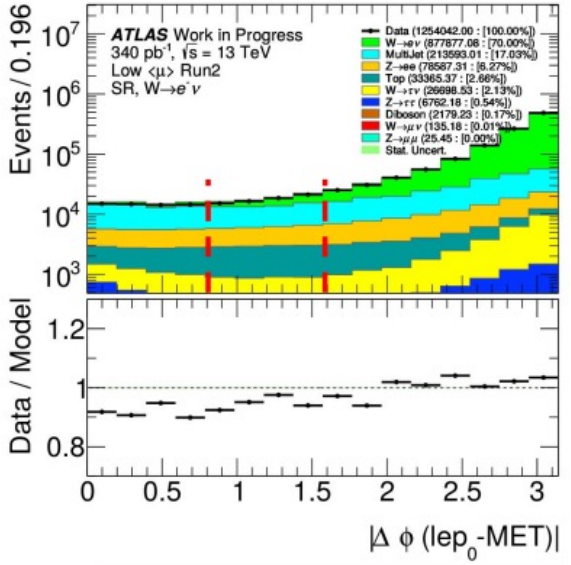

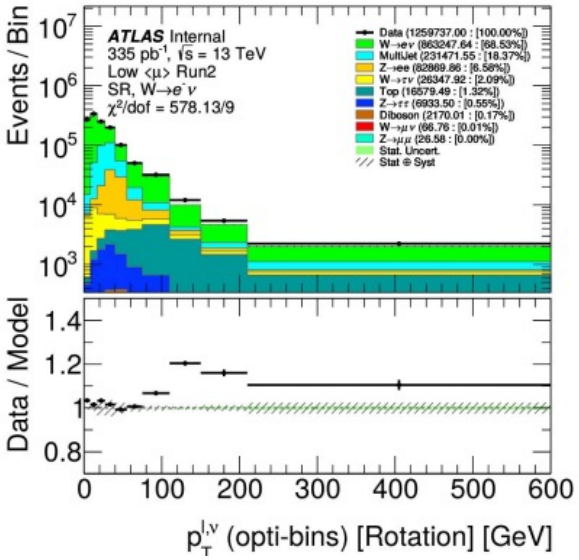

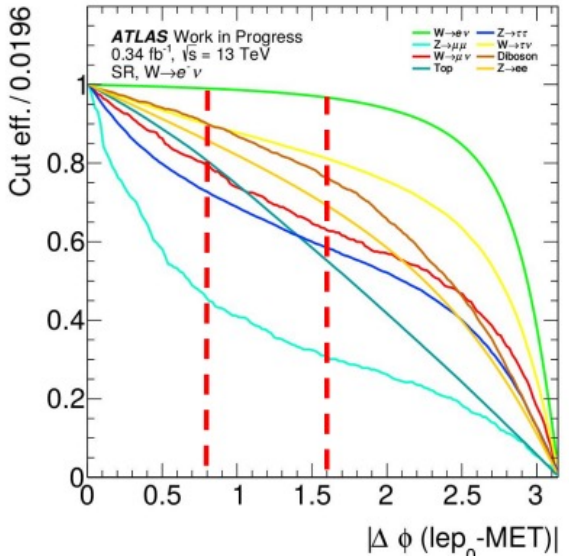

Top Background (2)

Both signal and background at high p_T lose all $\cos\theta_{CS}$ shape information and causing large uncertainty.

Addition of MET cut reduces background but also signal too much.

From our studies the top background seems irreducible.

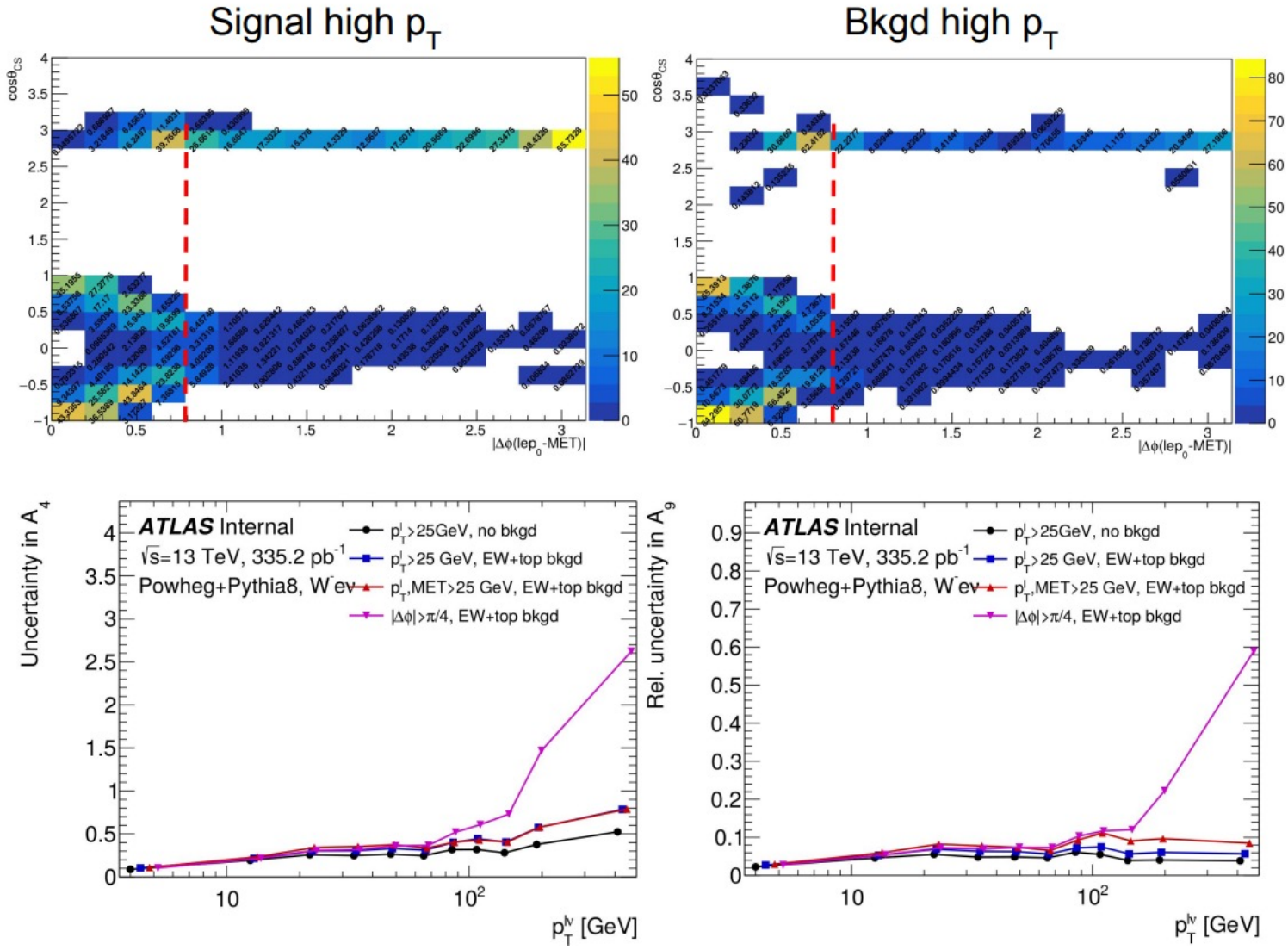

Event selection: Sensitivity Comparison

A_0

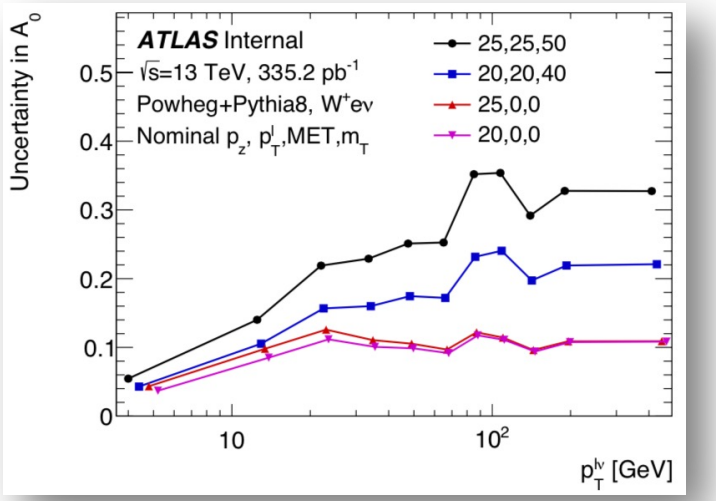

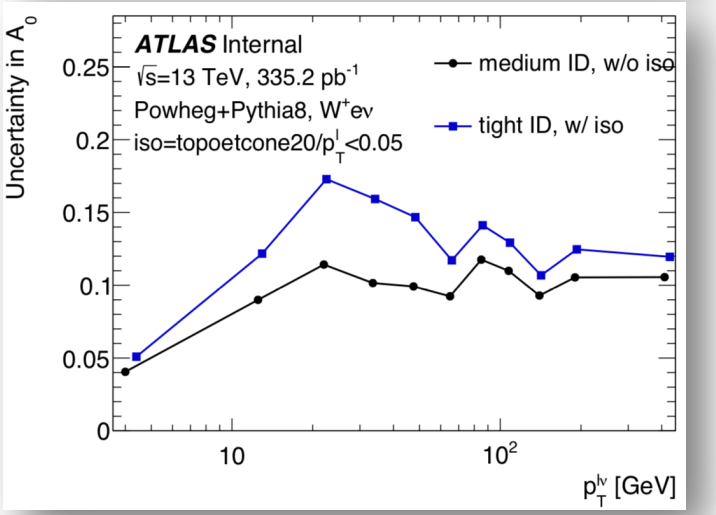

A_4

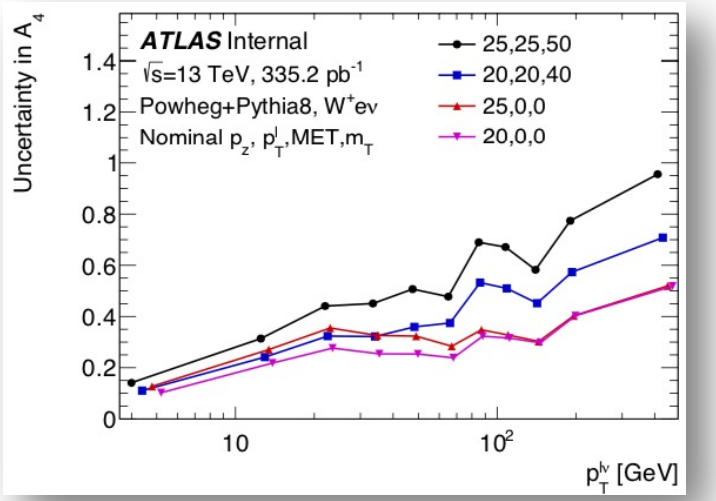

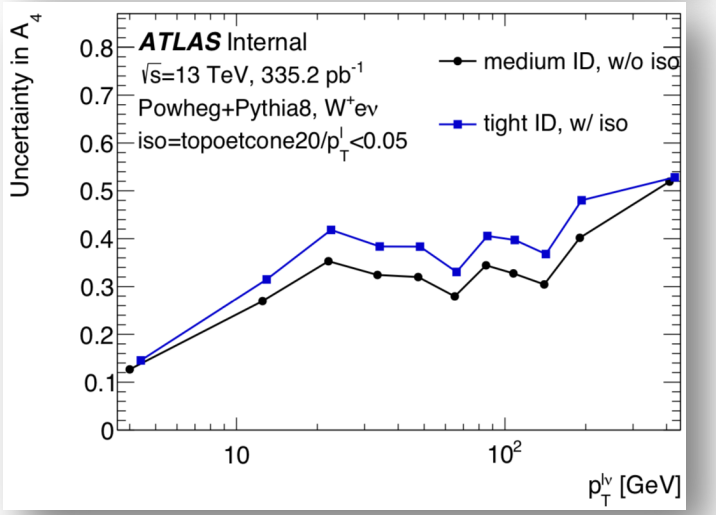

Systematics

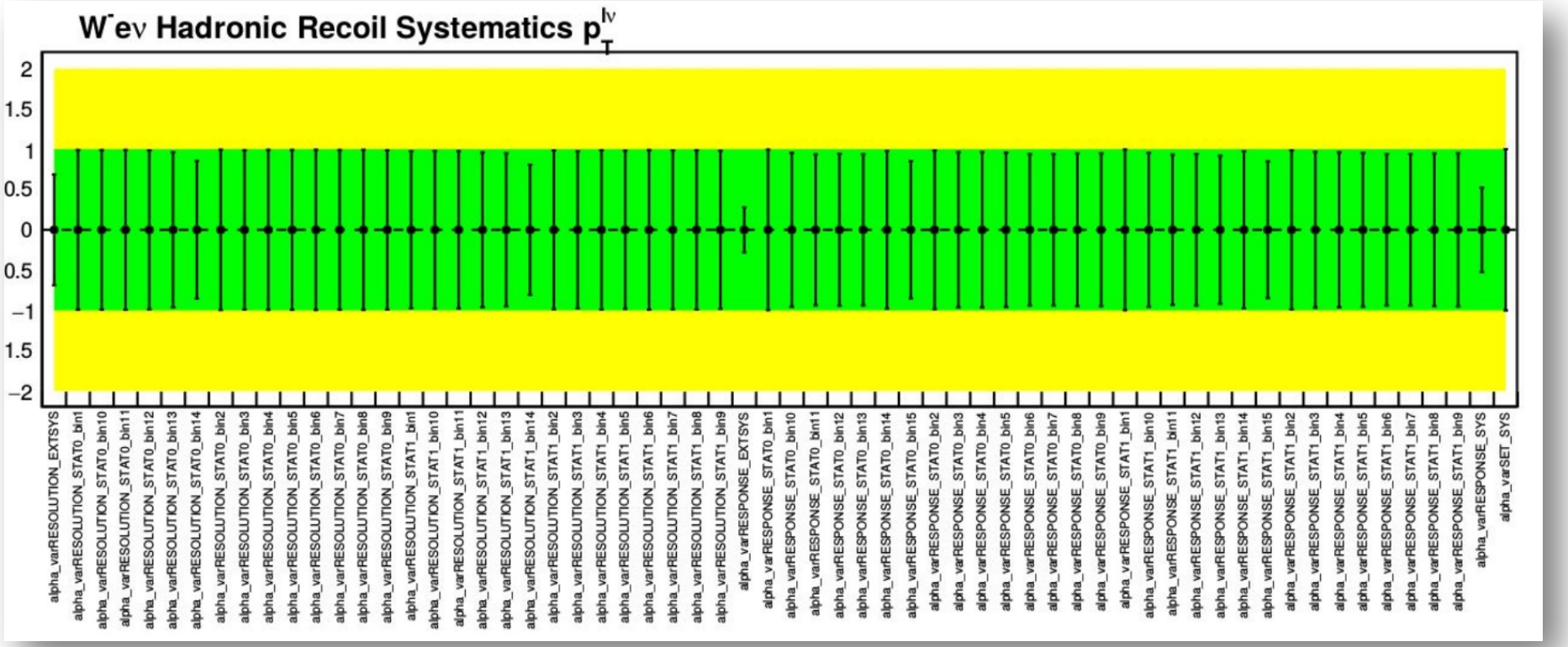

- Have tested 2 largest expected systematics (Hadronic Recoil and Background) independently
- MJ NPs heavily constrained, still being understood.

MJ Acceptance Systematic (8 < pT < 17 GeV)

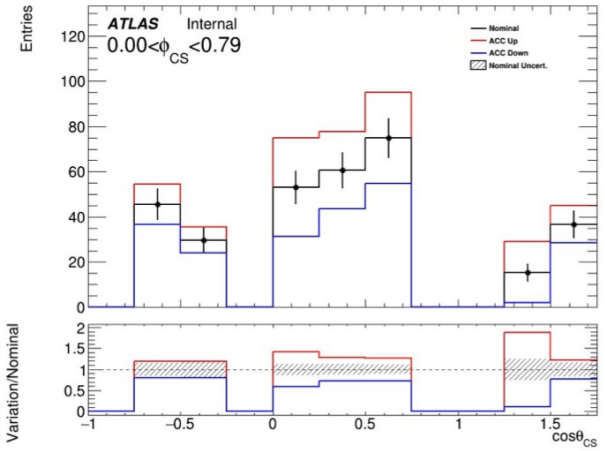

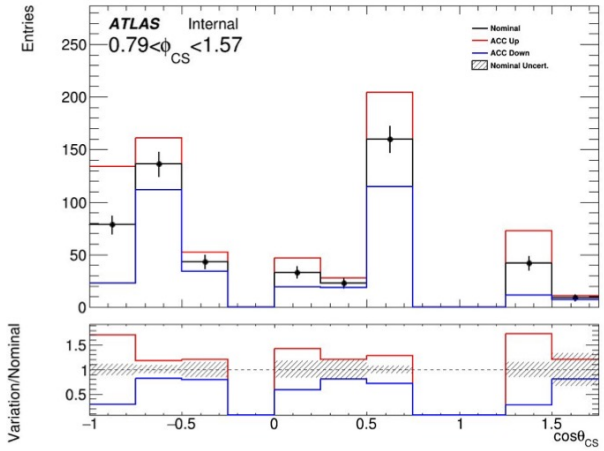

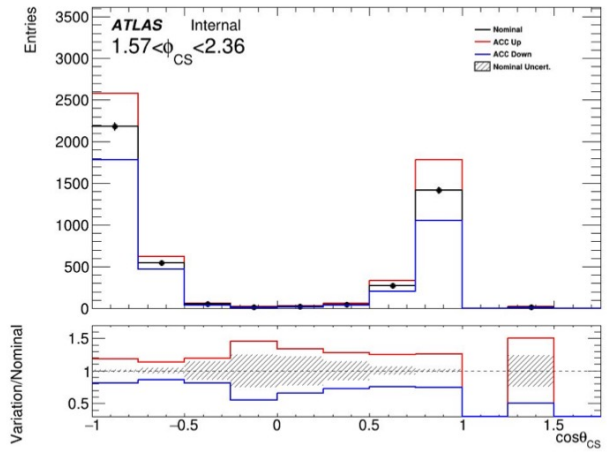

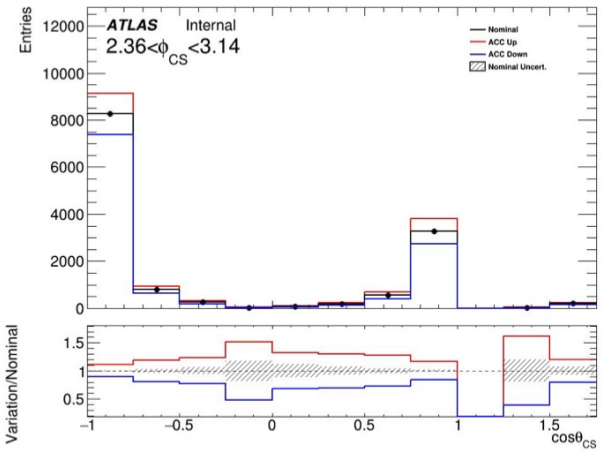

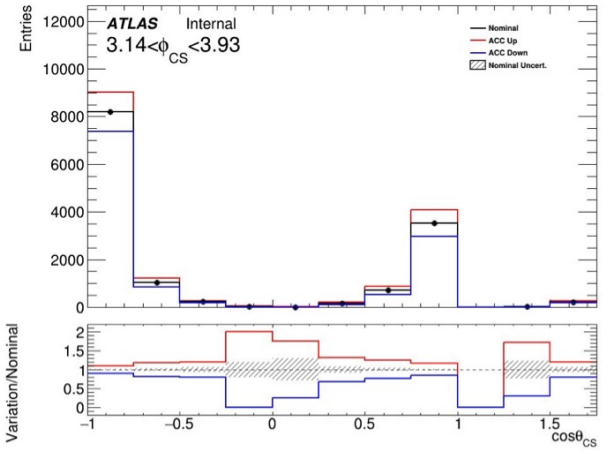

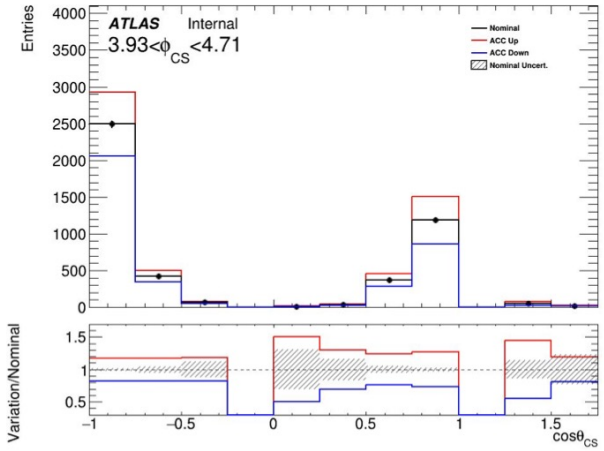

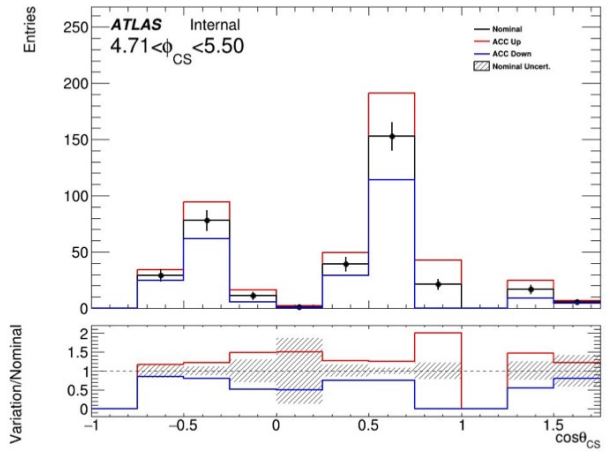

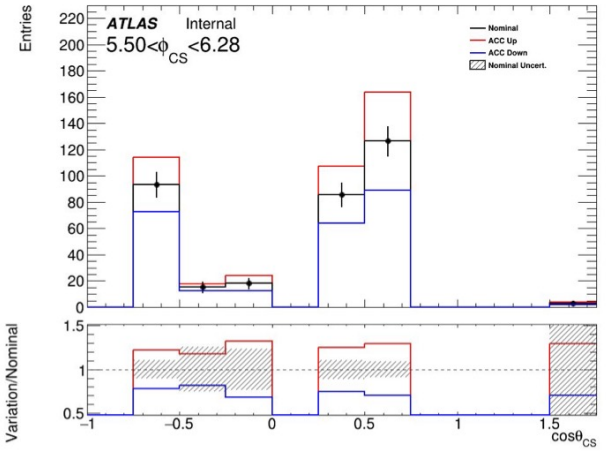

MJ Shape Systematic (8 < pT < 17 GeV)

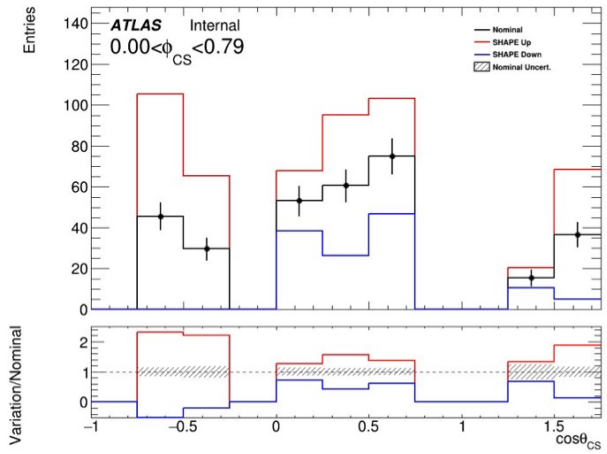

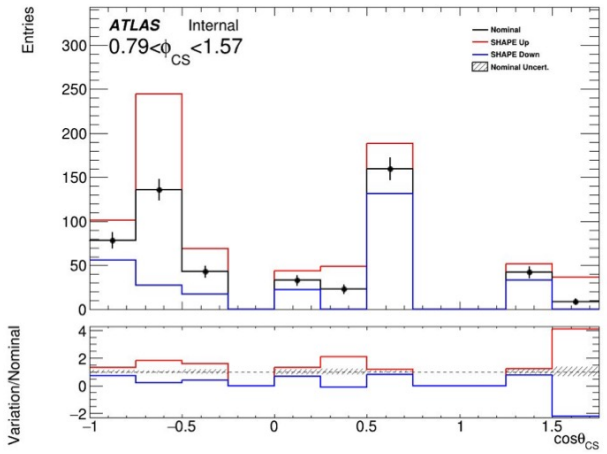

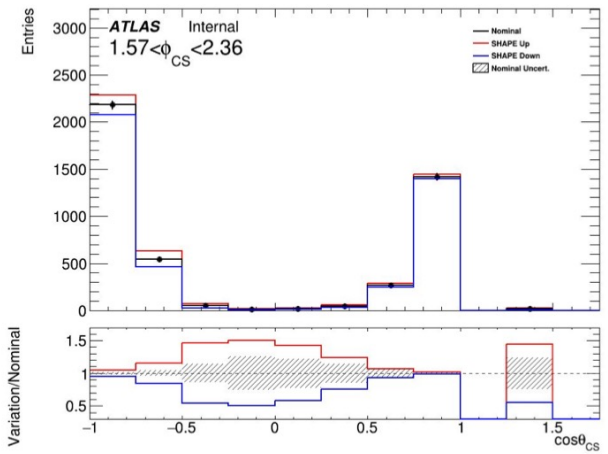

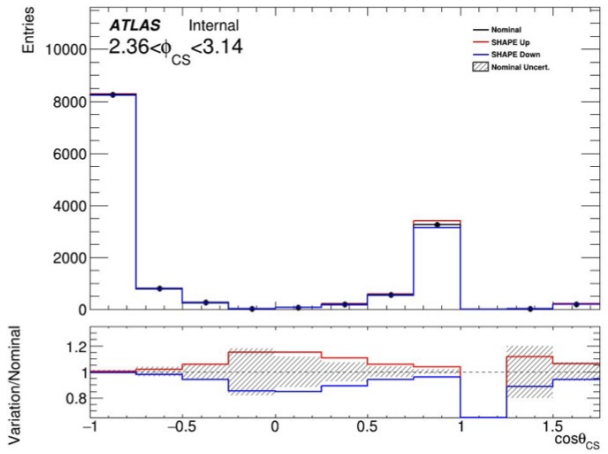

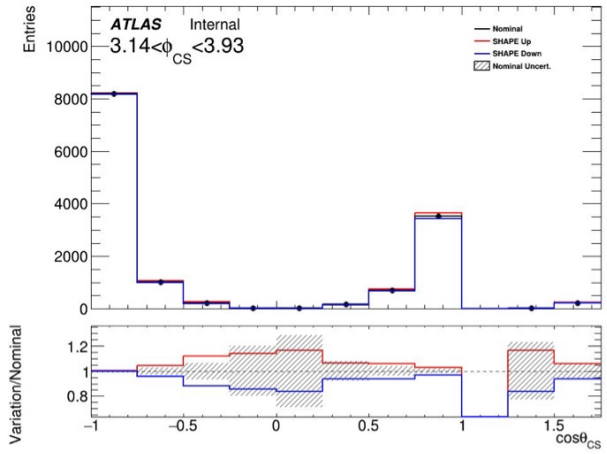

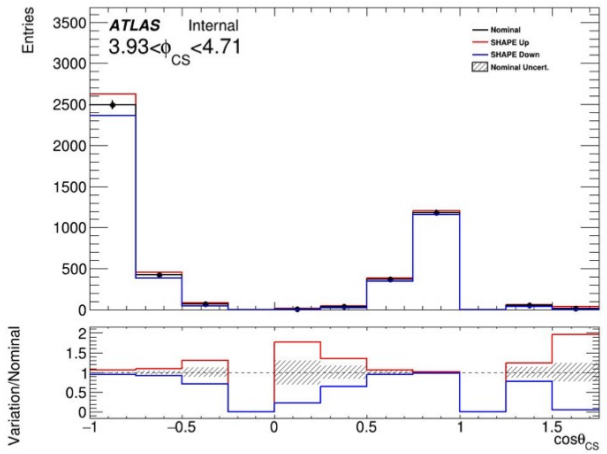

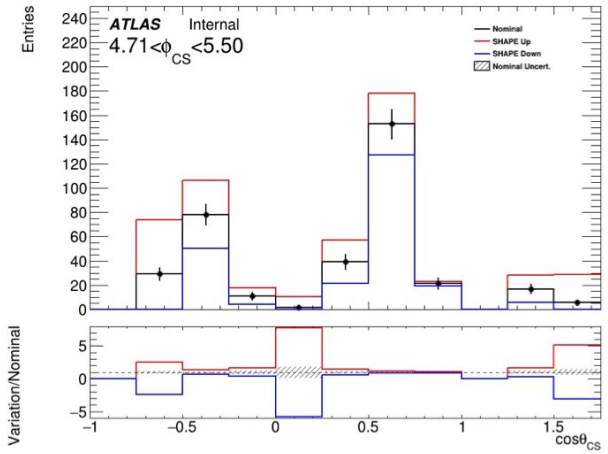

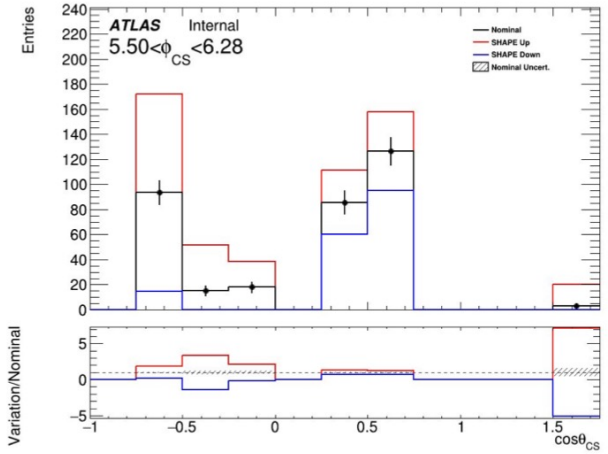

MJ templates derived for pure DD and predicted by QCD MC

$W \to e^- \nu$

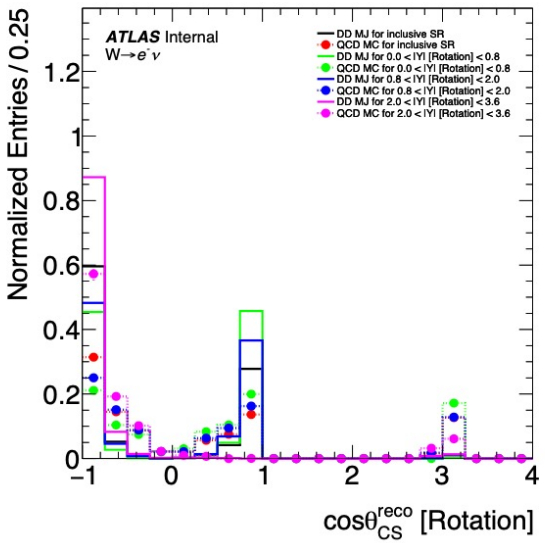

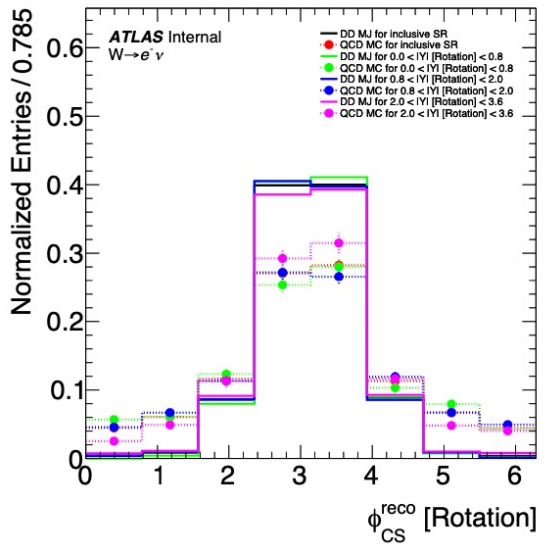

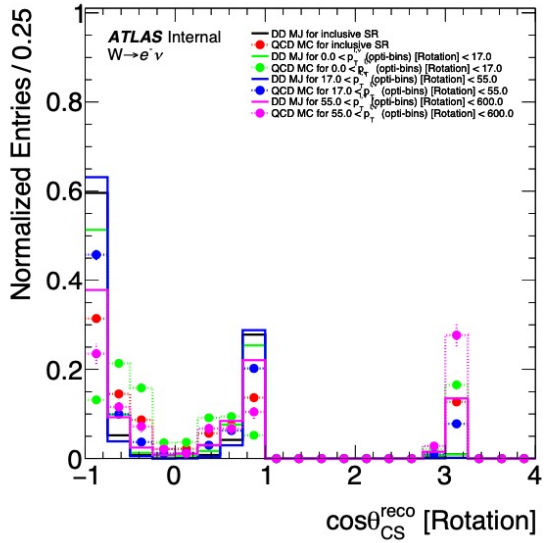

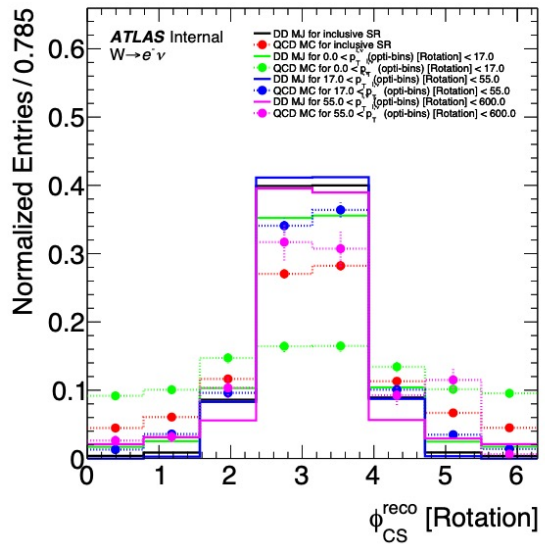

$W \to \mu^- \nu$

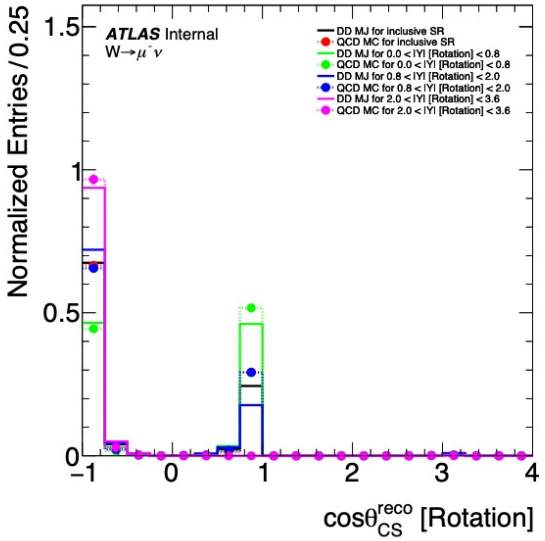

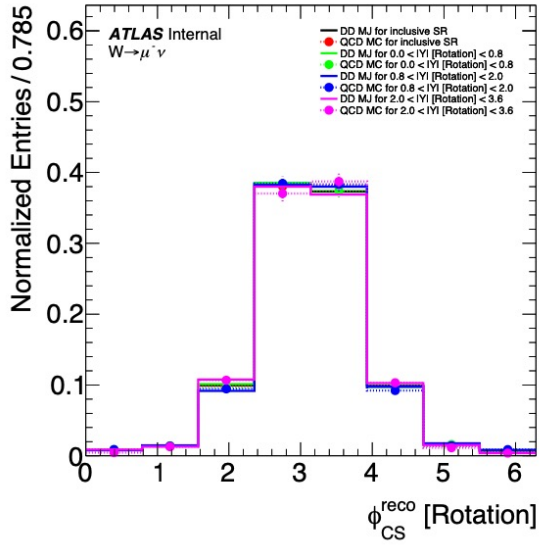

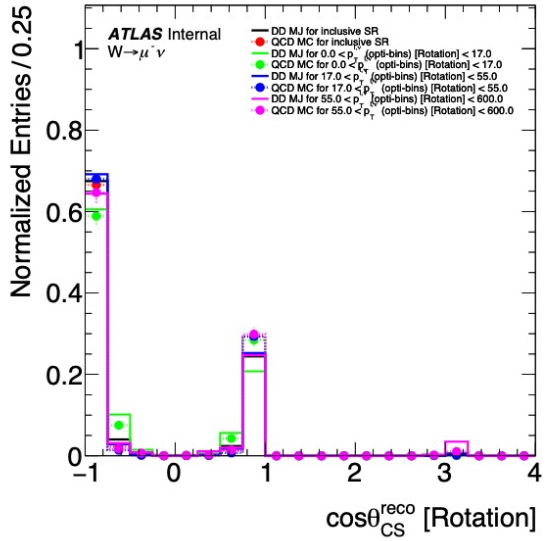

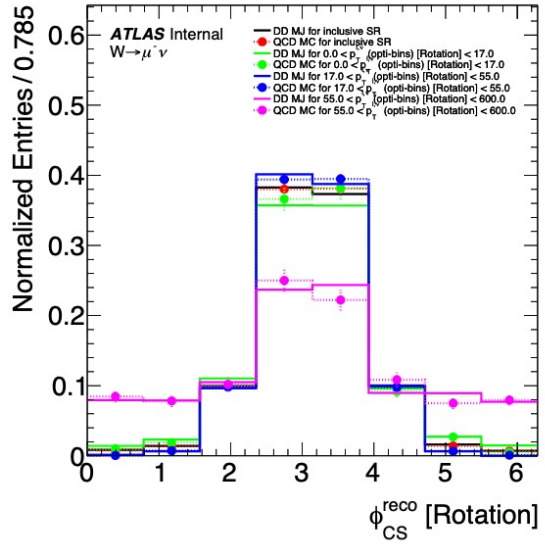

Debugging: MJ templates derived by accCorr

$W \to e^- \nu$

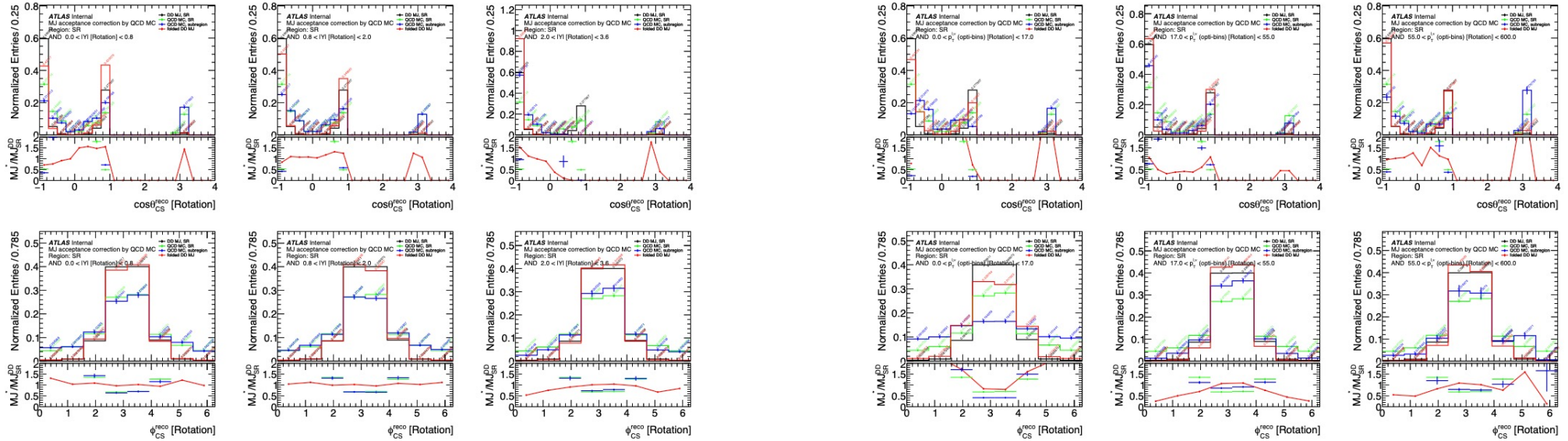

$W \to \mu^- \nu$

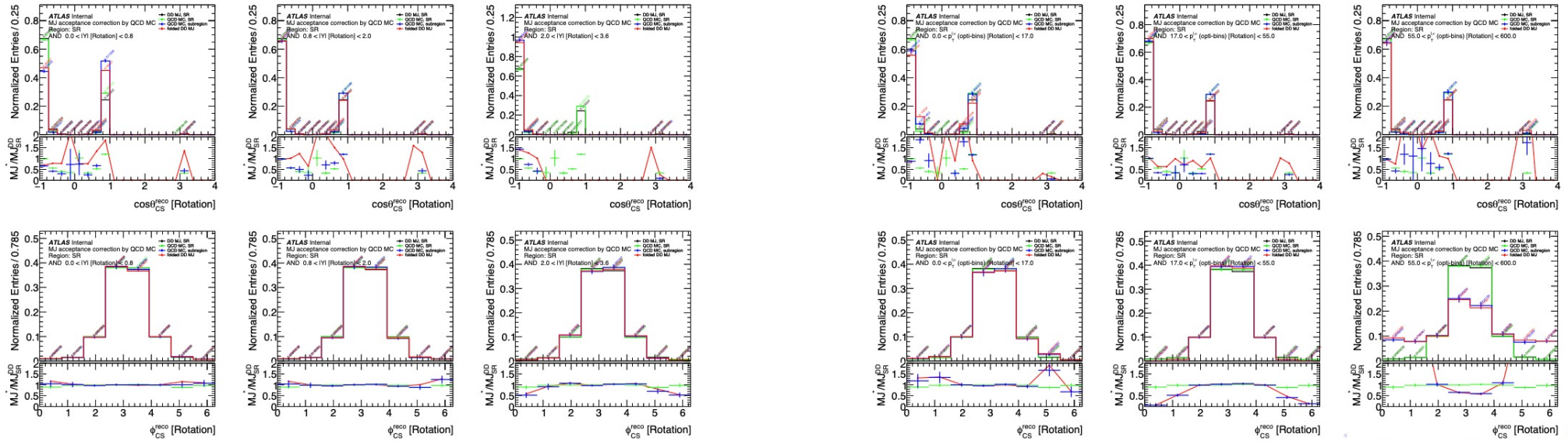

Debugging: accCorr functions

$W \to e^- \nu$

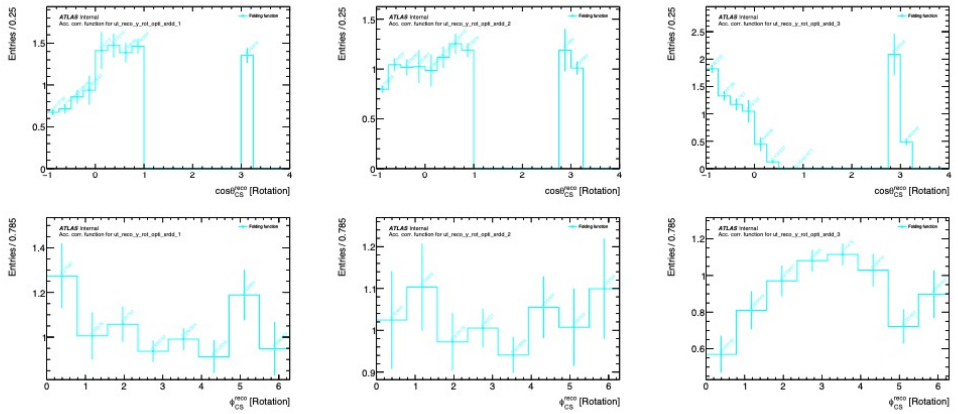

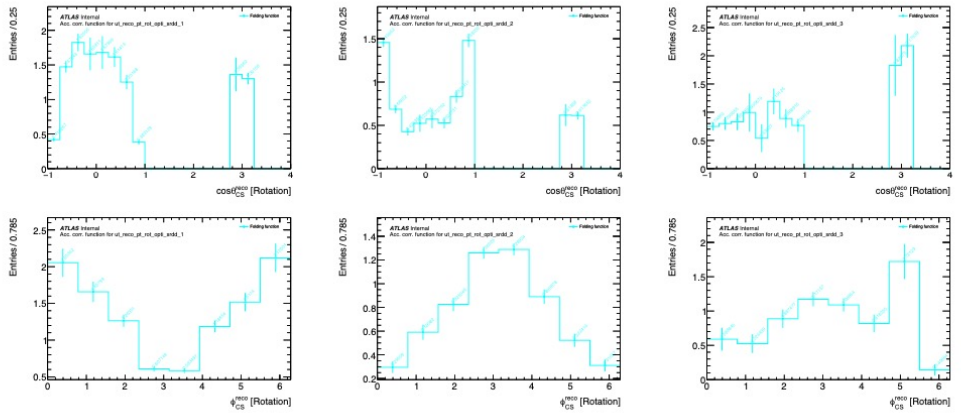

$W \to \mu^- \nu$

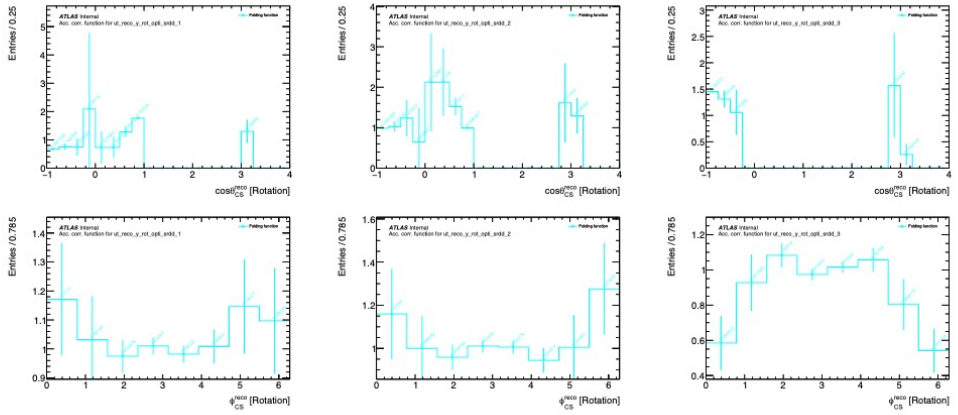

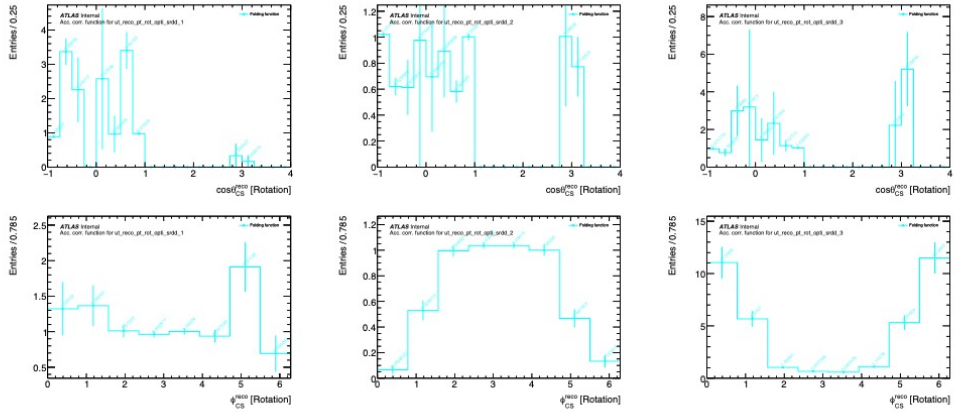

Acc Correction for 3D templates

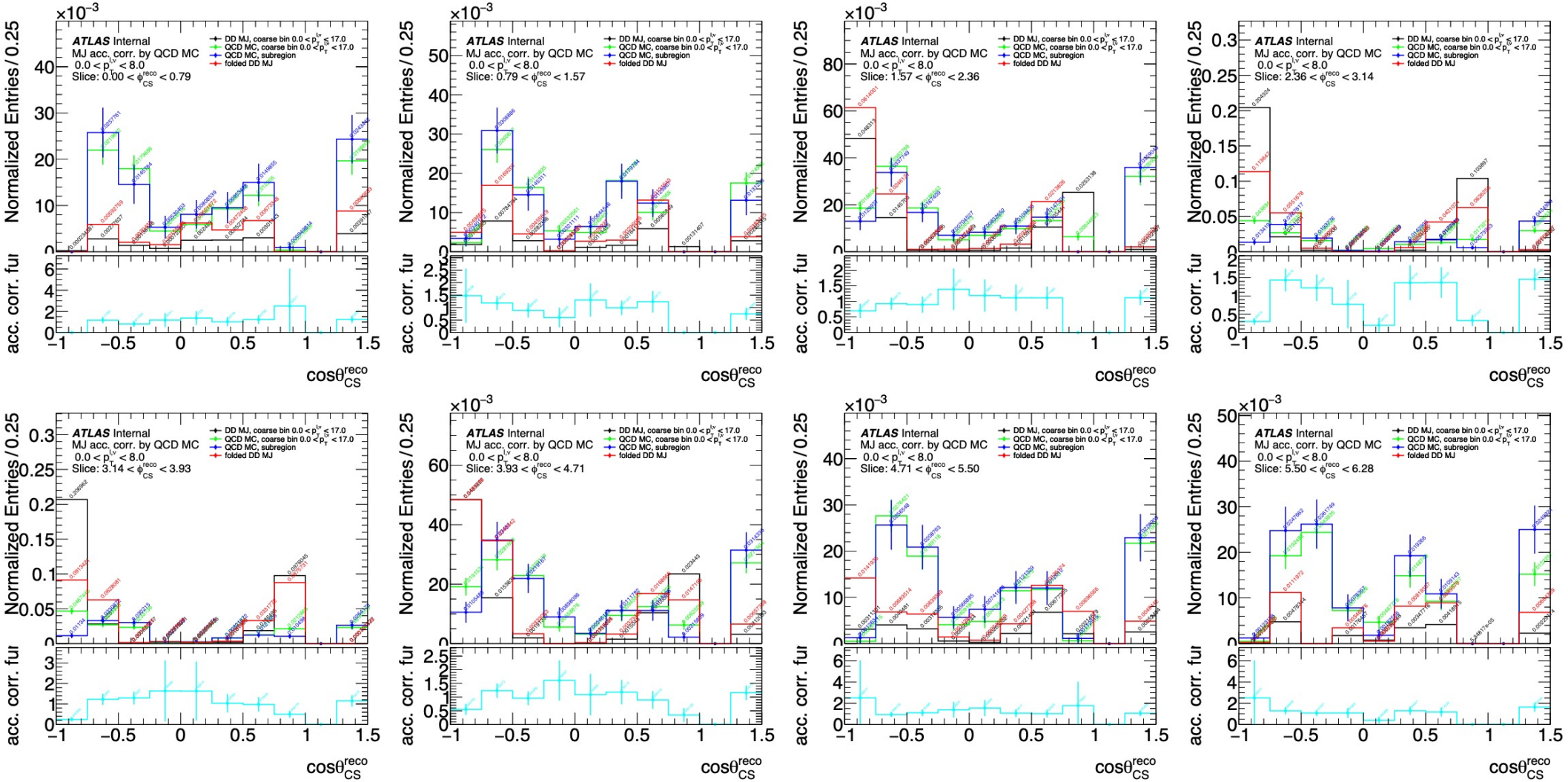

Figure 161: Multi-jet background template acceptance correction functions for $\cos\theta_{CS}$ as slices of ϕ_{CS} for $0 < p_T^{\ell,\nu} < 8$ GeV bin for $W^- \to e^-\overline{\nu}$ channel. Distributions are normalized over ϕ_{CS} slices. Error bands represents statistical uncertainties.

Acc Correction for 3D templates

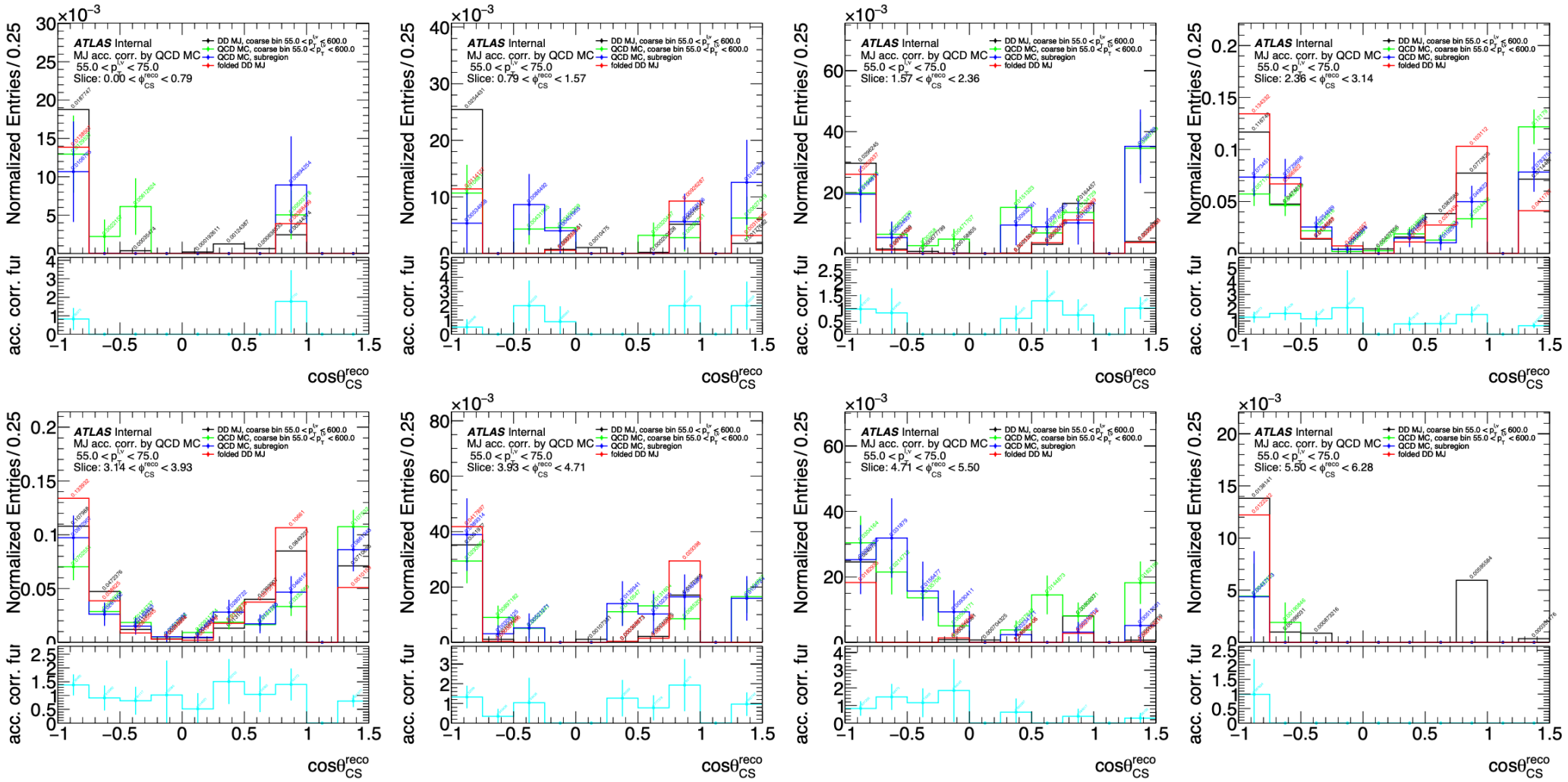

Figure 166: Multi-jet background template acceptance correction functions for $\cos\theta_{CS}$ as slices of ϕ_{CS} for $55 < p_T^{\ell,\nu} < 75$ GeV bin for $W^- \rightarrow e^-\bar{\nu}$ channel. Distributions are normalized over ϕ_{CS} slices. Error bands represents statistical uncertainties.

Acc Correction for 3D templates

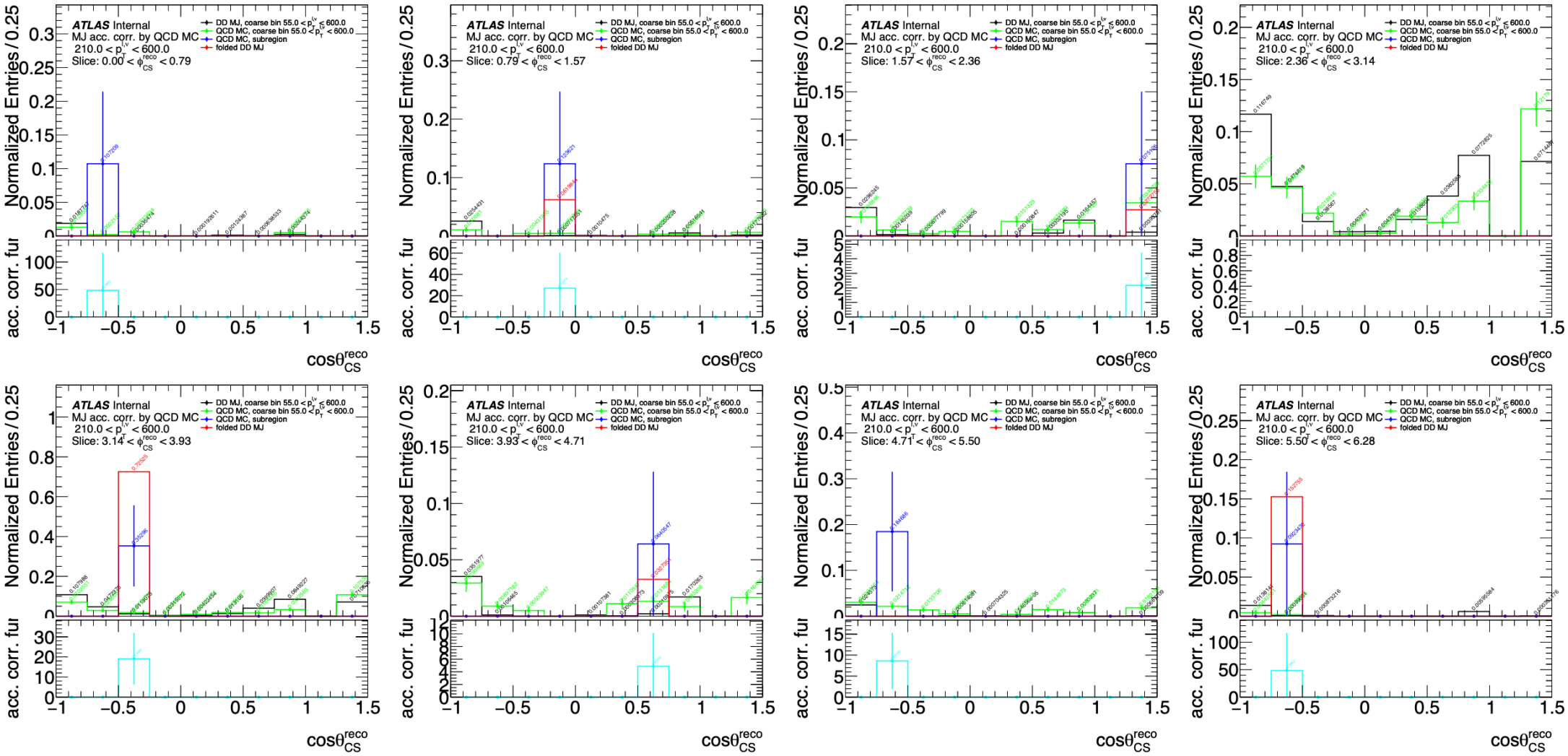

Figure 170: Multi-jet background template acceptance correction functions for $\cos\theta_{CS}$ as slices of ϕ_{CS} for $210 < p_T^{\ell,\nu} < 600$ GeV bin for $W^- \to e^-\overline{\nu}$ channel. Distributions are normalized over ϕ_{CS} slices. Error bands represents statistical uncertainties.